

Advanced Reactor Physics Methods for Transient Analysis of Boiling Water Reactors

Zur Erlangung des akademischen Grades
Doktor der Ingenieurwissenschaften (Dr.-Ing.)
der Fakultät für Maschinenbau
Karlsruhe Institut für Technologie

genehmigte

Dissertation

von

Jose Angel Gonzalez Vargas

geboren in Ometepec, Guerrero, Mexiko

Hauptreferent:	Prof. Dr.-Ing. Robert Stieglitz Karlsruhe Institut für Technologie
Korreferent:	Univ.-Prof. Rafael Macián-Juan, Ph.D. Technische Universität München (TUM)
Tag der Einreichung:	07.08.2017
Tag der mündlichen Prüfung:	27.10.2017

2017

Hiermit erkläre ich, dass ich die vorliegende Arbeit selbständig angefertigt und keine anderen als die angegebenen Quellen und Hilfsmittel benutzt sowie die wörtlich und inhaltlich übernommenen Stellen als solche kenntlich gemacht und die Satzung des KIT zur Sicherung guter wissenschaftlicher Praxis in der jeweils gültigen Fassung beachtet habe.

Karlsruhe, den 07. December 2017

José Ángel González Vargas

A mi hijo Uriel Tonatiuh y a mi esposa Olivia

A mi padres Susana y Ángel

A mis hermanos Susana y Fernando

A mis sobrinos Judas, Santiago y Bárbara

Por creer siempre en mí y por todo su amor

Acknowledgements

First of all I would like to thank to the CONACYT-DAAD scholarship program for all the financial and administrative support during the development of this thesis.

Moreover, I would like to express my deepest gratitude to Prof. Dr-Ing. Robert Stieglitz for their invaluable guidance, encouragement and useful feedback during this PhD work. I also want to thank to Dr. Victor Hugo Sanchez Espinoza not only because he gave me the opportunity to come to Germany, but also because he has always believe in me. I am in debt to him for his support but overall for his friendship. I am also very grateful to Prof. Dr. Rafael Macian from the Technical University of Munich (TUM), who accepted to be one of my supervisors.

I specially thank Dr. Javier Jimenez Escalante, who was not only a college but also became a good friend, for his invaluable support in programming issues and operating systems.

My special thanks to the members of the Nuclear System Department of the National Institute for Nuclear Research of Mexico (ININ), especially to Dr. Javier Ortiz Villafuerte, Dr. Rogelio Castillo Duran, Dr. Armando Miguel Gomez Torres and the master students Guillermo and Miguel for the support and hospitality received during my internship for the development of the cross section methodology.

I wish to thanks my colleges at the Institute of Neutron Physics and Reactor Technology of the Karlsruhe Institute of Technology (INR-KIT) that supported me in the desperate moments, particularly Nerea Diez, Veronica Jauregui, Dr. Ignacio Gomez, Joaquin Basualdo, Yousef Alzaben, Thomas Schaub and Dr. Wadim Jäger. Also, I want to express all my gratitude to the secretaries of INR, Petra Klug and Birgit Zagolla.

Last but not least, I want to thank and dedicate this PhD to my son Uriel Tonatiuh and to the love of my live and wife Olivia. They are my best motivation to overcome every difficulty.

Abstract

The safety assessment of nuclear power plants requires the consideration of the several physical phenomena taking place in the reactor core. Since the last decade, the simulations are performed using the so-called Best-Estimate (BE) thermal-hydraulic system codes coupled with 3D nodal diffusion reactor dynamics solvers. These numerical tools are well developed and validated for PWR but for BWR there are still improvements and developments to be done. In addition, homogenized cross sections libraries, depending on the individual thermal-hydraulic state parameters, e.g. fuel temperature, moderator density, etc., must be supplied to take into account the interdependencies of the involved physics.

In this PhD a new coupled code system named TRADYN was developed that consists of the novel and innovative integration of the core simulator DYN3D into the code system TRACE/PARCS using compiler preprocessor directives. This has the advantage to preserve the original TRACE/PARCS system “untouch” and to facilitate the maintenance, modification and debugging. In order to manage the transfer information between TRACE and DYN3D, a General Interface and Specific Data Map routines in FORTRAN were developed. To properly describe the tightly-coupled neutronics and thermal-hydraulic phenomena within the core of a BWR, different physical models were extended and new ones implemented in DYN3D and PARCS.

Another contribution of this doctoral thesis is the development of a new in-house methodology called GENSIM-XS for the generation of nodal cross sections for BWRs considering history effects of control rods and void. GENSIM-XS is able to greatly simplify the number of the neutronics regions present in the reactor core. This new methodology uses the AUDIT option of SIMULATE-3 (S3) to report the cross sections on the output file. Then, they are extracted and written in multi-group tabulated cross sections in NEMTAB format in an automatized manner using Python scripts.

The validation of TRADYN is based on Boiling Water Reactor Turbine Trip (TT) benchmark data, where TRADYN has demonstrated its capability to predict the stationary plant conditions as well as the temporal evolution of the main plant parameters, showing a good agreement with the measurements e.g. core power and dome pressure.

The static core of the cycle 4 of BWR Laguna Verde nuclear power plant was selected as second case for the validation not only of the GENSIM-XS methodology but also of TRADYN. The TRADYN results such as k -eff, axial power profile, axial void fraction exhibit an excellent agreement with the reference values. This underpins the capabilities of the new methodology to generate cross-sections for coupled thermal-hydraulic/neutronics calculations accounting also for history effects for BWR core analysis.

Kurzfassung

Die Sicherheitsbewertung von Kernkraftwerken erfordert die Berücksichtigung mehrerer physikalischen Phänomene, die im Reaktorkern stattfinden. In der jüngeren Vergangenheit erfolgten die Simulationen mittels sogenannte „Best-Estimate“ (BE) thermohydraulischen Programme. Diese werden mit 3D nodalen Reaktordynamik-Programmen gekoppelt. Diese Simulationsprogramme werden in westlichen Druckwasserreaktoren (DWR) aber wenigsten Siedewasserreaktoren (SWR) validiert. Bei letzterem gibt es noch einen erheblichen Entwicklungs- und Verbesserungsbedarf. Diese gekoppelten Neutronik-Thermohydraulik-Codes benötigen homogenisierte und kondensierte Wirkungsquerschnittsbibliotheken, die werden von den thermalhydraulischen Kernparametern wie Brennstofftemperatur, Kühlmitteldichte, abhängen.

In dieser Doktorarbeit wurde ein neues gekoppeltes Codesystem, genannt TRADYN, entwickelt. Dieses neuartige Programmsystem besteht aus der Integration des Kernsimulators DYN3D in das Codesystem TRACE/PARCS unter Verwendung von Präprozessordirektiven. Der Vorteil von TRADYN besteht darin, dass das ursprüngliche TRACE/PARCS System „unberührt“ bleibt und somit die Wartung, Modifizierung und das Debugging erleichtert werden. Zum Datentransfer zwischen TRACE und DYN3D wurden eine allgemeine Schnittstelle sowie verschiedene FORTRAN-Routinen entwickelt. Zur Beschreibung der neutronenphysikalischen und thermohydraulischen Wechselwirkung innerhalb des Kerns eines SWR, wurden verschiedene physikalische Modelle in DYN3D und PARCS implementiert.

Ein weiterer Beitrag dieser Arbeit ist die Entwicklung einer neuen Methode, genannt GENSIM-XS, zur Erzeugung von Wirkungsquerschnittsbibliotheken für einen SWR, die Historieneffekte wie z.B. von Absorber-Kreuzen und Dampfgehalt berücksichtigt. GENSIM-XS ermöglicht die Anzahl der Neutronik-Regionen im Reaktorkern erheblich zu reduzieren. Diese neue Methodik verwendet die „AUDIT“ Option von SIMULATE-3 (S3), um die Querschnitte in eine der Ausgabedatei zu schreiben. Danach werden sie automatisiert mit Hilfe eines Python-Skripts ausgelesen und tabellarischen in das NEMTAB-Format geschrieben.

Zur TRADYN Validierung wurden experimentelle SWR Daten einer Turbinenschnellabschaltung (TT) verwendet. Dabei konnte gezeigt werden, dass TRADYN in der Lage ist, die stationären Betriebsbedingungen vor dem Test sowie den zeitlichen Verlauf wichtiger Kernparameter wie der Reaktorleistung und den Druck im oberen Plenum des Reaktordruckbehälters mit hoher Genauigkeit zu berechnen.

Weiterhin wurden die Messdaten des Zyklus 4 des stationären Betriebszustand vom SWR Laguna Verde zur Validierung der entwickelten Methode zur Wirkungsquerschnittserstellung GENSIM-XS und auch der Voraussagbarkeit vom TRADYN genutzt. Die mit TRADYN berechneten Parameter wie k -eff, axiale Leistungsverteilung und Dampfgehaltsverteilung zeigen eine gute Übereinstimmung mit den Referenzwerten. Diese Ergebnisse dokumentieren die Leistungsfähigkeit von GENSIM-XS zur Kernsimulationen gekoppelte Neutronik/Thermohydraulik Fragestellung unter Berücksichtigung von Historie Effekten bei SWR-Kernen.

Publications related to this thesis

1. Gonzalez-Vargas Jose Angel, Sanchez-Espinosa V and Jimenez J. Internal Coupling of the Code DYN3D with the USNRC Code TRACE - First Results. In *Proceedings of the Physor 2016 conference*. Sun Valley, USA, 2016.
2. Gonzalez-Vargas Jose Angel, Sanchez-Espinosa, V., Stieglitz R and Macian-Juan R. Development and Validation of the New Coupled Code System TRADYN. *Accepted to be published in Annals of Nuclear Energy*, 2017

Contents

1	Introduction.....	7
1.1	Motivation.....	7
1.2	Overview of the current boiling water reactors.....	7
1.3	Main Objectives of the thesis.....	11
1.4	Structure of the thesis.....	11
2	State-of-the-art of Boiling Water Reactor Simulations	13
2.1	Multi-physics Methodologies.....	13
2.2	Thermal-hydraulic / Neutronics coupling approaches	15
2.2.1	Internal coupling	16
2.2.2	External coupling	17
2.2.3	Spatial coupling.....	17
2.2.4	Temporal coupling	20
2.3	Cross section generation for Thermal-hydraulic / Neutronics coupled calculation	21
2.4	Neutronics core characterization.....	24
2.5	Recent trends in coupling simulations	25
3	Principles of Thermal-Hydraulics/Neutron Kinetics Core Calculations	27
3.1	The Best-Estimate Thermal-Hydraulic Code System TRACE	27
3.1.1	Thermal-hydraulic 2 Phase Conservation Equations.....	27
3.1.2	Heat transfer at the interface and at the wall	29
3.1.3	Heat conduction model in solids	30
3.2	The reactor dynamic code PARCS.....	31
3.3	Thermal-hydraulic/Neutronics coupled system TRACE/PARCS.....	32
3.3.1	The General Interface.....	32
3.3.2	The PARCS-Specific Data Map Routine	33
3.3.3	The TRACE-Specific Data Map Routine.....	33
3.4	The multi-group reactor dynamic code DYN3D-MG.....	34
4	Thermal-hydraulic/Neutronics Coupled Code System TRADYN Development.....	37
4.1	Internal coupling approach.....	37
4.2	Steady State Coupling	40
4.3	Transient Coupling.....	41
4.4	Improved physics of TRADYN for BWR simulations	43
4.4.1	New DYN3D models for Gamma Heating and Bypass Correction	44
4.4.2	New DYN3D module to account for the orientation of ADF	45
4.4.3	New PARCS module for reading multi-group cross section in NEMTAB format	46

4.5	New post-processing capabilities in TRADYN	47
5	GENSIM-XS methodology for nodal cross section generation of BWR cores	49
5.1	The new GENSIM-XS methodology	49
5.2	Application of the GENSIM-XS Methodology to a real power plant.....	51
5.2.1	Description of the cycle 4 of Laguna Verde Nuclear Power Plant	51
5.2.2	Determination of the average fuel exposure.....	52
5.2.3	Determination of the average nodal values per subtype	56
5.2.4	Parameterization and generation of the cross section.....	57
6	Validation of TRADYN using the Peach Bottom Turbine Trip test	59
6.1	Definition of Peach Bottom Turbine Trip (TT) test and models.....	59
6.2	Comparison of TRADYN steady state predictions against test data.....	63
6.3	Comparison of TRADYN transient predictions against test data	66
7	Analysis of the Laguna Verde core using SIMULATE-3 and TRADYN using cross sections generated with GENSIM-XS	69
7.1	The neutronics and thermal-hydraulic Laguna Verde core models	69
7.1.1	The SIMULATE-3 core reference model.....	69
7.1.2	The PARCS and DYN3D core models	71
7.1.3	The TRACE thermal-hydraulic model	71
7.2	Comparison of TRADYN static core simulations with SIMULATE-3	73
8	Summary.....	81
9	Outlook.....	83
	List of figures.....	85
	List of tables.....	89
	Appendix A	91
	Appendix B	93
	Appendix C	97
	Appendix D.....	101
	Appendix E	107
	References.....	109

List of Acronyms

ADF	Assembly Discontinuity Factor
ANM	Analytical Nodal Method
ATWS	Anticipated Transient Without SCRAM
BE	Best Estimate
BOP	Balance of Plant
BWR	Boiling Water Reactor
CAMP	Code Application and Maintenance Program
CASL	Consortium for the Advanced Simulation of Light Water Reactor
CHF	Critical Heat Flux
CMFD	Coarse Mesh Finite Difference
CMS	Core Management System
CRDA	Control Rod Drop Accident
DDMR	DYN3D Specific Data Map Routine
DNBR	Departure from Nuclear Boiling Ratio
ENDF	Evaluated Nuclear Data File
EXP	Exposure
FMFD	Fine Mesh Finite Difference
G	Mass flow
GENSIM-XS	Methodology for generation of cross section for BWR
GI	General Interface
H	Enthalpy
HCRD	History Control Rod
HP	High Pressure
HTMO	History Moderator Temperature
HVOI	History Void fraction
HZDR	Helmholtz Zentrum Dresden Rossendorf

INR	Institut für Neutronenphysik und Reaktortechnik
JEFF	Joint Evaluated Fission and Fusion File
KIT	Karlsruher Institut für Technologie
LP	Low Pressure
LOCA	Loss Of Coolant Accident
LV	Laguna Verde
LVNPP	Laguna Verde Nuclear Power Plant
LWR	Light Water Reactor
MED	Data Exchange Model
MSLB	Main Steam Line Break
N	Neutronics
NEM	Nodal Expansion Method
NEMMG	Multi-group Nodal Expansion Method
NK	Neutron Kinetic
NSSS	Nuclear Steam Supply System
OTB	Onset of Transition Boiling
PBTT	Peach Bottom Turbine Trip
PDMR	PARCS Specific Data Map Routines
PVM	Parallel Virtual Machine
PWR	Pressurized Water Reactor
REA	Rod Ejection Accident
RPV	Reactor Pressure Vessel
S3	SIMULATE-3
SLB	Steam Line Break
TDMR	TRACE Specific Data map subroutine
TH	Thermal-hydraulics
THF	Thermal-hydraulics Feedback
TRACE	TRAC/RELAP5 Advanced Computational Engine
TRADYN	TRACE/DYN3D coupled system code
TSV	Turbine Stop Valve

TT	Turbine Trip
US NRC	United States Nuclear Regulatory Commission
VERA	Virtual Environment for Reactor Applications
XS	Cross-section

1 Introduction

1.1 Motivation

The safety assessment of nuclear power plants requires not only a deep understanding of the physical phenomena taking place in the core, but also the use of computer codes able to describe them in a more realistic way. Because several areas of physics play a role, the simulations were at the very beginning performed by independent codes handling a specific physical aspect of the system.

Nowadays the safety assessment can be performed using the so-called best-estimate (BE) coupled codes involving different areas of the physics. The BE methods depicts more realistic physics and reduce conservativeness and allow therefore for reduced safety margins. At present, the use of BE codes for licensing purposes according to regulatory requirements must be complemented with an uncertainty evaluation. Furthermore, the current nuclear power plants producing electricity must submit to the regulatory bodies the corresponding safety analysis reports to assure a safe operation of the power plant during the whole operating cycle. These analyses are performed considering several operating conditions scoping nominal operation, operational transients or postulated accidents (e.g. reactivity initiated transients, turbine trips, load rejection, station blackout, anticipated transients without scram (ATWS)). Therefore, there is a real necessity not only for the nuclear stakeholders but also for the regulatory bodies to have verified and validated computational codes that can be used to perform these analyses. On the other hand, most of the current nuclear power plants producing electricity belong to either Pressurized Water Reactors (PWR) or Boiling Water Reactors (BWR). This PhD work is focused in the last one.

1.2 Overview of the current boiling water reactors

In a BWR, one main component is the Nuclear Steam Supply System (NSSS), consisting of the recirculation pumps, steam lines and the reactor pressure vessel (RPV), where the core and the separators/dryers are located. Other big component is the balance of the plant (BOP) including the high pressure turbine (HP) and low pressure turbines (LP), condenser, feedwater pump, heaters, etc. In a BWR reactor, the coolant enters into the core with a certain subcooling; vertically upward flowing coolant heats up reaching saturation condition already at the lower part of the core. Thereby, vapour is generated in the core, which flows upwards. In the vapour flow water droplets are entrained, which are separated from the steam in the separators/dryers.

This liquid is returned to the core, while the steam produced flows through the steam lines to the turbines where it is expanded. After that, the steam is cooled down and condensed in a condenser to be later reheated and reinserted by means of recirculation pumps into the core, completing a closed circuit. A general overview of a BWR plant, showing the main components, is presented in Figure 1-1.

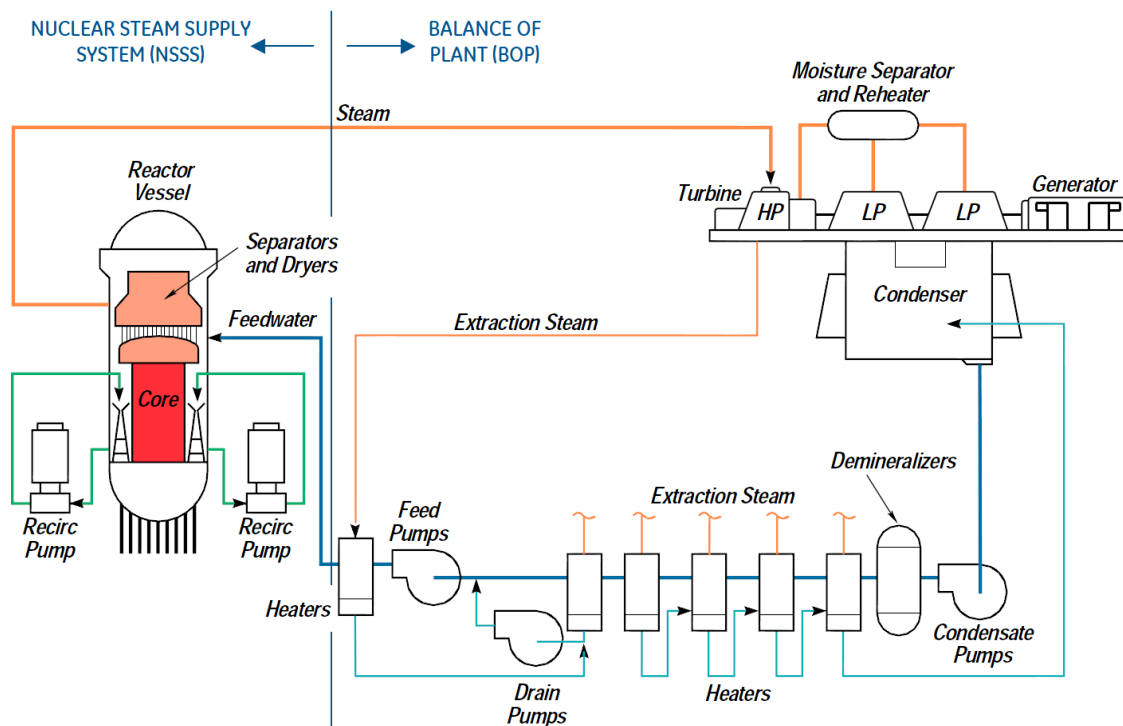


Figure 1-1 General scheme of a Nuclear Power Plant with a Boiling Water Reactor taken from (Chaparro-Vega, 2014).

The Figure 1-2 depicts a more detailed view of a typical BWR reactor pressure vessel and its internal structures. It can be seen that the core is located inside the core shroud and between core plate and top guide. The region between the core shroud and the vessel is called the “Downcomer region”. In this region, the water, coming from the separators and dryers, is mixed with the feedwater flow and pumped into the core by the recirculation system.

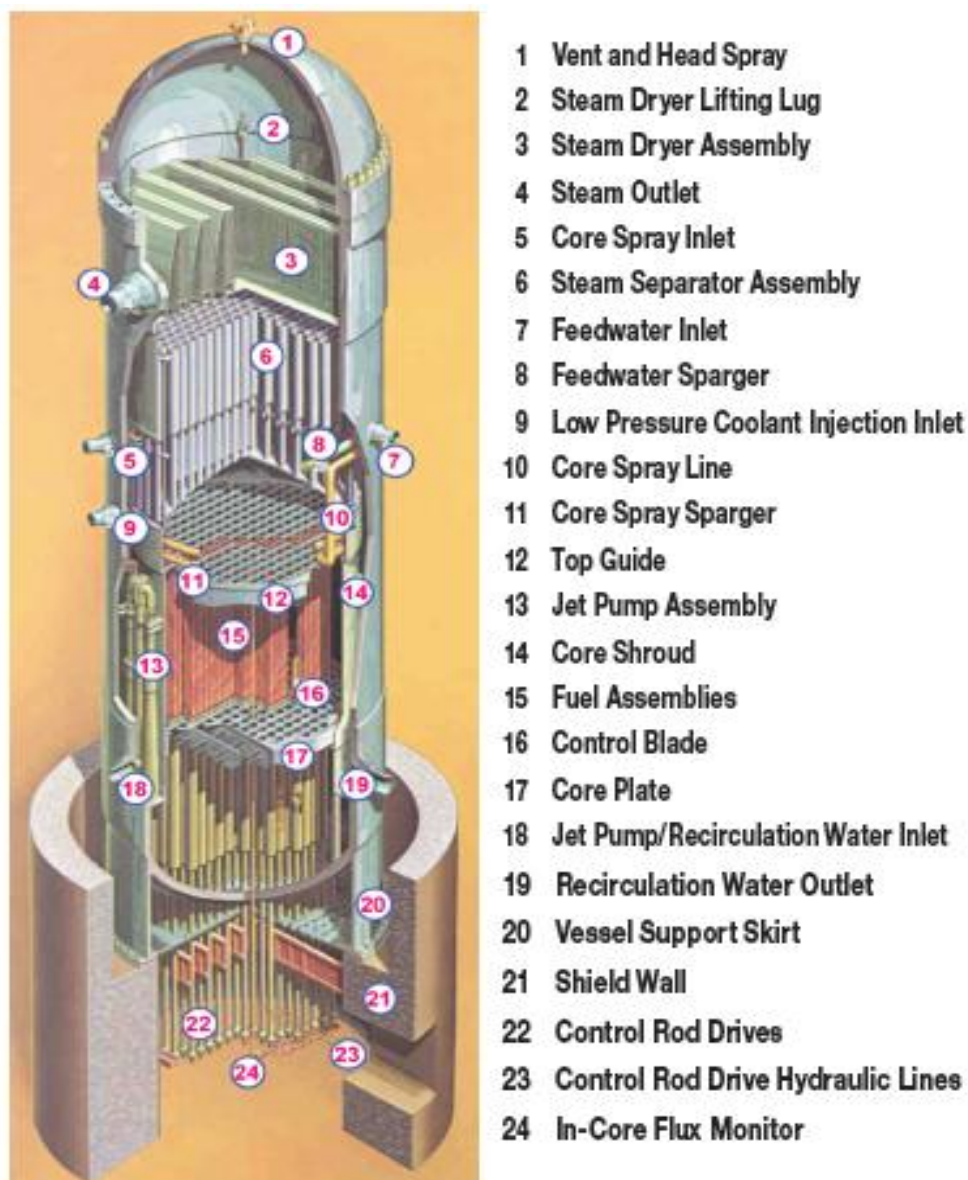


Figure 1-2 Detailed display of a typical BWR pressure vessel and its internal structures taken from (ANS , 2012).

The reactor cores of BWR are very large compared to the ones of PWR and in modern BWR core loading different types of fuel assemblies can be encountered which in general are characterized by water rods of different geometry and size (single tube, square or rhomboid tubes, etc.), a bypass flow around each fuel assembly canister, which is larger than the one of PWR. The Figure 1-3 depicts a typical BWR fuel assembly.

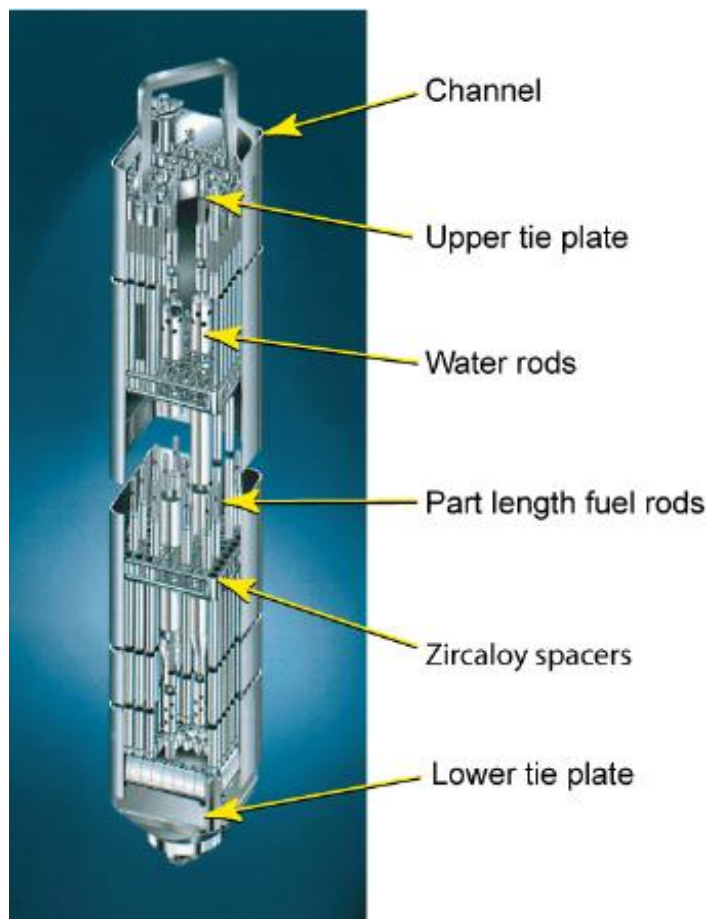


Figure 1-3 Example of a typical BWR fuel assembly taken from (ANS , 2012).

Through the water rods and bypass a considerable amount of water flows which remains cold compared to the coolant flowing inside the canister and in direct contact with the fuel rods. This contribute to an enhancement of the neutron moderation and hence on the fissions taking place inside the core. Hence, additional feedback effects between the core neutronics and the thermal hydraulics in a BWR must be considered in the coupled codes.

Other components present in the reactor core are the control rods. They are designed as long cross-shaped blades and inserted into the core from the bottom. The control rods represent the principal control mechanism of the core power level. Boron carbide is used as strong thermal neutron absorber to control the reactivity during operation and to shutdown the reactor. It is common to divide the control rods into 48 axial zones called “notches”. If a control rod is full inserted into the core it is referring to be located in the position 0, but if it is full withdrawn it is referring to be located in the position 48.

Since the last decade, coupled neutronics and thermal-hydraulic codes are being developed and validated for the simulation of plant transients, where a strong spatial power or temperature distortion within the core is expected to occur. These numerical tools are well developed and validated for PWR, but, for BWR there are still improvements and developments to be done.

1.3 Main Objectives of the thesis

The main goal of this PhD work is the further development of multiphysics coupling methodologies based on thermal-hydraulic and neutronics domains for transient analysis of boiling water reactors in order to describe the main interdependencies of different phenomena taking place in the reactor.

In order to reach these goals a coupling between the thermal-hydraulic code TRACE and the core simulator DYN3D (based on multi-group diffusion approximation) will be developed, tested and validated. In detail, the main scientific focus of the doctoral thesis is concentrated on the following areas:

- Development of a flexible coupling approach between DYN3D and TRACE without affecting the current coupling with PARCS.
- Review and extensions of BWR-related physical models of DYN3D for an improved description of the feedbacks between the neutronics and thermal-hydraulics.
- Development of a methodology for the generation of exposure dependent nodal cross sections considering history effects and written in an appropriate format (e.g. NEMTAB) for both DYN3D and PARCS.
- Testing, verification and validation of the developed schemes and the cross section methodology using code-to-code or code-to-data.

1.4 Structure of the thesis

Following this introduction, the state-of-the-art of Boiling Water Simulations focused on thermal-hydraulic and neutronics coupling is described in chapter 2. In chapter 3, the applied computational tools are briefly introduced. In chapter 4, the new coupled code system TRADYN developed entirely on this dissertation is presented in detail. Additionally, the improvements done in DYN3D and PARCS are also given. The chapter 5 is devoted to the description of a new methodology (GENSIM-XS) for the generation of nodal few-group cross section for BWR and its application to the cycle 4 of Laguna Verde Nuclear Power Plant (LVNPP). In chapter 6, the validation of TRADYN using the Peach Bottom Turbine Trip Benchmark considering steady state and transient calculations is described and the results are discussed. The objective of chapter 7 is to present the validation of the cross section generated in chapter 5 using TRADYN for steady state conditions. Finally a summary of the main investigations as well as an outlook with potential extensions and future work are given at the end of this dissertation.

2 State-of-the-art of Boiling Water Reactor Simulations

In this chapter, different multi-physics methodologies, mainly focused on thermal-hydraulics and neutronics domains, will be described. The importance of the cross section for the coupling simulations is also emphasized. Finally, the new trends for coupling simulations of nuclear systems are briefly presented.

2.1 Multi-physics Methodologies

The simulation of the different operating conditions of Boiling Water Reactors has been improved in the last decades. On the one hand devoted to the rapid progressing of the computational power and on the other hand due to the better understanding of the physical phenomena taking place in a nuclear power plant.

At the very beginning, the simulations were treated or described separately in different computer programs using simplified models in order to describe every field, but the interrelation between them was not taken into account. Traditionally, two independent fields were mainly considered during the simulations, the thermal-hydraulics (TH) and the neutronics (N). The first one is in charge of the fluid dynamics and heat transfer mechanisms throughout the reactor coolant system and especially in the core region of the reactor, whereas the second one is dealing with the balance of neutrons in the core.

On one hand, in the last decades the so called “Best-Estimate” (BE) thermal-hydraulic system codes with one dimensional thermal-hydraulic models were well developed and widely validated using experimental data from specially designed scaled down test facilities or data from nuclear power plants in the framework of international benchmarks. Very well-known codes belonging to this category are TRAC-BF1 (Borkowski, et al., 1992), RELAP5 (RELAP5, 2001), ATHLET (Lerchl, 1998), among others. Moreover, these systems have been continuously evolved by adding new models for a 3D representation of the physical processes inside de reactor pressure vessel and other components. As a result, system codes with 3D model capability are now available such as: RELAP-3D (RELAP, 2005), CATHARE-3 (Emonot, et al., 2011) TRACE (TRACE, 2013), or the ongoing 3D ATHLET model (Schöffel, et al., 2016), etc.

On the other hand, the main goal of the reactor physics (neutron kinetics) calculations is to determine the neutron distribution and reaction rates, depending usually on the time and the position in the core. In fact, the time dependent Boltzmann transport equation can be used to

describe the behaviour of neutrons exactly. However, only approximated forms of this equation are solved due to its integro-differential nature. It is not the scope of this dissertation to make an exhaustive description of the different approximations. A complete description can be found in (Bell, et al., 1970). Nonetheless, some important approaches will be here summarized in the following paragraphs.

There are two main branches for dealing with the transport equation:

- **The stochastic methods**, also referring as **Monte Carlo Method**

Its applicability comes from the fact that the macroscopic cross sections (XS) can be interpreted as a probability of interaction per unit distance travelled by a neutron. Hence, in the Monte Carlo method, a set of neutron histories is generated by following individual neutron through successive collisions, which may result in scattering, radiative capture or fission. By following the behaviour of the neutrons until they are either absorbed or escaped from the system, the characteristic of the system can be evaluated by performing a statistical average of many neutron histories. This probabilistic approach is extremely computer-intensive, since many neutrons are required in order to obtain results having a statistical significance and since nuclear cores are large systems to be modelled. On the other hand, some of the advantages of the Monte Carlo method are the exact geometry representation of the system and almost no approximations involved in the calculations, i.e. continuous in energy variation of microscopic cross section. Examples of codes implementing this methods are MCNP (X-5 Monte Carlo Team, 2003), OpenMC (Romano, et al., 2013), Serpent (Leppänen, 2013), among others.

- **The deterministic methods**

The solution of the neutron transport equation can be tackled by using discretization in angular direction, space and energy as function of time. Additionally, depending of the form of the equation, different methods can be applied, such as: the collision probabilities or the method of characteristics. These methods are used by APOLLO (Sanchez, et al., 2010), DRAGON (Marleau, 2001), HELIOS-2 (Wemple, et al., 2008), CASMO-4 (Knott Dave, 1995) or POLARIS (Jessee, et al., 2014) for the generation of cross sections of a heterogeneous lattice in 2-Dimensions. Other methods such as: Spherical Harmonics (P_N) and some simplification (SP_N) have been implemented for example in PARCS (Downar, et al., 2013), DYN3D-SP3 (Grundmann, 2009), CRONOS2 (Mignot, et al., 2004); or the Discrete Ordinates method has been implemented in DORT (Schunert, et al., 2013) or NEWT (Jessee, et al., 2015) of the SCALE sequence.

However, most of the current production codes modelling the existing Light Water Reactors (LWRs) are based on the diffusion approximation, considering either 2 energy

groups or several groups, and discretization in space using a large coarse mesh (of an assembly size) of so-called *nodes* (circa of 15-20 cm). The Nodal Expansion Method (NEM) and the Analytical Nodal Method (ANM) are the most common methods currently used. Prominent examples codes using this methods are NEM (Beam, et al., 1999), PARCS (Downar, et al., 2013), DYN3D (Grundmann, et al., 2005), SIMULATE-3 (S3) (Cronin, 1995), SIMULATE-3K (S3K) (Grandi, 2005), etc.

It can be stated that in the last decades, important progress in the development of TH and N codes has been done. However, coupling of the system and neutronics codes (diffusion) have been carried out in order to allow for a more realistic description of the core behaviour during non-symmetrical transients, where the strong interaction of thermal-hydraulic and neutronics plays an important role, e.g. during ATWS, steam line break (SLB), rod ejection accident (REA) in PWRs or the control rod drop accident (CRDA) in BWRs. Some well-known examples of these coupling systems are TRAC/NEM (Beam, et al., 1999), CATHARE-CRONOS2-FLICA (Mignot, et al., 2004), TRAC-M/PARCS (Lee, et al., 2004) (Xu, et al., 2009), RELAP5-PARCS (Bousbia-Salah, et al., 2004), ATHLET-QUABOX/CUBBOX (Langenbuch, et al., 2004), DYN3D/ATHLET (Kozmenkov, et al., 2015), TRACE/S3K (Nikitin, et al., 2010), etc. These coupled systems have been validated against several cases including, but no limited to plat data or international benchmarks such as: PWR Main Steam Line Break (MSLB) (Ivanov, et al., 99), the Peach Bottom Turbine Trip (PBTT) (Solis, et al., 2001), the VVER-1000 Coolant Transient (Ivanov, et al., 2002) and Oskarshamn-2 Stability Event (Kozlowski, et al., 2014). These Benchmarks offer one option for verifying the capabilities of the coupled codes to analyse complex transients, where the neutronics and thermal-hydraulics interact each other strongly.

2.2 Thermal-hydraulic / Neutronics coupling approaches

A broad spectrum of code systems with coupling of thermal-hydraulic system (TH) codes and neutron-kinetic (NK) codes has been developed due to the continuously increasing computing capabilities. All necessary requirements for developing these systems were well summarized in (CRISSUEV2, 2004) and some details can be found in (Ivanov, et al., 2007), (Bousbia-Salah, et al., 2007). The objective of these requirements is to provide accurate solutions in a reasonable amount of CPU time in coupled simulations of detailed operational transients and accident scenarios. The key issues in coupled codes are:

- Coupling approach (internal or external).
- Spatial and temporal coupling.
- Appropriate convergence criteria for coupling.

2.2.1 Internal coupling

Within the internal coupling the modules of the neutronics code are directly implemented into the thermal-hydraulic system code, in order to replace e.g. corresponding point kinetics or 1D kinetics subroutines. The thermal-hydraulic behaviour of all components of the plant including the reactor core is modelled by the system code. Thermal-hydraulic feedback (THF) parameters for each node are transferred to the neutron kinetic model, and power densities are transferred back from the neutronics model for each heat conduction volume in the system code's nodalisation, see Figure 2-1. This way of coupling is the most consistent way of coupling. One major disadvantage of this method is that it involves significant modifications in both codes. Nevertheless, the modifications can be done in a way that if new versions of the codes are released, or if it is desired the coupling with some other code, no changes or minimal changes of the new coupling routines are necessary to generate the coupled code. This coupling scheme is adopted in the basic TRACE/PARCS coupling.

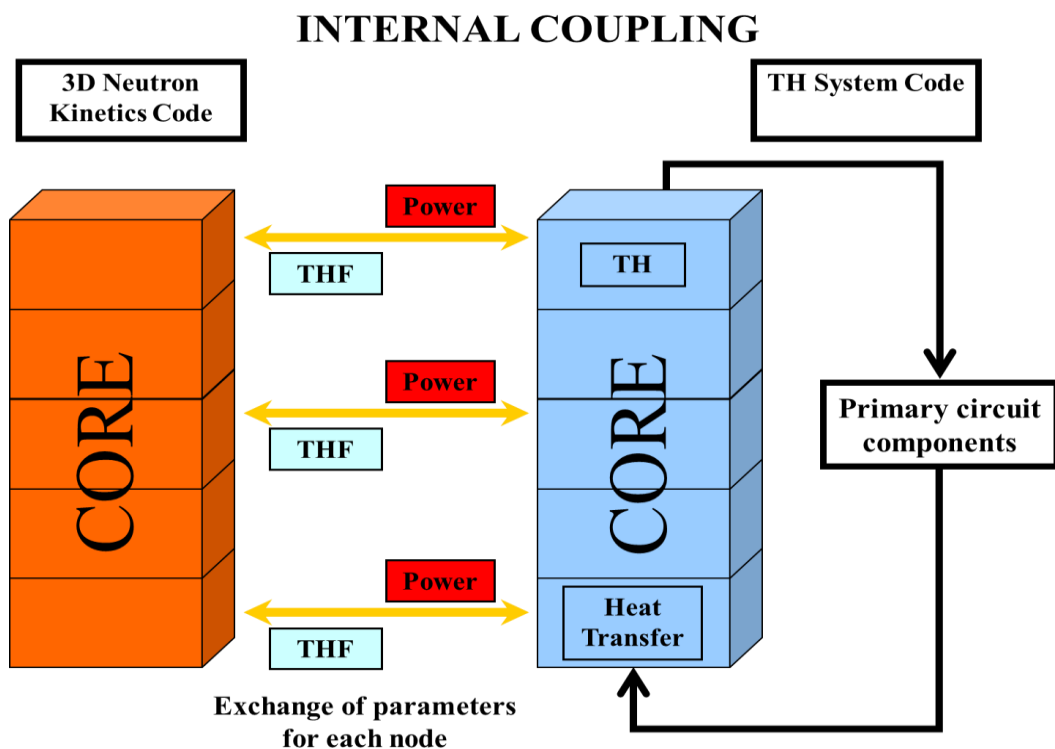


Figure 2-1 Internal Coupling between a neutron kinetic code and a system code from (Gomez-Torres, 2011).

2.2.2 External coupling

In the external coupling, the reactor core is completely modelled by the 3D reactor-dynamic model, including thermal hydraulics. The system code models the whole plant thermal hydraulics except the reactor core. Core inlet and outlet boundary conditions such as pressure (p), mass flow (G) and enthalpy (H) or coolant temperature, are exchanged between the two sub-models, see Figure 2-2. External coupling is easy to implement, however in some cases, it may lead to unstable numerics and slow convergence, especially in cases with strong interaction between thermal hydraulics and neutronics, e.g. for BWR.

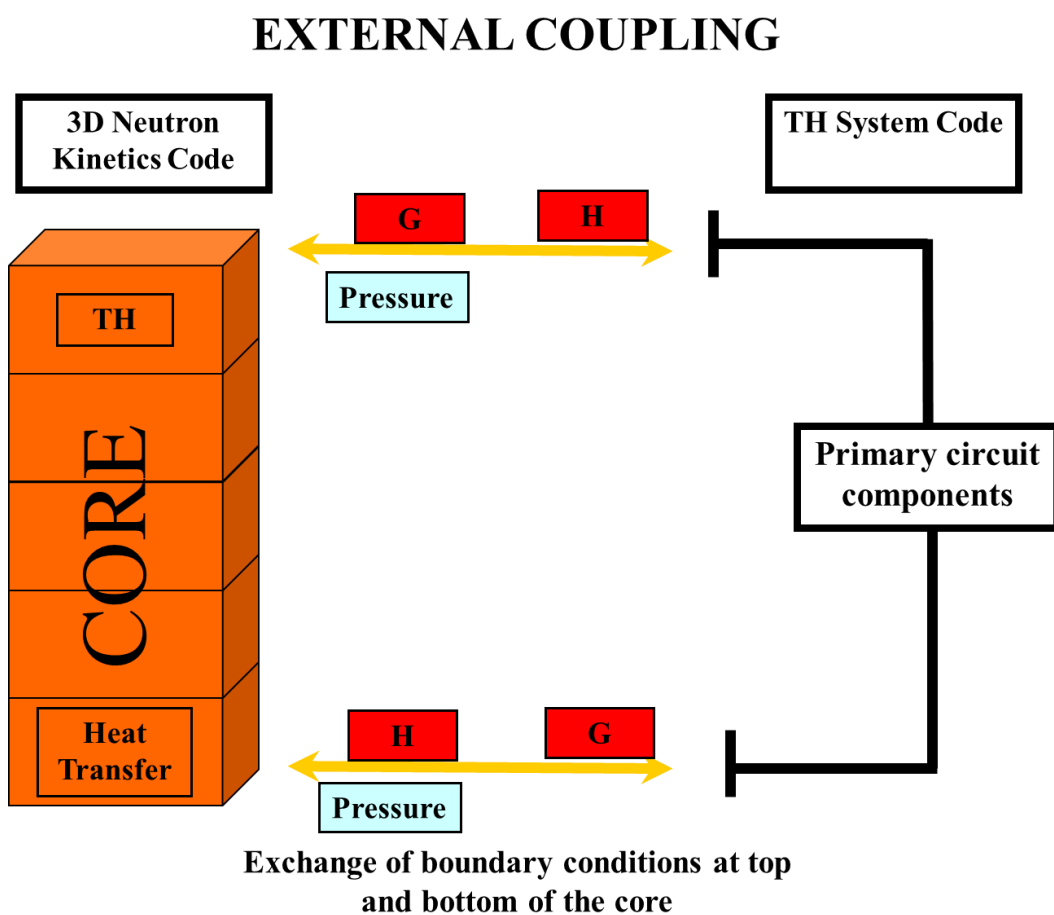


Figure 2-2 External coupling between a reactor dynamics code and a system code from (Gomez-Torres, 2011).

2.2.3 Spatial coupling

The spatial (radial and vertical) mapping between the neutronics and thermal-hydraulic codes plays an important role to assure the proper exchange of information and accuracy of the results.

In most of the current coupled TH/NK codes, this mapping is either fixed or flexible. In the first one usually one thermal-hydraulic channel (or node) represents one neutronics assembly (or node), while in the flexible coupling the user can specify the radial or axial mapping schemes. The determination of the proper mapping can be a challenging task and is problem dependent. Nevertheless, for detailed representations both radial and axial mapping have to be considered.

In order to map consistently neutronics assemblies to thermal-hydraulic channels, several rules usually are to be respected:

- Assemblies with similar neutronics design are mapped to one TH channel.
- Special attention must be paid to important variables such as: relative power, coolant flow, void fraction, type of bundle throttling (orifice), type of fuel (enrichment), etc.
- The core symmetry must be matched.

A boiling water reactor core contains a large number of fuel assemblies (usually about 800). The exact, detailed TH and kinetics modelling of such core requires significant computational resources. Thus the optimization of coupled neutronics/thermal-hydraulic calculations represents a considerable challenge. Calculation costs could be reduced if similar assemblies can be collapsed into a single TH channel, while maintaining the detailed neutronics modelling. Furthermore, collapsing the number of T-H channels smooths the power distribution and the resulting reactivity feedback. Finding an optimized number of TH channels helps to improve the accuracy and duration of calculation.

Modern reactor analysis codes, such as TRACE, have two different geometrical representations for the three-dimensional components, Cartesian and cylindrical. In either case, for detailed representations, both the axial and radial mappings have to be considered.

The Figure 2-3 and Figure 2-4 depict the radial mapping and axial mapping, in which the numbers indicate the different thermal-hydraulic channels, between the TH and N domains, used for the Peach Bottom Turbine Trip Benchmark discussed in the results of section 6.2.

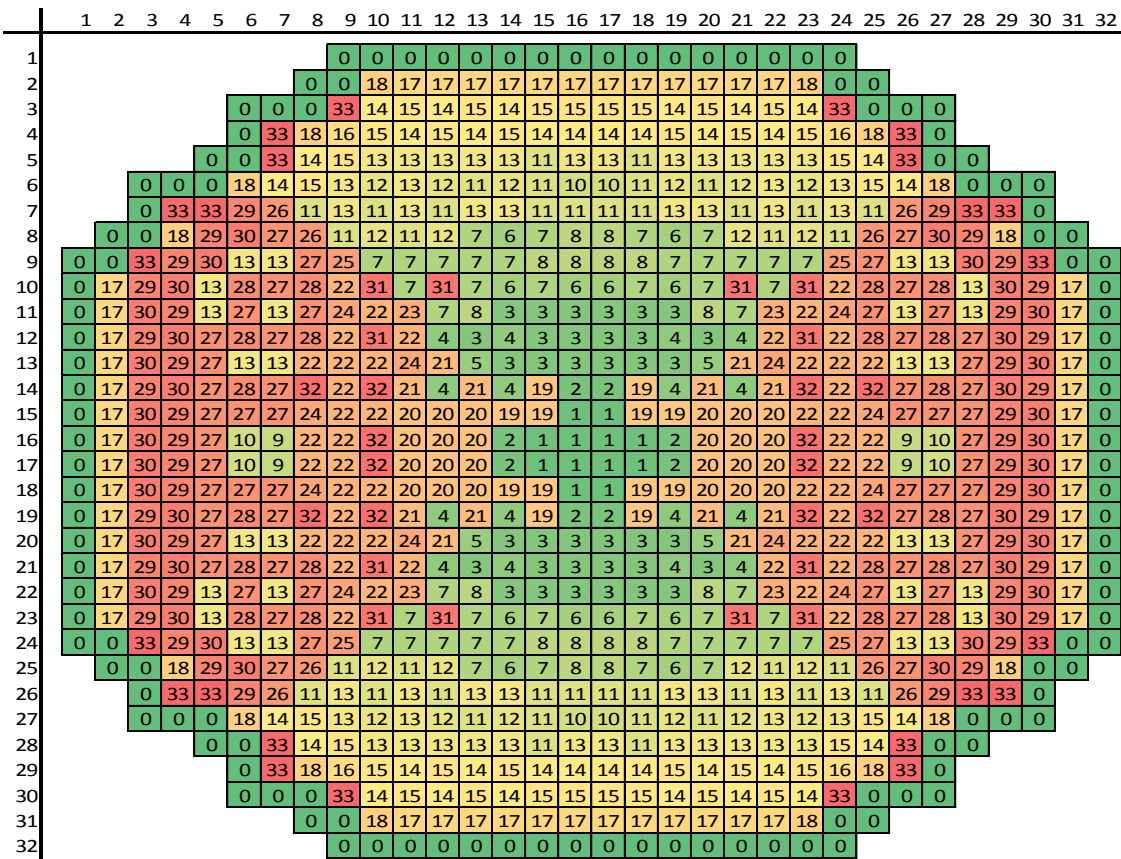


Figure 2-3 Thermal-hydraulic channels of the radial mapping scheme used to represent the Peach Bottom reactor core (Solis, et al., 2001).

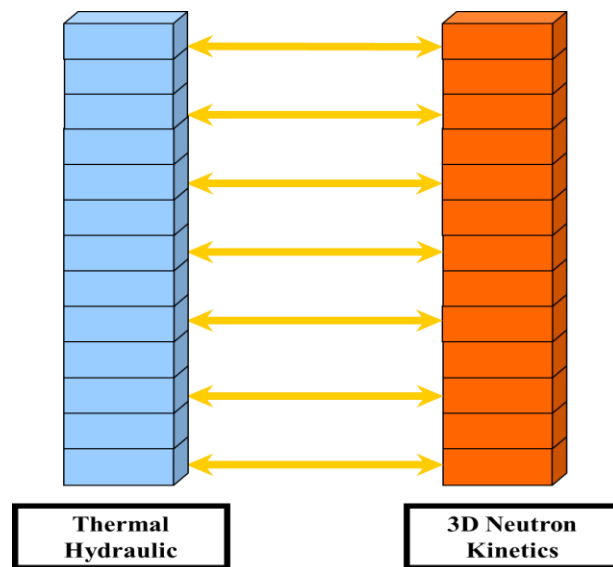


Figure 2-4 Scheme used for the axial mapping between Thermal-hydraulic and Neutronics domains used in the Peach Bottom Turbine Trip benchmark.

2.2.4 Temporal coupling

The temporal coupling and synchronization are essential for the coupling of two different codes e.g. a thermal-hydraulics and neutron-kinetics. Usually each code has its own time-step selection algorithms based on the nature of the physical problem to be solved. The easiest and the most straightforward technique is to select one code e.g. the thermal-hydraulics as the master code and to make the time-step size of the slave code (e.g. the neutronics solver) equal to the size of master. For instance, in TRACE/PARCS system, TRACE is the master and PARCS the slave. This means that the time step selection is based on the convergence of the thermal-hydraulics parameters and global power but not the local neutron fluxes. Therefore, in some situations smaller time-step sizes will be necessary to achieve a solution convergence. Care has to be taken to assure that time-steps are small enough to resolve local flux distributions in fast transients with fast power changes. During one time step, the TH data calculated by the TH code (i.e. moderator density and temperature, vapour density, void fraction, boron concentration, average fuel temperature, fuel centreline temperature and fuel surface temperature) is passed to the NK code. In the NK solution that information impacts via the cross sections the feedback. Finally the NK code returns the local power as feedback to the TH model.

Beyond the time step size, the point at which data is exchanged between the two codes is important. It can be classified in three types of couplings namely explicit, implicit and semi-implicit (Watson, 2010). All three of them exhibit advantages and drawbacks.

The explicit coupling is the simplest one and probably the most widely used method. In this approach the master code converges first (1) and sends its feedback parameters to the slave code (2), afterwards the slave code converges (3) and it sends data back to the master (4). At every time step the process is repeated, until the last TH time step is reached. This approach is used in TRACE/PARCS system, where TRACE is the master code and PARCS the slave. Both codes use the same time step calculated by the TRACE. The Figure 2-5 illustrates the temporal coupling approach in TRACE/PARCS.

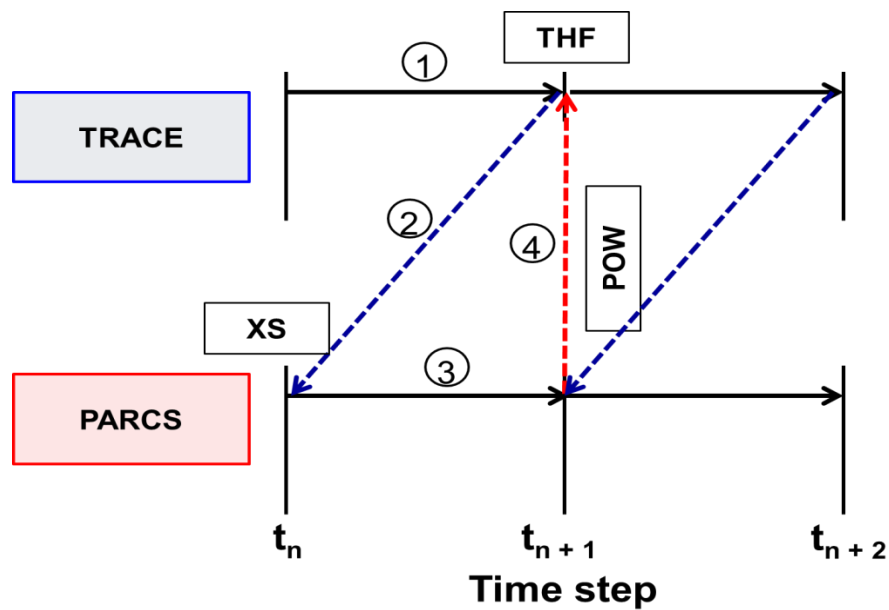


Figure 2-5 Explicit temporal coupling approach in TRACE/PARCS system; both codes use the same time step calculated by TRACE (master).

The semi-implicit method uses feedback parameters considering the previous and the actual time step. This type of scheme is implemented into TRAC-PF1/NEM. In this case, the fluxes and powers at the current time-step are calculated combining the values of the thermal-hydraulic condition and the fuel rod temperatures calculated from the current and previous time-step. The disadvantage of the explicit and semi-implicit methods is that both codes converge individually during the time step. Thus small time steps are required to maintain the accuracy of exchanged parameters.

In implicit time integration scheme not only the individual codes have to match convergence criteria but also the feedback parameters. An implementation based on this approach for TRACE/PARCS was proposed by Watson (Watson, 2010).

2.3 Cross section generation for Thermal-hydraulic / Neutronics coupled calculation

In the coupled N/TH codes, the feedback between the neutronics and thermal-hydraulics is taken into account via the nodal homogenized cross sections which are generated in advance in dependence of feedback TH parameters in so called branch calculations using lattice physics codes. In detail, the nodal cross sections are determined based on the fuel types, neutron energies, operating conditions and depletion history parameters, etc. In the current BWR analysis, the generation of nodal cross sections starts from the extraction of the cross section

information from a Data Library using the processing tool (e.g. NJOY). Then the lattice code performs the homogenization by an energy collapsing. Finally, the generated cross section sets are supplied to the core simulator. This process can be splitted into two main stages (see Figure 2-6): **a)** the generation of effective cross sections at cell level varying with the temperature and density (TH values) of the materials using lattice physics codes, and **b)** the use of the generated nodal two-group cross sections by the core simulator in order to solve the diffusion equation after their update according to the actual TH conditions within the core. A description of the stage **a)** is presented in the following section and the stage **b)** will be discussed in the subsequent sections.

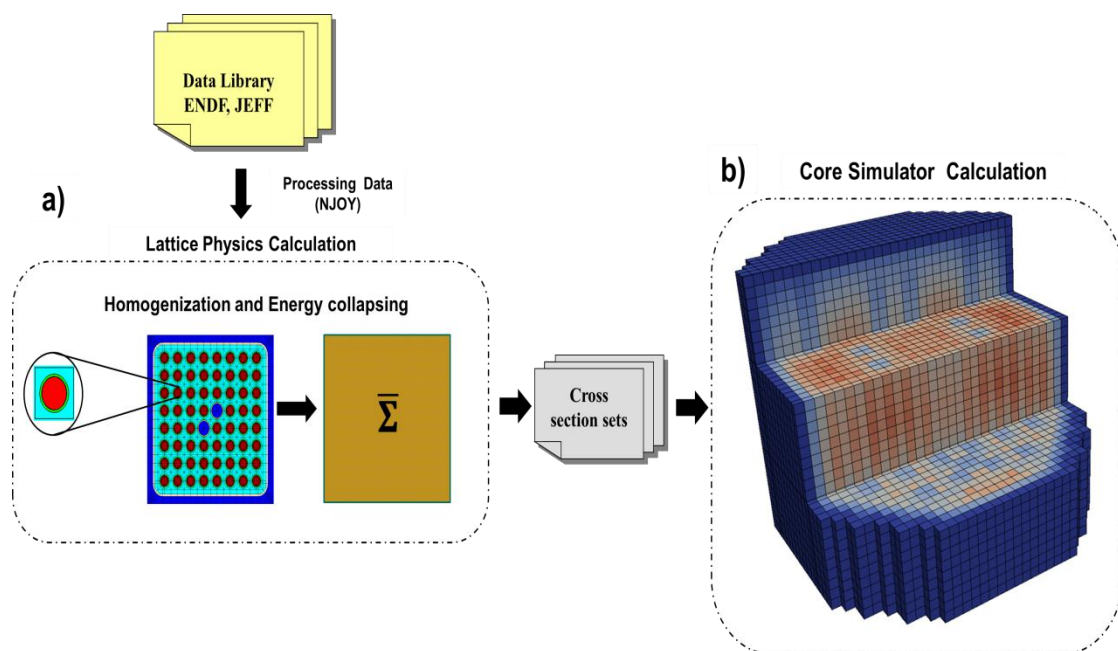


Figure 2-6 Global computational scheme for a deterministic reactor physics calculation.

Use of Lattice Codes for Generation of Cross Sections

In the first step of this stage **a)**, the evaluated nuclear data library e.g. ENDF/B (Chadwick, et al., 2011) or JEFF (Santamarina, et al., 2009) containing continuous energy nuclear cross-section data is converted into a multi-group cross section library by a nuclear data processing code, for instance NJOY (MacFarlane, et al., 2012). It is important to mention that, all the cross sections are available as a function of the energy of the incoming neutron, as well as a function of the temperature of the target.

In the second step of stage **a)**, a heterogeneous 2D multi-group transport calculation of each fuel assembly (homogenized) type is done. For this purpose, information about the material composition e.g. fuel type and enrichment of U-235 or Pu fissile, cladding material, moderator, exposure as well as geometrical data of the fuel assembly and the pins, guide tubes is needed. In

addition, the temperature and density of the materials (fuel, cladding) is also required. Finally, radial boundary conditions must be defined. When doing such simulations, the lattice physics codes use the nuclear data contained in a master multi-group library generated in advance by e.g. NJOY to get the energy-dependent microscopic cross sections. During the homogenization process the reaction rates in the single cell geometry are preserved. However, when the cell is put in the real reactor core it has a different environment than during the homogenization process. Therefore, the homogenized flux solution will be not continuous at the cell boundary. In order to correct these deficiencies the so-called assembly discontinuity factors (ADF) were proposed by (Smith, 1986). The ADF (f) is the ratio of the heterogeneous (ϕ_{het}) to homogeneous (ϕ_{hom}) flux at the boundary of the assembly.

$$f = \frac{\phi_{het}}{\phi_{hom}}. \quad (2-1)$$

After the corrections are done in step two, the multi-group structure of the cross sections is finally collapsed a few-group structure (usually two groups for LWR, thermal spectrum for energies $< 1\text{eV}$ and fast spectrum $> 1\text{eV}$).

In order to cover the whole TH conditions of the reactor core, two types of calculations are performed: 1) branch calculations using several combinations of material properties (temperatures and densities) and 2) depletion calculation for the effect of the exposure during the cycle. The depletion calculations consider that the state parameters, e.g. void fraction, fuel and moderator temperature, control rod position, and their history values, are constant during at each exposure step. The importance of considering the history effects was addressed by (Watson, et al., 2002) (Hartmann, 2016). The cross section obtained can be arranged in look-up tables in order to be used in a 3D core simulator.

The process described above is followed by the current conventional deterministic codes such as HELIOS-2, CASMO-4, NEWT or POLARIS. However, the application of continuous-energy Monte Carlo technics has become more interesting in the nuclear community (Fridman, et al., 2011), (Yoshioka, et al., 2011). Furthermore, methodologies for generating cross sections based on both deterministic and Monte Carlo code have been developed SIMTAB (Roselló, 2004), CreateXSlib (Daeubler, 2015).

2.4 Neutronics core characterization

The neutron multiplication factor and the reactivity are important parameters characterizing the core reactor state. For any infinite nuclear reactor the neutron multiplication factor is defined as (Duderstadt, et al., 1976) :

$$k_{inf} = \frac{\text{neutron generation}}{\text{neutron consumption}} \quad (2-2)$$

In a real finite reactor core the leakage of neutrons is taken into account with the non-leakage probability P_{NL} to obtain the effective multiplication factor:

$$k_{eff} = k_{inf} P_{NL} \quad (2-3)$$

The reactor state is referred as subcritical, critical and supercritical if k_{eff} is smaller, equal or larger than one, respectively. Other way to characterize the reactor state is by the reactivity, which is defined as:

$$\rho = \frac{k_{eff} - 1}{k_{eff}} \quad (2-4)$$

The reactivity is commonly in units of pcm (1 pcm = 10^{-5}) or relative to the delay neutron fraction β_{eff} in units of dollar (\$). Reactivity smaller, equal or larger than zero indicates a subcritical, critical or supercritical, respectively.

Reactivity coefficients

The reactivity coefficients are used to describe the change in core reactivity due to changes of thermal-hydraulic parameters or material composition. Important coefficients for BWR cores are fuel temperature, coolant void and control rod.

The fuel temperature reactivity coefficient (also called Doppler reactivity coefficient) determines the reactivity change caused by the variation of the fuel temperature in the reactor core. The increasing of the fuel temperature leads to stronger absorption of thermal neutrons in the resonances of the fertile material in the fuel (Doppler effect). This coefficient is sensitive on fuel composition and changes due to fuel depletion.

The coolant void coefficient reactivity is of prime importance for BWR since any change in the void fraction in the reactor core impacts the neutron moderation due to the change in the coolant

density. The presence of voids causes a hardening of neutron spectrum in the reactor core resulting in higher resonance absorption.

The control rod coefficient reactivity determines the reactivity change due to the movement of control rods in the reactor core. The insertion or withdrawing of control rods into the core affects directly the power due to changes in the material composition. This coefficient is also referred as external reactivity.

2.5 Recent trends in coupling simulations

Aside from the multiphysics coupling at nodal level, in the recent years several developments based on refined spatial resolution have been done. This new tendency is also known as high fidelity simulations, which include not only multiphysics but also multiscale coupling approaches. The objective of them is to describe the phenomena at pin and subchannel level. It allows the prediction of local safety parameters such as: fuel rod enthalpy, departure from nucleate boiling ratio (DNBR) in PWR, onset of transitional boiling (OTB) in BWR, burn-out, maximum fuel rod cladding temperature, fuel rod centre-line temperature, etc. Example for those coupled code systems (based on diffusion and pin power reconstruction) are e.g. TRAC-BF1/NEM/COBRA-TF (Solis, et al., 2002), RELAP5/PANBOX (Jackson, et al., 1999), CATHARE/CRONOS/FLICA4 (Mignot, et al., 2004) and PARCS/SUBCHANFLOW (Basualdo, et al., 2017). In addition, other coupled codes such as COBAYA3/COBRA-TF (Jimenez, et al., 2010), COBAYA3/SUBCHANFLOW (Calleja, et al., 2014) are able to simulate whole cores at pin and subchannel level using a multi-group diffusion approximation. Furthermore, the codes such as DYN3D/SUBCHANFLOW (DYNSUB) (Gomez-Torres, et al., 2012a) (Daeubler, et al., 2015), DeCART (Joo, et al., 2004), MPACT/CTF/ORIGEN (Godfrey, et al., 2017) simulate LWR cores at pin/subchannel level using simplified SP3 or MOC neutron transport solvers.

Finally, Monte Carlo codes are being coupled with subchannel codes for the pin/subchannel-level solutions of fuel assemblies, FA-clusters as it is the case for the coupled codes MCNP/CTF (Sanchez, et al., 2009), MCNP/CTF/NEM/NJOY (Puente-Espel, et al., 2010), OpenMC/COBRA (Mylonakis, et al., 2014), and for full cores such as MCNP-SUBCHANFLOW (Ivanov, et al., 2013) and Serpent-SUBCHANFLOW (Daeubler, et al., 2014).

Other trends are focused on the coupling of neutronics, thermal-hydraulic and fuel thermo-mechanics for a better description of the core behaviour at any time window during a cycle. Coupled codes that can be mentioned in this category are TORT-TD/CTF/FRAPTRAN (Magedanz, et al., 2015), DYN3D-TRANSURANUS (Holt, et al., 2015), HEXTRAN-FINIX

(Ikonen, et al., 2016), PARCS-SUBCHANFLOW- TRANSURANUS (Basualdo, et al., 2017), etc.

Last but not least, several interesting and ambitious projects in the field of reactor multiphysics simulations have been launched around the world with the aim of developing powerful simulation platforms for core and safety analysis. One is the European NURESIM platform developed during the EU projects NURESIM, NURISP and NURESAFE (Chanaron, et al., 2015). Another one is the Virtual Environment for Reactor Applications (*VERA*) of the Consortium for the Advanced Simulation of Light Water Reactors (*CASL*) that comprises a suite of tools for scalable simulation of nuclear reactor core behaviour (Turinsky, 2013). The Mexican simulation platform named AZTLAN is being developed by a consortium of research centres and universities (Gomez Torres, et al., 2015).

3 Principles of Thermal-Hydraulics/Neutron Kinetics Core Calculations

3.1 The Best-Estimate Thermal-Hydraulic Code System TRACE

The reactor system analysis code TRACE (TRAC/RELAP5 Advanced Computational Engine) is been developed by the United States Nuclear Regulatory Commission (U.S. NRC). TRACE combines the capabilities of four major system codes (TRAC-P, TRAC-B, RELAP5 and RAMONA). It is designed to perform best-estimate computations for loss-of-coolant accidents (LOCAs), operational transients, and other accident scenarios in LWR. It can also model phenomena occurring in experimental facilities designed to simulate transients in reactor systems. Models applied in the code include multidimensional two-phase flow, non-equilibrium thermo-dynamics, generalized heat transfer, reflood, level tracking, and reactor kinetics. The code also provides automatic steady-state and dump/restart capabilities.

TRACE is the current thermal-hydraulic reference code of the U.S. NRC for safety investigations of LWR, but some other types are been investigated. In the frame of an international project - Code Application and Maintenance Program (CAMP) - codes of the U.S. NRC (e.g., TRACE, RELAP5, PARCS, etc.) are distributed to the CAMP-members for validation and application purposes.

TRACE code has many components e.g. VESSEL, PIPE, CHAN, HEATSTR, POWER, VALVE, PUMP, JETPUMP, FILL, BREAK, SIGNALS, TRIPS and CONTROL Systems, etc. that allow to represent the complete systems and components of a nuclear power plant including operator actions such as the opening of a valve, the shutdown of a pump.

3.1.1 Thermal-hydraulic 2 Phase Conservation Equations

The derivation of the set of equations of TRACE starts with single phase Navier-Stokes equations in each phase, and jump conditions between the phases. Time averaging is applied to this combination of equations, to obtain a useful set of two-fluid, two-phase conservation equations. TRACE uses this flow model in both one and three dimensions (TRACE, 2013).

The six partial differential equations for mass, energy and momentum conservation in the TRACE code are presented in the equations (3-1) to (3-6). In these equations the subscripts “*g*” and “*l*” distinguish between gas specific and liquid specific terms. On the other hand, α represents the fraction of vapour in the two-phase flow mixture and Γ , E_i and \vec{M}_i represent the

total contributions of time averaged interface jump conditions to transfer of mass, energy and momentum respectively. Furthermore, q' is the conductive heat flux, q_d is the direct heating.

The equations for the mass conservation are expressed by:

$$\frac{\partial}{\partial t} [(1 - \alpha) \cdot \rho_l] + \nabla [(1 - \alpha) \cdot \rho_l \cdot \vec{v}_l] = -\Gamma, \quad (3-1)$$

$$\frac{\partial}{\partial t} [\alpha \cdot \rho_g] + \nabla [\alpha \cdot \rho_g \cdot \vec{v}_g] = \Gamma. \quad (3-2)$$

The conservation of energy is based on a formulation with the internal energy:

$$\begin{aligned} \frac{\partial}{\partial t} \left[(1 - \alpha) \cdot \rho_l \cdot \left(e_l + \frac{v_l^2}{2} \right) \right] + \nabla \cdot \left[(1 - \alpha) \cdot \rho_l \cdot \left(e_l + \frac{v_l^2}{2} \right) \vec{v}_l \right] = \\ -\nabla \cdot \left[(1 - \alpha) \vec{q}'_l \right] + \nabla \cdot \left[(1 - \alpha) (T_l \cdot \vec{v}_l) \right] + (1 - \alpha) \rho_l \vec{g} \cdot \vec{v}_l - E_i + q_{dl}; \end{aligned} \quad (3-3)$$

$$\begin{aligned} \frac{\partial}{\partial t} \left[\alpha \cdot \rho_g \cdot \left(e_g + \frac{v_g^2}{2} \right) \right] + \nabla \cdot \left[\alpha \rho_g \cdot \left(e_g + \frac{v_g^2}{2} \right) \vec{v}_g \right] = \\ -\nabla \cdot \left[\alpha \vec{q}'_g \right] + \nabla \cdot \left[\alpha (T_l \cdot \vec{v}_g) \right] + \alpha \rho_g \vec{g} \cdot \vec{v}_g - E_i + q_{dg}. \end{aligned} \quad (3-4)$$

The conservation of momentum for the two phases is expressed by:

$$\frac{\partial}{\partial t} [(1 - \alpha) \rho_l \vec{v}_l] + \nabla \cdot [(1 - \alpha) \rho_l \vec{v}_l \vec{v}_l] = \nabla \cdot [(1 - \alpha) T_l] + (1 - \alpha) \rho_l \vec{g} - \vec{M}_i; \quad (3-5)$$

$$\frac{\partial}{\partial t} [\alpha \rho_g \vec{v}_g] + \nabla \cdot [\alpha \rho_g \vec{v}_g \vec{v}_g] = \nabla \cdot [\alpha T_g] + \alpha \rho_g \vec{g} - \vec{M}_i. \quad (3-6)$$

TRACE does not solve the field equations in the form presented above. To cut complexity and computer time of the numerical solution, the fully conservative forms of the energy and momentum equations are rearranged to provide internal energy and motion equations. The steps to the next form of the field equations are rigorous mathematically, and involve no formal approximations. However, in finite volume form, the internal energy equations have problems with large spatial and temporal pressure changes between two cells that are not present if the fully conservative forms of the energy equations are implemented directly into a finite volume approach.

In order to mathematically close the set of conservation equations, a lot of empirical correlations –called constitutive equations or closure laws- are needed which describe e.g. the wall/fluid and interface mass and heat transfer, the wall and interface friction, etc.

3.1.2 Heat transfer at the interface and at the wall

The liquid and gas field momentum equations include terms for the interfacial shear force and the wall drag force. In order to determine these forces it is necessary to know the flow regime. In the following sections a brief description of the flow regimes available in TRACE for both at the interface and at the wall are presented.

Interfacial drag

The “six-equation” two fluid model used in TRACE provides two characteristic velocities in each coordinate direction. In a 1D component, for example, there are two velocities at every junction (connection). One velocity corresponds to the liquid phase and another to the combined gas/vapour mixture. The equations of motion for these two velocities are coupled by two interfacial terms: one resulting from the interfacial drag force between the phases and the other from the momentum transfer associated with mass transfer.

In TRACE, there are three distinct classes of flow regimes for the interfacial drag:

- Pre- Critical Heat Flux (CHF): Including bubbly/slug and the annular/mist regimes.
- Stratified: the horizontal stratified flow regime is available for 1-D components that are either horizontal or inclined.
- Post-CHF: this encompasses the "inverted" flow regimes that occur when the wall is too hot for liquid-wall contact.

The Figure 3-1 depicts four flow regimes for the Pre-CHF class available in TRACE. It is worth to remark that the bubbly/slug flow regimes include the dispersed bubble, slug flow and Taylor cap bubble regimes. In fact, BWR fuels operate in the Pre-CHF regimes. The models and correlations used for the interfacial drag in the bubbly/slug and annular/mist flow regimes are applied to both vertical and horizontal geometries. But, for the horizontal case, a special horizontal stratification model is applied.

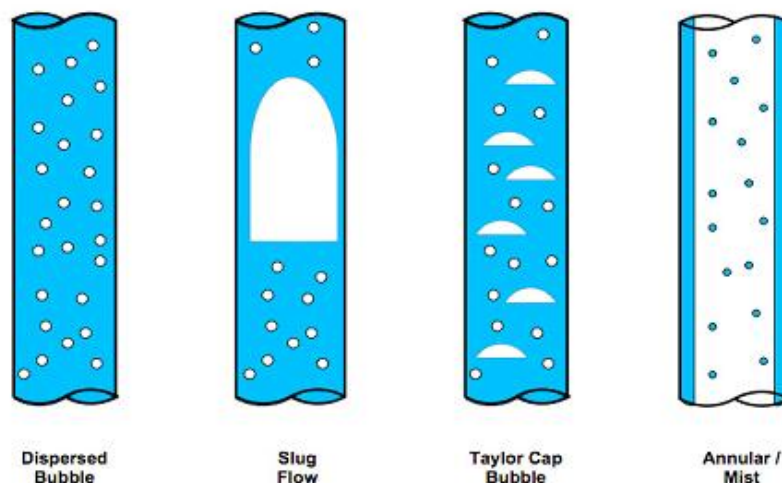


Figure 3-1 Different vertical flow regimes available in TRACE for the Pre-CHF at the interface taken from (TRACE, 2013).

In the Stratified class, for the horizontal and inclined pipes, there is the possibility for the flow to become stratified at low velocity conditions as gravity causes the phases to separate. Finally for the Post-CHF, when the temperature of a surface is above the minimum stable film boiling temperature, the liquid phase cannot contact the hot surface. This gives rise to a family of "inverted" flow regimes with the gas phase in contact with the wall. Three principal inverted flow regimes are modelled in TRACE for post-CHF conditions: inverted annular, inverted slug, and dispersed flow. A detailed description of stratified and post-CHF classes can be found in (TRACE, 2013).

Wall drag

Two types of frictional pressure losses are modelled in TRACE:

- Wall Drag: models the fluid-wall shear using a friction factor approach, and;
- Form Drag: models geometry specific pressure losses through user specification of additive loss coefficients for irreversible form losses due to abrupt or semi-abrupt flow area expansions and contractions, thin-plate-orifice-type flow restrictions, and flow redirection (turning) at an elbow or tee.

3.1.3 Heat conduction model in solids

The TRACE heat conduction model is used to simulate the heat transfer between reactor structure (such as fuel, piping, wall, vessel walls, internal vessel) and the fluid in the reactor.

The heat conduction process in a solid material with a generic geometry can be described by means of the equation (3-7) in a simplified manner:

$$\rho C_p \frac{\partial T}{\partial t} = \nabla \cdot (k \nabla T) + q''' \quad (3-7)$$

where, ρ is the density, C_p the specific heat capacity, T the temperature, k the thermal conductivity and q''' the heat generation rate per unit of volume.

The thermal conditions of the reactor structures are obtained from a solution of the heat conduction equation applied to different geometries. These geometries include cylindrical walls, slabs and core fuel rods. In fact, there are two heat conduction models in TRACE. The first one deals with cylindrical walls. The second type describes the heat transfer within structural components (slabs or fuel rods) as e.g. in the vessel.

3.2 The reactor dynamic code PARCS

PARCS is a three-dimensional reactor core simulator that solves the steady-state and time dependent neutron diffusion or SP3 transport equations to predict the dynamic response of the reactor to reactivity perturbations such as control rod movements, boron concentration or changes in the temperature/fluid conditions in the reactor core. There are many solvers implemented in PARCS for the spatial discretization of the equations mainly considering nodal or cell level. In case of square geometries, the following solvers can be used: the Analytical Nodal Method (ANM), the multi-group Nodal Expansion Method (NEMMG), the Coarse Mesh Finite Difference (CMFD) and the Fine Mesh Finite Difference (FMFD) (Downar, et al., 2012).

The major calculation features in PARCS are the abilities to perform eigenvalue calculations, transient (kinetics) calculations, Xenon transient calculations, decay heat calculations, pin power calculations, depletion calculations. In fact, PARCS have been extended to include not only Light Water Reactors, but also the Pressurized Heavy Water and High Temperature Gas Reactors

PARCS is coupled directly to the thermal-hydraulics system code TRACE, which provides the temperature and flow field information to PARCS during steady state and transient calculations via the few-group cross sections. PARCS is also coupled to the systems code RELAP5 using the Parallel Virtual Machine (PVM) message passing interface. Furthermore, PARCS is available as a standalone code for performing calculations by means of the new thermal-hydraulic module PATHS, therefore it does not require necessarily a coupling to TRACE or RELAP5.

3.3 Thermal-hydraulic/Neutronics coupled system TRACE/PARCS

In order to improve the accuracy in TRACE simulations for some reactor transients or accidents scenarios the 3D power distribution has to be determined. Therefore, PARCS is integrated into TRACE forming the TRACE/PARCS system. Some of the main features of TRACE/PARCS version 5.890, which is used in this work, can be listed as follow:

- An internal integration scheme has been used in the TRACE/PARCS system, where the thermal-hydraulic conditions of the core and system are obtained by TRACE and the spatial kinetics solution by PARCS.
- A General Interface (GI) manages all the information transfer between both codes, a detailed description can be found in (Barber, et al., 1998). However, special attention must be paid to the new coupling strategy (the “Virtual Channel”) implemented in the recent versions of TRACE/PARCS (Hudson, et al., 2015).
- The GI communicates with the secondary interfaces of PARCS and TRACE, the so called, PARCS-Specific data map routine (PDMR) (Barber, 1998) and the TRACE-Specific data map subroutine (TDMR) see e.g. (Miller, et al., 2000).
- The TH data calculated by TRACE (i.e. moderator density and temperature, vapour density, void fraction, boron concentration, average fuel temperature, fuel centreline temperature and fuel surface temperature) is used by PARCS in order to incorporate the feedback effects into the cross sections.
- The spatial kinetics solution from PARCS (i.e. power distribution) is used by TRACE for solving the heat conduction in the core structure components.
- A one-to-one time step selection is implemented in TRACE/PARCS system, where the time step selection is done based on the convergence criteria of TRACE (master code). PARCS (the slave code) uses the same time step as TRACE.
- Regarding the time coupling approach, an explicit approach is used in the TRACE/PARCS system.

3.3.1 The General Interface

The General Interface was designed for managing the transfer of information between TH and NK codes. It is a set of FORTRAN 90 subroutines divided in 3 independent modules, also a module for error checking is included. In the first release of the GI, the PVM package was used to control all communication operations, but in more recent versions this package was removed, because the GI was fully merged into PARCS source code as a separated module. The transfer of information (buffers and vectors) is done through the shared memory (Ward, et al., 2013).

The first unit of the GI is in charge of the initialization process. Here, the mapping between the TH and NK domains and all the geometry information is transfer to the GI and stored for use in the two subsequent variable mapping units. The second unit transfers the TH data to the NK code. Finally, the third unit manages the transfer of the power distribution determined by the NK code back to the TH code. It is worth to mention, that the error checking unit is called for each unit for checking the correct transfer of information and detecting possible failures in the coupled code. During the three stages, the GI communicates with the respective unit of the TH and NK code.

3.3.2 The PARCS-Specific Data Map Routine

The main function of the PARCS-Specific Data Map Routine is to act as secondary interface between the GI and PARCS. In order to be consistent with the design requirements of the GI and TRACE, the PDMR is divided in 3 units. The first unit reads not only the mapping information provided by the user in the *maptab* file, but also the geometry from PARCS input deck. Then this information is sent to the GI. The second unit transfers the TRACE TH data stored in the GI to PARCS. Finally, the third unit transfers the PARCS power distribution to the GI. Like in the GI, a module dealing with the correct transfer of information in the coupled code is included.

3.3.3 The TRACE-Specific Data Map Routine

The TRACE-Specific Data Map Routine acts as secondary interface between the GI and TRACE. For consistency with the design requirements of the GI, the TDRM is divided in 3 units. The first unit (initialization) transfers the mapping information to the GI. The second unit transfers the TRACE data to the GI. Finally, the third unit transfers the PARCS power distribution stored in the GI to TRACE. Like in the GI and PDMR, a module dealing with the correct transfer of information in the coupled code is included.

The Figure 3-2 depicts a schematic diagram of the communication between TRACE and PARCS through the GI. It can be seen that TRACE sends the thermal-hydraulic feedback parameters e.g. average fuel temperature (\bar{T}_f), fuel centreline temperature (T_f^{cl}), fuel surface temperature (T_f^{sf}), moderator temperature (T_m) and density (ρ_m) and boron concentration (B) to the general interface and the GI passes them over to PARCS. Then PARCS updates the nodal cross sections based on these thermal-hydraulic conditions of the core and solves the neutron diffusion equation. The so predicted 3D nodal power distribution is then sent to the GI and from there it is transferred to TRACE.

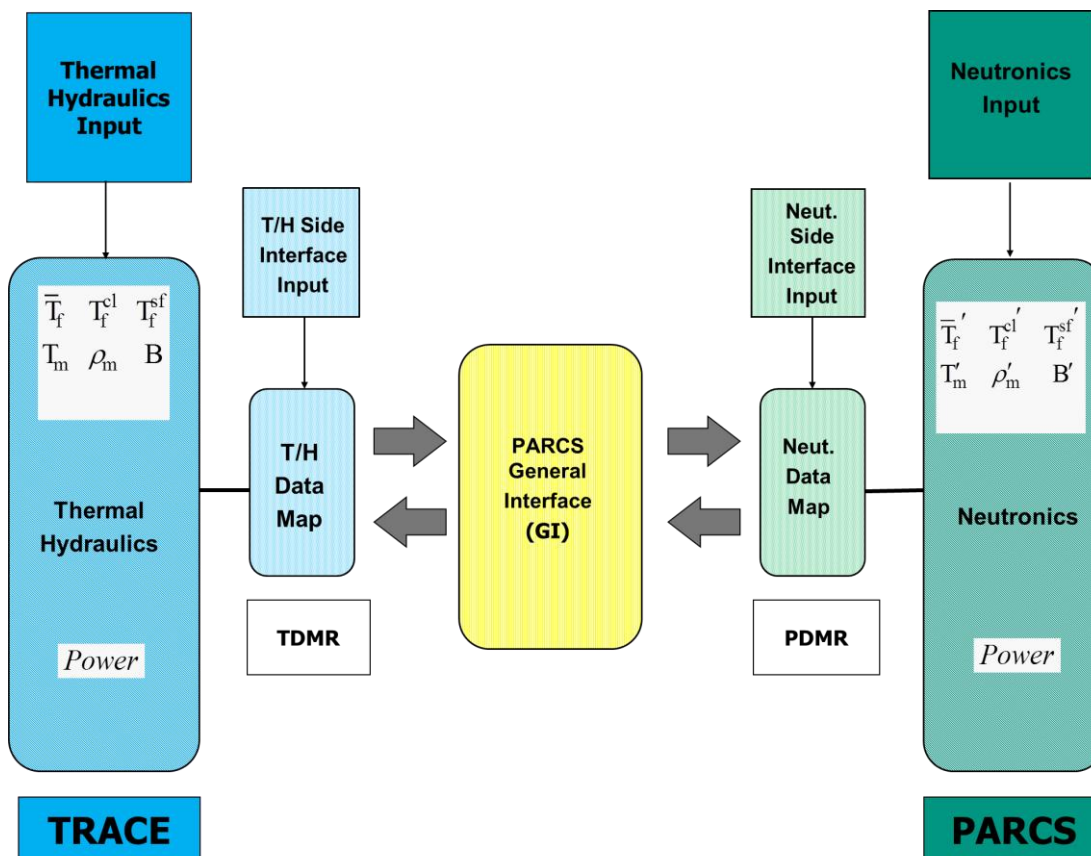


Figure 3-2 Schematic diagram of the data exchange between TRACE and PARCS via the General Interface (Barber, et al., 1998).

3.4 The multi-group reactor dynamic code DYN3D-MG

DYN3D is a **DY**Namical **3-D**imensional best-estimate tool for simulating steady state and transient conditions of LWRs developed at the Helmholtz Zentrum Dresden-Rossendorf (HZDR) since 20 years. The neutron kinetic module comprises the solution of three dimensional two-group or multi-group neutron diffusion equations or simplified transport equations by means of nodal expansion methods depending of the geometry of the fuel assemblies.

The two-group version was originally developed for the analysis of reactivity-initiated transients and accidents of Russian VVER-type reactors. This version has been widely validated not only for VVER but also for Western PWR reactor cores by means of several benchmark problems, a complete description of DYN3D applications can be found in (Rohde, et al., 2016). Additionally, it has been coupled with: thermal-hydraulic system codes, such as ATHLET (Kozmenkov, et al., 2015), RELAP (Kozmenkov, et al., 2007); CFD codes, ANSYS-CFX (Grahn, et al., 2015); and fuel performance codes, TRANSURANUS (Holt, et al., 2015).

DYN3D-MG is the code version of DYN3D developed based on the two-group diffusion code DYN3D to perform both diffusion- and SP3-based core simulations at pin or fuel assembly level. In this doctoral thesis, the version DYN3DMG-V2.0, called hereafter DYN3D, is used. This version has been validated for western PWR and its SP3 solver has been coupled with the sub-channel code SUBCHANFLOW (Imke, et al., 2012), developed at the Institute for Neutron Physics and Reactor Technology (INR) of the Karlsruhe Institute of Technology (KIT), in order to develop the best-estimate coupled code DYNSUB (Gomez-Torres, et al., 2012a) (Gomez-Torres, et al., 2012b). Almost no validation of the DYN3DMG-V2.0 nodal diffusion solver is available for BWRs, which formulates one goal of this dissertation. Afterwards, in this work, DYN3D is referred to the DYN3D multi-group version.

The Multi-group Diffusion Solver of DYN3D

The multi-group diffusion equation solved in DYN3D can be expressed by:

$$\begin{aligned}
 \underbrace{\frac{1}{v_g} \frac{\partial}{\partial t} \phi_g(\vec{r}, t)}_{\text{change in time of neutron density}} &= \underbrace{\nabla \cdot D_g(\vec{r}, t) \nabla \phi_g(\vec{r}, t)}_{\text{leakage}} - \underbrace{\Sigma_{R,g}(\vec{r}, t) \phi_g(\vec{r}, t)}_{\text{loss by absorption+scattering}} \\
 &+ \underbrace{\sum_{\substack{g'=1 \\ g' \neq g}}^G \Sigma_{s,g' \rightarrow g}(\vec{r}, t) \phi_{g'}(\vec{r}, t)}_{\text{scattering in group } g} \\
 &+ \underbrace{\frac{\chi_g}{k_{eff}}}_{\text{prompt neutron fission spectra in group } g \text{ over } k_{eff}} \underbrace{\sum_{g'=1}^G (1 - \beta_{g'}) v_{g'}(\vec{r}, t) \Sigma_{f,g'}(\vec{r}, t) \phi_{g'}(\vec{r}, t)}_{\text{total fission production}} \\
 &+ \underbrace{\sum_{i=1}^{I_p} \chi_{g,i} \lambda_i C_i(\vec{r}, t)}_{\text{total delay precursors}} \quad g = 1, \dots, G.
 \end{aligned} \tag{3-8}$$

$$\begin{aligned}
 \underbrace{\frac{\partial}{\partial t} C_i(\vec{r}, t)}_{\text{change in time of neutron precursors}} &= \frac{1}{k_{eff}} \underbrace{\sum_{g=1}^G \beta_{g,i} v_g(\vec{r}, t) \Sigma_{f,g}(\vec{r}, t) \phi_g(\vec{r}, t)}_{\text{precursor production due to fission}} \\
 &- \underbrace{\lambda_i C_i(\vec{r}, t)}_{\text{loss by decay}} \quad i = 1, \dots, I_p.
 \end{aligned} \tag{3-9}$$

The removal cross section $\Sigma_{R,g}(\vec{r}, t)$ is defined as:

$$\Sigma_{R,g}(\vec{r}, t) = \Sigma_{t,g}(\vec{r}, t) - \Sigma_{s,g \rightarrow g'}(\vec{r}, t), \quad (3-10)$$

where, the total cross section $\Sigma_{t,g}(\vec{r}, t)$ includes macroscopic absorption $\Sigma_{a,g}(\vec{r}, t)$ and scattering $\Sigma_{s,g}(\vec{r}, t)$. Similar to PARCS, the cross-sections sets used by DYN3D are dependent on the medium temperature. In the frame of a coupled N/TH simulation using DYN3D with any thermal-hydraulic solver, these cross sections needs to be updated if the thermal conditions of the medium change. Thereby, the feedback effects between thermal-hydraulic and neutronics codes are taken into account.

The equations (3-8) and (3-9) are solved in DYN3D by using nodal methods, where the quantities at interfaces between nodes are preserved. One of the most common techniques applied for Cartesian geometry is the transversal integrated nodal method, where the three-dimensional neutron balance equation is replaced by three one-dimensional equations along each of the directions. A detailed description can be found in (Beckert, et al., 2008).

The nodal power $P^n(t)$ produced in a node n at time t by fission is calculated in DYN3D (also PARCS) by means of the equation (3-11):

$$P^n(t) = \sum_{g=1}^m \varepsilon_g^n \Sigma_{f,g}^n(t) \phi_g^n(t), \quad (3-11)$$

where, ε_g^n is the energy release per fission ($\sim 200\text{MeV}$), $\Sigma_{f,g}^n$ is the fission cross section for the group g in node n at time t and $\phi_g^n(t)$ is the average neutron flux for the group g across the node n .

4 Thermal-hydraulic/Neutronics Coupled Code System TRADYN Development

TRADYN (**TRACE/DYN3D**) is the new coupled code system where the thermal-hydraulic system code TRACE is internally coupled to two reactor dynamic codes (PARCS and DYN3D) using a GI (Gonzalez-Vargas, et al., 2016) (Gonzalez-Vargas, et al., 2017). This new system is innovative, because DYN3D was integrated using compiler preprocessor directives. This has the advantage to preserve the original TRACE/PARCS system “untouch” and to facilitate the maintenance, modification and debugging. Hereafter, a description of the GI and the subroutines (DDMR) developed herein are presented. Then, the coupling approach developed for TRACE and DYN3D for steady state and transient simulations is described. Finally, the improvements on the physical models of the neutronics codes inside TRADYN are provided.

4.1 Internal coupling approach

The reactor dynamic code DYN3D has been coupled internally to TRACE. Now DYN3D is fully integrated in TRACE as an internal module. Therefore, a new GI is developed and Specific Data Map routines (DDMR) for DYN3D, which manage the transfer information to TRACE, are integrated.

The developed DYN3D general interface has the same structure as the PARCS GI. It is divided in 3 independent units performing the initialization, the transfer of TRACE TH data to DYN3D and the transfer of DYN3D power distribution to TRACE. Like in the PARCS GI, a module for error checking is included.

On the other hand, the DYN3D-Specific Data Map routines act as secondary interface between the GI and DYN3D. The DDMR is also consistent with the design requirements of the GI and TRACE. Then it is divided in 3 independent units.

The first unit (initialization) reads the geometry given in DYN3D input deck and sends it to the GI. During this stage the spatial coupling of TRACE and DYN3D is carried out. It is necessary that the user specifies the correspondence between the thermal-hydraulic volumes and the neutronics nodes. This is realized via a *maptab* file. In the TRACE/DYN3D coupling, the DDMR module reads the *maptab* file and automatically associates the neutronics nodes with the corresponding thermal-hydraulic nodes. It is worth to mention that both vessel and channel TRACE components can be mapped to the neutronics nodes. Examples for the mapping schemes used in TRADYN are presented in the validation section.

The second unit of the DDMR module transfers the TRACE TH data stored in the GI to DYN3D. Finally, the third unit transfers the DYN3D power distribution to the GI. Like in the GI, a module dealing with the correct transfer of information in the coupled code is included, see Figure 4-1.

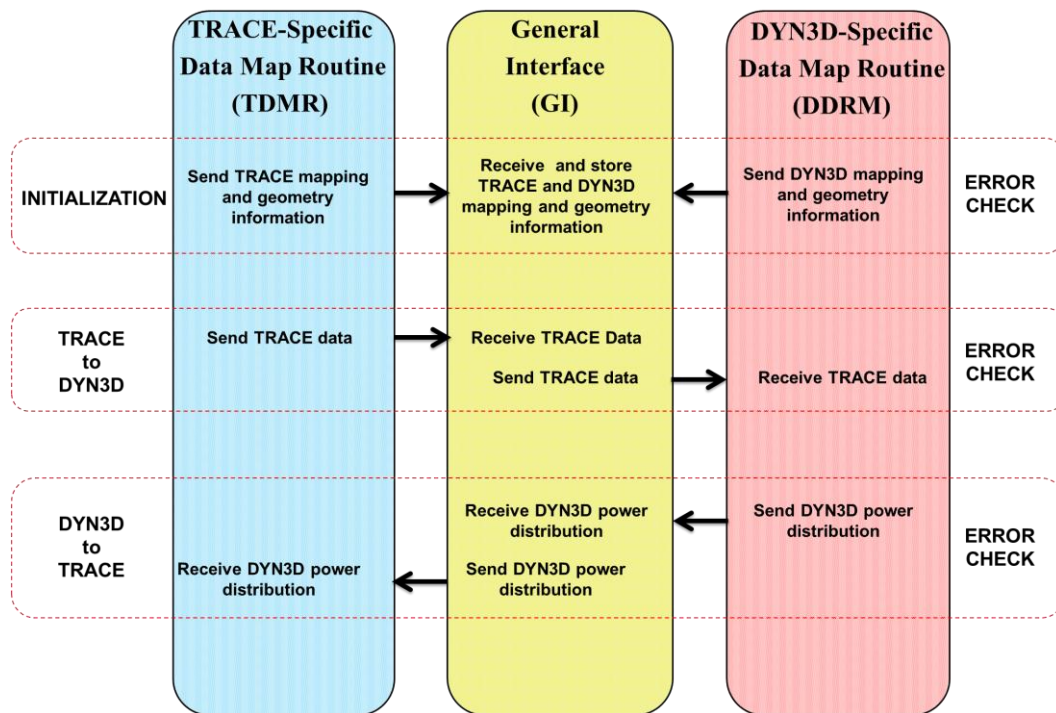
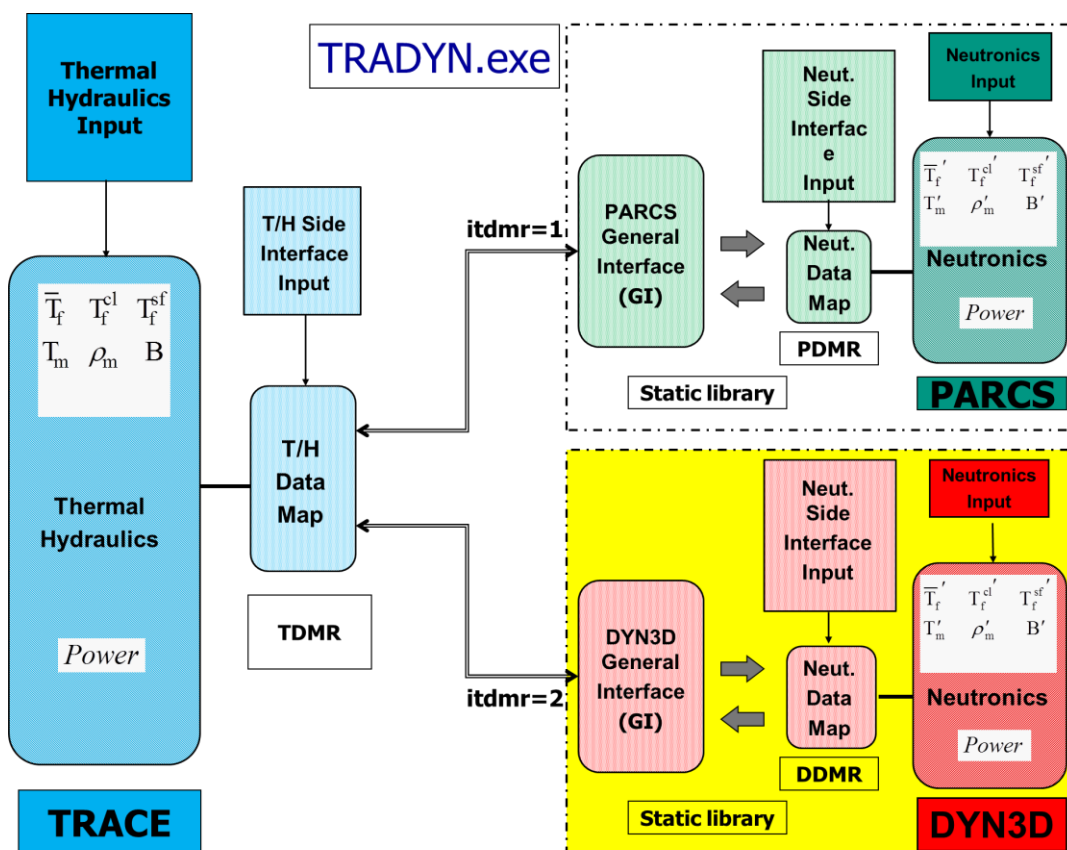


Figure 4-1 Flow of information between TRACE and DYN3D through the TDMR, GI and DDMR modules.

Additionally, TRACE source code modifications, especially related to the TDMR unit are required. Thereby, TRACE exchanges information with DYN3D in addition to PARCS. By this coupling approach, TRACE is the master and PARCS and DYN3D are slaves. In TRADYN, the code DYN3D and the developed GI and DMMR units are modules compiled as static libraries and linked to TRACE in order to generate a single executable. In Figure 4-2, a schematic diagram of the data exchange between TRACE and DYN3D (yellow highlighted) in addition of PARCS is depicted.



Adapted from D. Barber, 1998

Figure 4-2 Schematic diagram of the data exchange between TRACE and DYN3D, now the user can select between PARCS and DYN3D as neutronics solver, just by changing a single variable (*itdmr*) in the TRACE input.

In Figure 4-2, it can be seen that TRACE sends the thermal-hydraulic feedback parameters to the general interface and the GI passes them over to DYN3D. Then DYN3D updates the nodal cross sections based and solves the neutron diffusion equation. The so predicted 3D nodal power distribution is then sent to the GI and from there it is transferred to TRACE. On the other hand, the input deck of TRADYN consists of the DYN3D (or PARCS) and the TRACE stand-alone inputs. Additionally, few modifications of the TRACE input deck are needed. The coupling implemented allows the user the option to select either PARCS or DYN3D as a neutronics solver just by changing a single variable *itdmr* (1 for PARCS and 2 for DYN3D) in the TRACE input deck.

The implementation of a new GI in DYN3D source code required the creation of several new FORTRAN modules and subroutines. The Table A-1 and Table A-2 in the Appendix A contain a list with a short description of all new modules integrating the DYN3D general interface and the DDMR module respectively.

4.2 Steady State Coupling

In TRADYN steady state coupling approach, the main program TRACE reads the input decks and initializes the variables and arrays. If DYN3D is selected as neutronics solver, DYN3D starts reading the input decks, gets the thermal-hydraulic conditions from TRACE and updates the cross sections. Then DYN3D performs a “first steady state calculation” (a), in order to determine the nodal power distribution, which is passed to TRACE.

As next, an iterative loop between TH and NK is started, where TRACE first calls the subroutine trans.f90. At each time-advancement, DYN3D is called in steady state mode to perform following task: 1) read TH conditions and update cross sections, 2) calculate steady state eigenvalue, 3) predict nodal power distribution and 4) send nodal power to TRACE. Once TRACE convergence criteria are met, TRACE calls DYN3D for finishing the coupled simulation. The flow diagram for the steady state coupled calculation is shown in Figure 4-3.

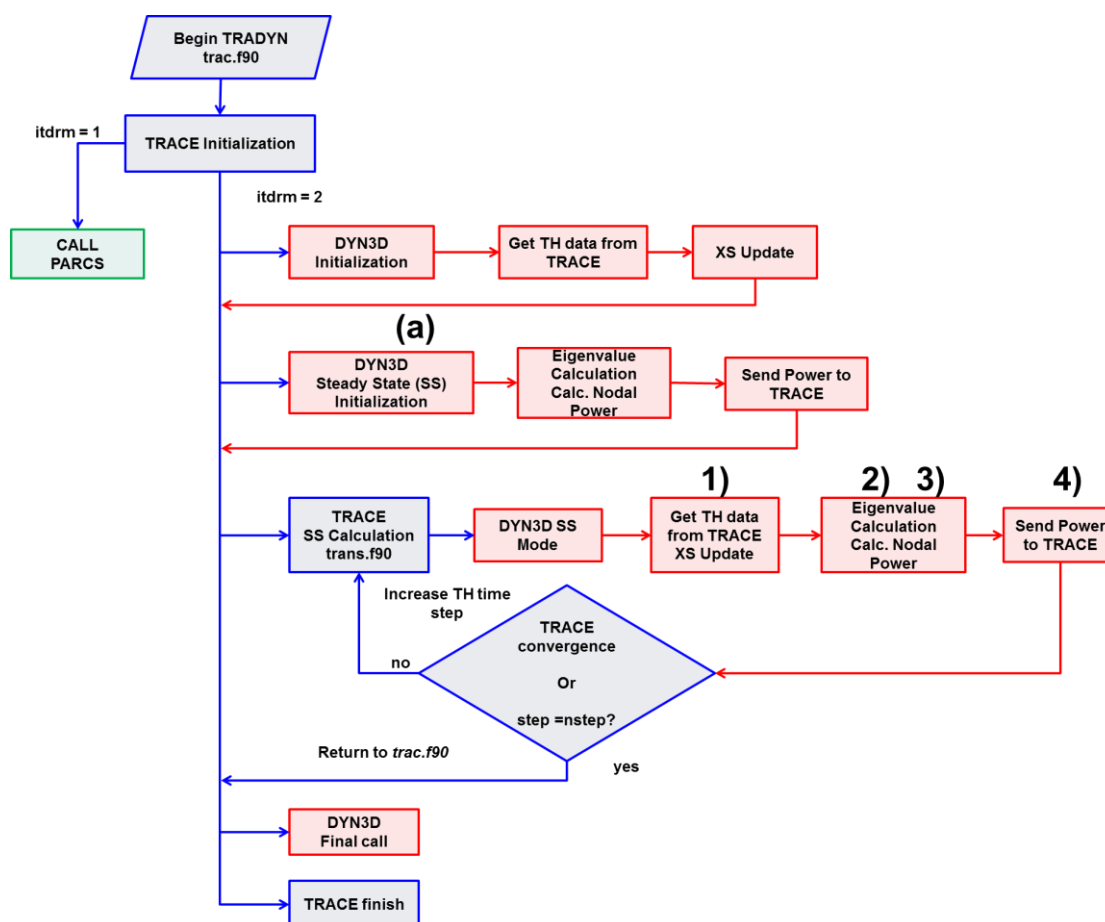


Figure 4-3 Flow diagram for the steady state calculation in TRADYN, when DYN3D is selected as neutronics solver.

4.3 Transient Coupling

In the transient coupling approach of TRADYN, the same flow chart that in the steady state coupling is followed. But the main difference is in the TRACE TH-NK iterative loop. There DYN3D is called in transient mode performing the subsequent tasks: 1) read the TH feedback parameters 2) fission source iteration 3) 3D nodal power prediction and 4) send 3D power to TRACE. Once this iteration process is completed i.e. if the problem time is reached (the nstep value is reached), TRACE calls DYN3D for finishing the coupled simulation. The flow diagram for the coupled transient calculation is shown in Figure 4-4.

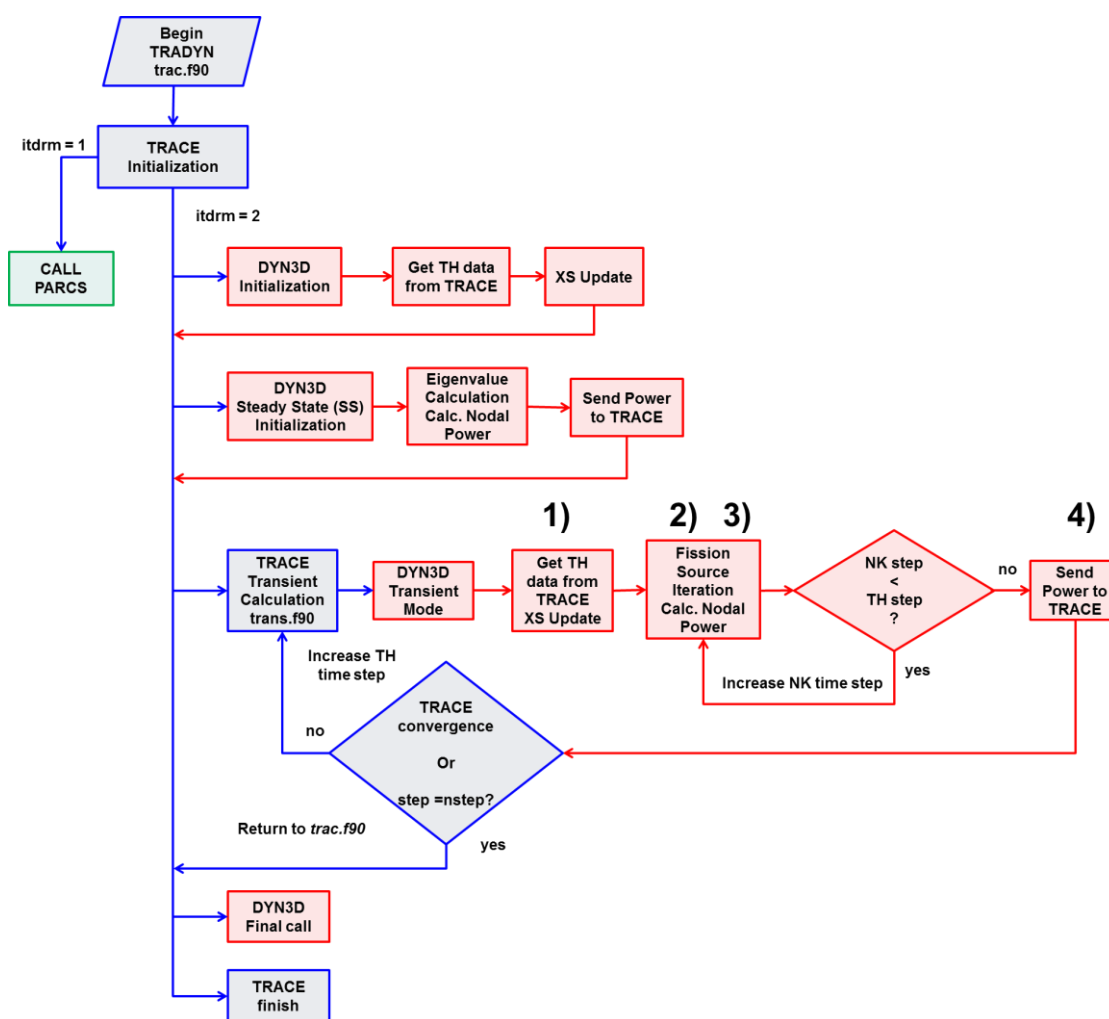


Figure 4-4 Flow diagram for the transient calculation in TRADYN, when DYN3D is selected as neutronics solver.

Temporal coupling

The temporal coupling and the time step selection play an important role in the TH/N coupling. One approach is to use a straightforward strategy, i.e. one-to-one time step selection, where the time step determined by the thermal-hydraulic code (master) is also used by the neutron kinetic code (slave). By this approach, the time step selection is done based on the convergence of the local parameters of the master code. This approach is already implemented in TRACE/PARCS system. Hence, the same approach has been implemented for TRACE and DYN3D coupling. Now the master code TRACE has PARCS or DYN3D as slave codes.

It is worth to note that DYN3D has a variable time step control algorithm, which allows the selection of several NK time steps inside one TH-time step. It makes DYN3D suitable for transients characterized by fast neutron flux gradients. In the case of DYN3D stand-alone calculation, the neutronics solver of DYN3D acts as master and the internal thermal-hydraulic module (FLOCAL) as slave. Because in TRADYN, the logic is arrayed vice versa this required some code structure changes to account for it. While in TRACE/PARCS the time step selection is one-to-one, TRACE/DYN3D has the advantage to select a one-to-one time step or several NK time steps for one TH time step. There are also limitations: first a TH-step can only be subdivided in an integer number of NK steps and the second, NK time steps must be smaller or equal to TH time steps.

Furthermore, the time at which data between the NK and TH domains is exchanged, is very important in coupled simulations. In TRADYN, the explicit operator splitting coupling approach is already implemented in TRACE/PARCS and the same approach was used for TRACE/DYN3D coupling. In this approach the master code TRACE converges first (1) and sends its feedback parameters (THF) to the slave code (PARCS or DYN3D) (2), after the slave code converges (3), it sends data back to TRACE (4). At every time step the process is repeated, until the last TH time step is reached, see Figure 4-5. Also, it can be seen the subdivision of the NK time step within one TH time step as explained above.

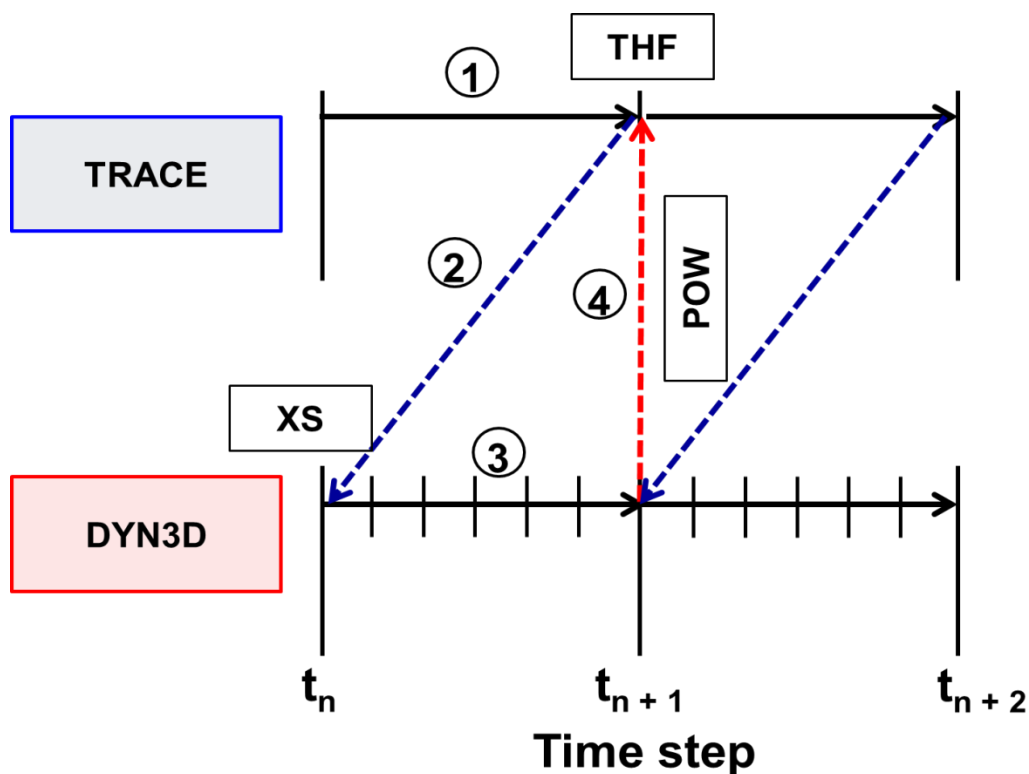


Figure 4-5 Explicit coupling scheme between TRACE and DYN3D. It can be noticed the subdivision of the DYN3D time step within one time step of TRACE.

4.4 Improved physics of TRADYN for BWR simulations

After a deep review of the BWR capabilities of multi-group version of DYN3D implemented in TRADYN, missing models for the simulation of BWR cores were identified, e.g. for:

- The gamma heating.
- The correction of coolant density along the core taking into account the higher density of the bypass flow as an important feedback parameter to be considered during the cross section update.
- The ADF models to take into account all possible orientations of the fuel assembly.

Since DYN3D is using nodal cross sections in the NEMTAB format, it has been necessary to implement a new module in PARCS to facilitate the use of the multi-group tabulated cross sections in NEMTAB format so that a code-to-code comparison using DYN3D and PARCS can be done. These implementations in TRADYN are described in the following subchapters. Additionally the post-processing capabilities of TRADYN are extended so that, the 3D results of both PARCS and DYN3D simulations can be post-processed using the ParaVis tool inside

the NURESIM platform thanks to the automatic generation of MED files, where important core parameters (neutronics and thermal-hydraulics) are included for 3D plots. Finally, DYN3D code modifications were necessary to increase and reformat the output of important parameters for a better code-to-code comparison with PARCS increasing the readability of the code. These modifications are presented in the Appendix B.

4.4.1 New DYN3D models for Gamma Heating and Bypass Correction

In order to calculate the thermal-hydraulic conditions in the core accurately power produced by the nuclear fuel must be known. Usually, just the instant power (power produced by fission) is considered in the simulations of PWR. However in case of BWR cores, where the fuel rods are surrounded by a wide channel, it is important to consider additionally the gamma heating, i.e. the amount of power that is deposited directly in the coolant (~ 2%), bypass and water rods (~1.7%). The original version of DYN3D does not cover this aspect. After source code modifications, the TRACE/DYN3D coupled option within TRADYN is now able to take into account the power deposited in a BWR core in a more realistic manner than before.

Furthermore, it has been necessary to modify the DYN3D source code to account for the moderator density correction before the nodal cross sections are updated. Since the water in the channel bypass (see Figure 4-6) is not directly in contact with the fuel rods (heat source), its density is bigger than the water density inside the coolant channel. This correction plays an important role for the neutron moderation in the upper part of the core and it improves the neutron balance within the core. The following approach is used (Solis, et al., 2001):

$$\rho_{\text{act}}^{\text{eff}} = \frac{A_{\text{act}}\rho_{\text{act}} + A_{\text{byp}}(\rho_{\text{byp}} - \rho_{\text{sat}})}{A_{\text{act}}}, \quad (4-1)$$

where $\rho_{\text{act}}^{\text{eff}}$ is the effective average coolant density for cross-section calculation, ρ_{byp} is the average moderator coolant density of the bypass channel, ρ_{sat} is the saturated moderator coolant density of the bypass channel, A_{act} is flow cross-sectional area of the active heated channel and A_{byp} is the flow cross-sectional area of the bypass channel.

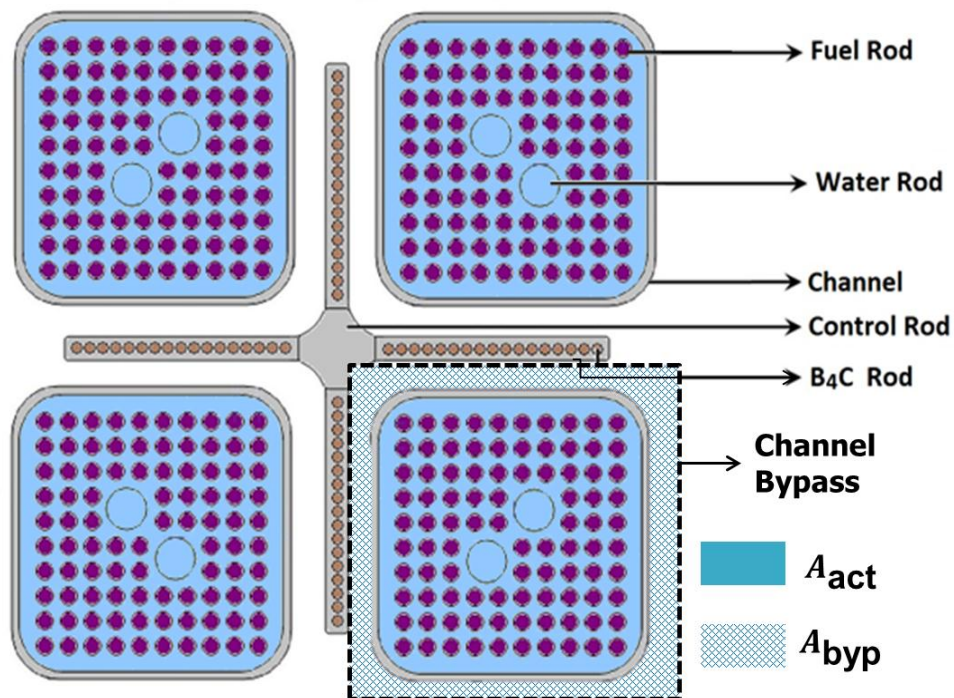


Figure 4-6 Channel bypass consideration in TRADYN for BWR fuel assemblies.

4.4.2 New DYN3D module to account for the orientation of ADF

The ADFs are usually generated by the lattice code (for example CASMO-4) considering that the control rod is located in the north-west corner, see Figure 4-7. Therefore, if one fuel assembly is located in a different position within the core, the ADFs must be rotated in order to correspond to the lattice code definition, here mentioned as “rotation = 0”.

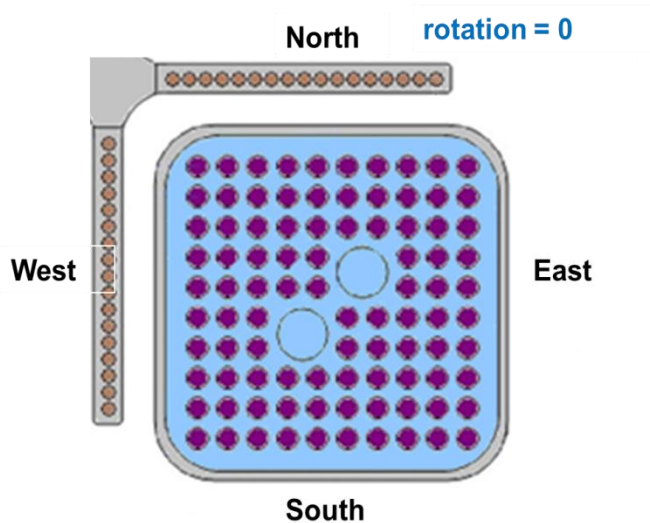


Figure 4-7 Fuel assembly orientation used by the lattice code CASMO-4 for ADF assignment, notice that the control rod is located in the top left corner.

The version of DYN3D inside TRADYN has the possibility to take into account per fuel assembly, in square geometry, one ADF (by using the XS library option 22) or four ADFs (by using the XS library option 26). Nevertheless in the last case, the rotation of the fuel is not considered at all. In order to take into account this rotation, modifications in the DYN3D source code are carried out. Now, depending on the position of the fuel assembly respect to the control rod the ADFs are rotated and enabling a more physical simulation of the core neutronics. In the Figure 4-8 the rotation of the fuel assembly is identified with the rotation index 1, 2, 3 that corresponds to the rotated assembly 90, 180, 270 degree anti-clock wise respectively.

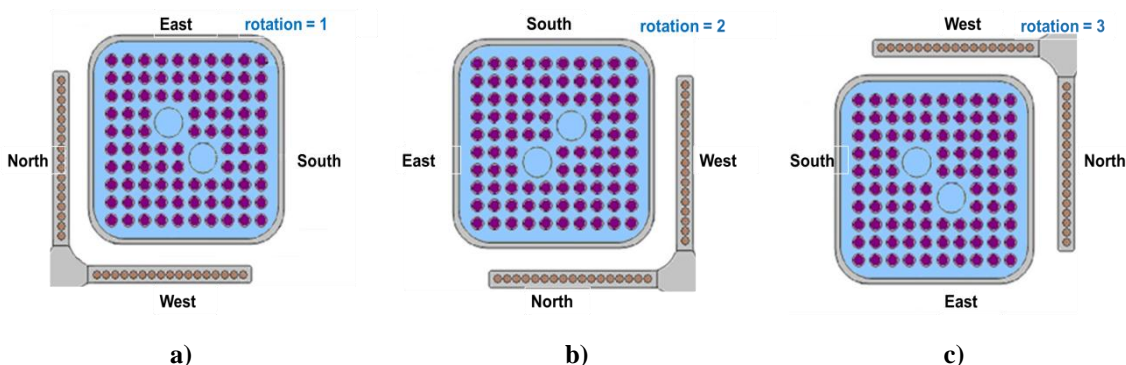


Figure 4-8 Fuel assembly rotation index depending on the rotation degree considered in DYN3D, a) rotated assembly 90 degree (index = 1), b) rotated assembly 180 degree (index = 2) and c) rotated assembly 270 degree (index = 3).

4.4.3 New PARCS module for reading multi-group cross section in NEMTAB format

A key requirement for neutronics simulations is the availability of nodal cross sections for real core loadings of BWR cores. As mentioned in 2.3, they are usually generated by codes such as CASMO-4, SERPENT, NEWT, POLARIS, etc. In order to use the generated cross sections in core simulators, they must be first written on the format that the simulator can handle.

In TRADYN, the neutronics solver DYN3D is able to read multi-group tabulated cross sections in NEMTAB format. On the other hand, PARCS can read PMAXS and an older NEMTAB format specifically developed for dedicated cases, such as PBTT, MSLB, VVER and the PWR MOX/UO₂ benchmarks (Kozlowski, 2003). If the user wants to supply the cross section for another reactor case, massive changes in PARCS source code are necessary. In order to overcome this problem, a new module for reading cross sections in PARCS has been implemented. Now the code PARCS in TRADYN is able to read the multi-group cross section in NEMTAB format (Kozlowski, 2003) for any reactor core loading. It is worth to note, that

these developments allow to compare the different neutronics codes of TRADYN (PARCS and DYN3D) using a unique cross sections format i.e. the multi-group NEMTAB format.

For testing of the source code modifications of PARCS to handle the NEMTAB format for any reactor core loading, the Peach Bottom Turbine Trip benchmark problem has been selected. The correct implementation and the verification of the new module are demonstrated and analysed in chapters 6 and 7.

4.5 New post-processing capabilities in TRADYN

TRADYN is extended to facilitate the post-processing of coupled simulations by the automatic generation of Data Exchange Model (DEM/MED) files. The MED files generated can be visualized and post-processed using the ParaVis tool inside the European simulation platform NURESIM (Chauliac, et al., 2011) that is based on SALOME platform (<http://salome-platform.org>) an open source and very powerful tool used in the scientific community. This improvement has paved the way for having a real 3D representation of the core where the evolution of the feedback variables can be followed during the whole simulation. Now in TRADYN using DYN3D or PARCS as neutronics solvers, the power, the neutron scalar flux, fuel temperature, moderator density and moderator temperature at nodal level are saved in the MED files, more details can be found in (Gonzalez-Vargas, 2017). Pictures demonstrating the post-processing capability of TRADYN are presented in Appendix D and Appendix E.

5 GENSIM-XS methodology for nodal cross section generation of BWR cores

The development of TRADYN requires the provision of cross section in NEMTAB format for which, several methodologies based on different lattice codes can be found. All of them contain proprietary information and therefore cannot be shared freely. This demands a new methodology for the cross section generation of BWRs considering history effects to be developed. This methodology can be extended to PWRs by adding the boron concentration and adapting the geometry according to fuel assembly dimension and reactor geometry.

The main goal of the GENSIM-XS methodology is to simplify the number of the neutronics domains in the reactor core. This new methodology uses the SIMULATE-3 (S3), which is part of the Core Management System (CMS) package, to transfer the cross sections into an output file. Then, they are extracted and written in multi-group tabulated cross sections in the NEMTAB format. In the following subsections, the GENSIM-XS methodology and the application to the cycle 4 of the Mexican Laguna Verde Nuclear power plant (LVNPP) for generating the cross sections are presented.

5.1 The new GENSIM-XS methodology

In real 3D reactor core geometry, each neutronics node differs from the others, so that the cross sections for the total nodes in the core have to be evaluated. This represents a huge computational effort for integration in a core simulator. The development of the GENSIM-XS methodology aims to reduce the number of the neutronics domains within the reactor core by simultaneously preserving the accuracy of the calculation.

The GENSIM-XS methodology is programmed entirely in Python language. It allows the creation of several functions in order to perform all the calculations automatically. The methodology starts with the “core follow files” generated with the code SIMULATE-3 and considers the exposure as the most representative parameter for simplifying the materials in the core. This is reasonable because fuel assemblies having the same exposure have been likely operated at similar conditions of power, void, control rod, and thus exhibit similar history effects (Watson, et al., 2002). The output files of S3 are supplied as input files for GENSIM-XS. The Figure 5-1 depicts the flowchart of the methodology. The chronology of the individual steps reads to:

1. Determination of the average fuel (2D) exposure (from S3 output file) for all the fuels in the core.
2. All the fuel elements belonging to one fuel type are grouped together. Then for each fuel type a range of exposure exists. If the difference of the exposure between two fuel elements of the same type is larger than a delta of exposure (user defined), these two elements are considered as different ones. By doing so for one fuel type several subtypes can exist. Thus a new radial map with new fuel subtypes is determined.
3. From S3 output the exposure, history void fraction (HVOI) and history control rod insertion (HCRD) for all the axial levels of every fuel subtype present in the core are extracted. Then an average exposure is calculated for every axial level.
4. Using the average values calculated above, a new S3 input decks are generated for each fuel subtype. As additional feature the user can specified if history effects (void, control rod or both) are considered or not. On these new inputs, the AUDIT option is activated in order to ask S3 to report the cross section for every “average node” with control rod present (rodded) and without control rod present (unrodded), which depends on the fuel temperature and the moderator density for BWR. In case of PWR’s the boron concentration can be added.
5. Finally, the cross section are extracted and written on NEMTAB format producing two files for each “average node”, one for the materials with control rod and one for the material without control rods.

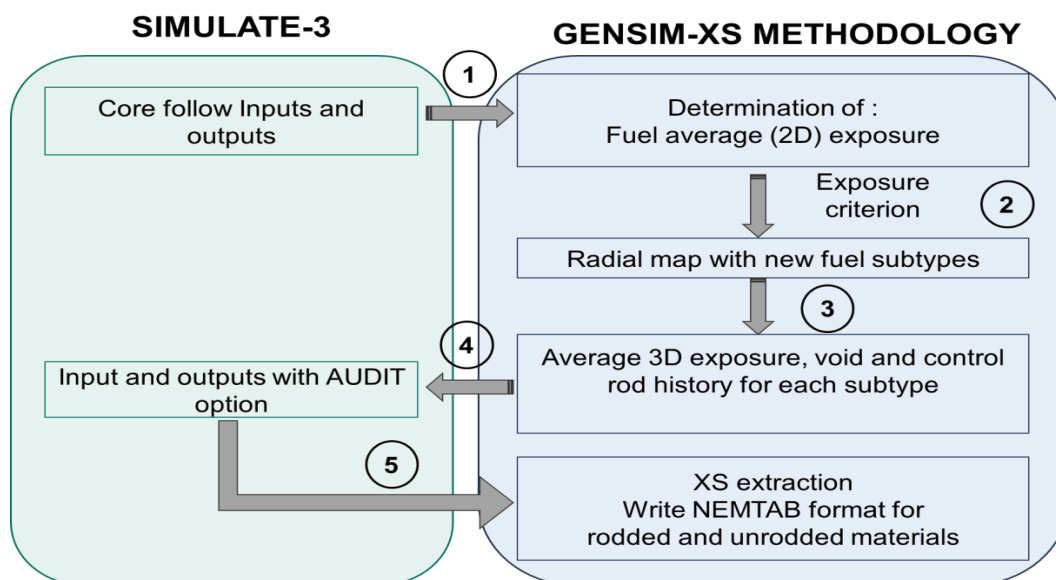


Figure 5-1 Flowchart of the information transfer between SIMULATE-3 and the GENSIM-XS methodology.

In the next section, the application of the GENSIM-XS methodology to the cycle 4 of Laguna Verde Nuclear Power Plant (LVNPP) is presented.

5.2 Application of the GENSIM-XS Methodology to a real power plant

5.2.1 Description of the cycle 4 of Laguna Verde Nuclear Power Plant

The cycle 4 of unit 1 operated from 24.03.1994 to 15.04.1995. The nominal power and mass flow rate were 1931 MWt and 7748.87 kg/s respectively. In this cycle, 104 fresh fuels were loaded and the rest were loaded in the previous cycles, having in total 444 fuel assemblies with 9 different fuel designs. All designs have an active fuel length of 381 cm, which is divided into 25 axial levels. Additionally two nodes more are added and the bottom and upper part of the fuel to account for the bottom (BOT REF) and top (TOP REF) reflectors. The fuel assembly designs differ mainly in the enrichment of U-235 as exhibited in Table 5-1. In the Figure 5-2 the core configuration at the beginning of the cycle is depicted; in this map the fuel type 0 is used to represent the radial reflector (RAD REF).

Core follow simulations from the cycle 1 to cycle 4 of the unit 1 of Laguna Verde are reported by (Castillo, et al., 2013) using the CMS System Package. Therein, an instability event occurred almost at the end of the cycle, which was simulated using S3K. For the time before the event started the state of the core was also calculated with S3.

In this context static simulations for Laguna Verde are only conducted to illustrate the capabilities of the newly developed GENSIM-XS methodology. Hence, the steady state calculation is used as starting point for the methodology. The determination of the cross section is executed for a specific time of the cycle. At this point, the thermal power is 37 % corresponding to 714.8 MWth and the mass flow rate is 2928.89 kg/s.

Table 5-1: Different fuel designs present in cycle 4 of Laguna Verde Nuclear Power Plant.

Fuel type	Enrichment of U-235 (%)	Quantity	Cycle loaded
1	1.76	64	1
2	2.19	68	1
3	3.0	44	2
4	2.0	48	2
5	3.24	76	3
6	2.8	40	3

7	3.22	96	4
8	3.0	4	4
9	3.03	4	4

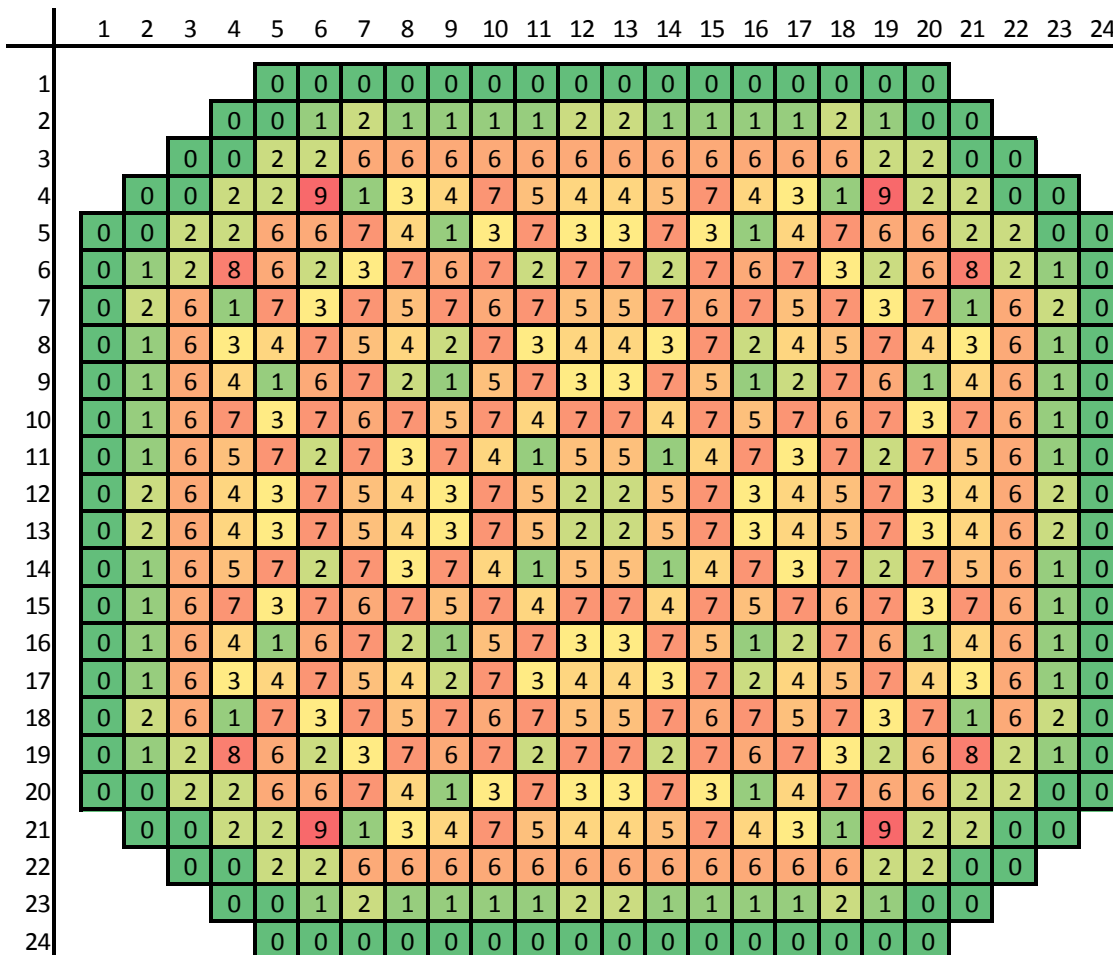


Figure 5-2 Core configuration at the beginning of cycle 4 of Laguna Verde Nuclear Power Plant, which is composed of 9 different fuel types, the fuel type 0 represents the radial reflector.

5.2.2 Determination of the average fuel exposure

The first step is to obtain the radial map of the average fuel exposure from the S3 output file, as illustrated in Figure 5-3. In the same figure, it can be seen for example that fuel element type 1 (highlighted in yellow) exhibits different exposure. Because the difference between the minimum value (18.42 GWd/t) and maximum (22.13 GWd/t) is around 3.71 GWd/t, it cannot be considered that all the elements belonging to fuel type 1 have the same neutronics properties.

The developed methodology automatically calculates (according to the exposure range and user defined exposure criterion) a delta exposure. If the difference in the exposure of two fuel elements of the same fuel type is larger than this delta, they are considered to exhibit different neutronics properties. If the same criterion is applied to all other fuel element types in the core, several subtypes for each fuel assembly type are obtained. Here, an exposure criterion of 1.5 GWd/t was used. The Table 5-2 shows all fuel subtypes (29) and their respective delta after applying this methodological approach. In Figure 5-4, the new subtype map according methodology is depicted. The number 0 is used for the radial reflector. At a first glance, the number of fuel types has increased. But it should be noted that the number of about 11100 (444 fuel assemblies * 25 axial nodes) neutronics domains can be reduced to 1450 (29 fuel subtypes * 25 axial nodes) domains with the corresponding cross section set. The cross sections sets are calculated considering also the control rod presence. The reduction in the number of cross sections sets results in a substantially minimized computation time for processing them using a core simulator.

Table 5-2: Exposure ranges calculated by the GENSIM-XS methodology (based on delta exposure) for every fuel type present in the cycle 4. As a result, every fuel type is divided in subtypes resulting in 29 fuel subtypes.

Fuel type	Exposure range (GWd/T)	Fuel subtype according to the methodology	Delta exposure
1	18.42 - 19.658	1	1.237
1	19.658 - 20.894	2	1.237
1	20.894 - 22.13	3	1.237
2	23.053 - 24.365	4	1.312
2	24.365 - 25.677	5	1.312
2	25.677 - 26.989	6	1.312
2	26.989 - 28.301	7	1.312
2	28.301 - 29.613	8	1.312
2	29.613 - 30.925	9	1.312
3	22.613 - 23.870	10	1.257
3	23.870 - 25.127	11	1.257
3	25.127 - 26.383	12	1.257
3	27.640 - 28.897	13	1.257
3	28.897 - 30.154	14	1.257
4	23.208 - 24.359	15	1.151

4	24.359 - 25.511	16	1.151
4	25.511 - 26.662	17	1.151
4	26.662 - 27.813	18	1.151
5	18.783 - 19.932	19	1.149
5	19.932 - 21.080	20	1.149
5	21.080 - 22.229	21	1.149
6	17.288 - 18.571	22	1.283
6	18.571 - 19.853	23	1.283
6	19.853 - 21.136	24	1.283
6	22.418 - 23.701	25	1.283
7	8.065 - 9.096	26	1.032
7	9.096 - 10.128	27	1.032
8	6.154 - 6.155	28	0.001
9	6.056 - 6.057	29	0.001

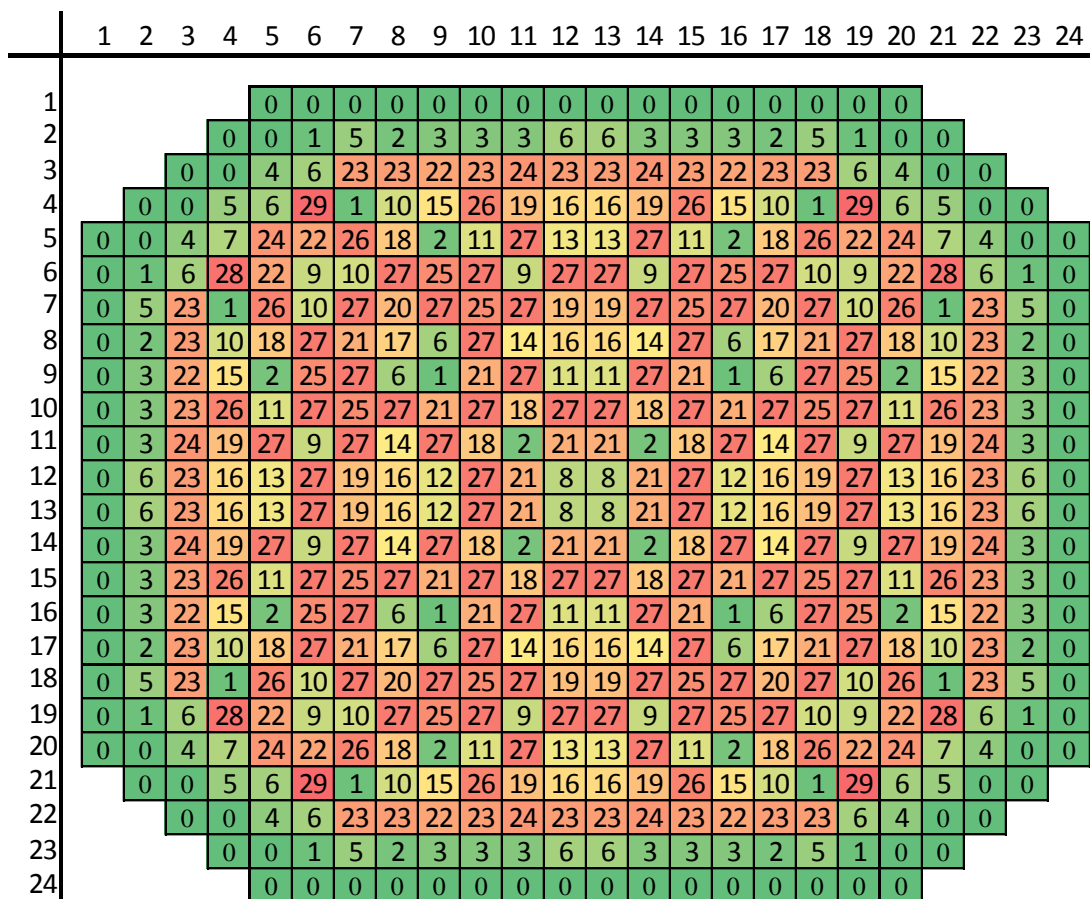


Figure 5-4 Radial core mapping of fuel assembly subtypes according to the exposure criterion methodology (GENSIM-XS) for the cycle 4 of LVNPP. The fuel type 0 represents the radial reflector.

5.2.3 Determination of the average nodal values per subtype

The axial material composition of the fuel assemblies loaded in the core and the reactor operating conditions, leads that the axial distribution of exposure, history void and control rod insertion to be unique for each fuel assembly. All the fuel assemblies belonging to one of the 29 subtypes, obtained in the previous stage, are different to each other. In Figure 5-4, it can be seen 20 fuel assemblies in the core belonging to the subtype 1, from all of them just one “average subtype 1” is required. The Table 5-3 shows the average nodal exposure at every axial level (including bottom and top reflectors) for the subtype 1. An equivalent calculation is done for the history void and history control rod insertion for the other 28 subtypes. As a result of this approach only 29*25 (subtypes*axial levels) neutronics regions or cross section sets are obtained. Additionally, 3 cross section sets have to be added to account for the reflectors adequately.

Table 5-3: Determination of the nodal axial average exposure (GWd/t) of all fuel elements belonging to subtype 1, the Bottom and top reflectors were also added.

Axial level	Exposure of the all fuel elements belonging to subtype 1					Average exposure (GWd/t)
	1	2	3	...	20	
BOT REF	0.0	0.0	0.0		0.0	0.0
1	4.154	4.151	4.315		4.154	4.2969
2	12.826	12.821	13.353		12.826	13.28135
3	16.785	16.782	17.555		16.785	17.43115
4	18.868	18.867	19.733		18.868	19.58465
5	20.19	20.19	21.032		20.19	20.89945
6	20.799	20.798	21.514		20.799	21.4546
7	20.922	20.921	21.4		20.922	21.4439
8	21.628	21.628	21.885		21.628	22.0404
9	21.974	21.973	22.022		21.974	22.34285
10	22.019	22.019	21.874		22.019	22.29185
11	22.523	22.523	22.19		22.523	22.6751
12	22.963	22.963	22.478		22.963	23.02495
13	22.976	22.976	22.294		22.976	22.8966
14	22.608	22.608	21.634		22.608	22.27725
15	23.057	23.057	21.857		23.057	22.5527

16	23.009	23.008	21.632		23.009	22.3524
17	22.386	22.386	20.75		22.386	21.50145
18	22.588	22.588	20.626		22.588	21.44035
19	22.551	22.551	20.38		22.551	21.29625
20	21.871	21.87	19.345		21.871	20.48265
21	20.586	20.586	17.887		20.586	19.0185
22	19.341	19.341	16.914		19.341	17.73385
23	16.527	16.527	14.42		16.527	14.9928
24	11.976	11.976	10.41		11.976	10.7646
25	5.439	5.439	4.77		5.439	4.9226
TOP REF	0.0	0.0	0.0		0.0	0.0

Regarding the void history, SIMULATE-3 calculates the quality in g/cc. To convert the moderator density into void fraction the Equation (5-1) is used. Therefore, the reference pressure (70 bar) is required to determine the saturation temperature (560 °K) as well as density for the liquid (0.738 g/cc) and vapour (0.038 g/cc) phases.

$$\alpha = \frac{\rho_m - \rho_l}{\rho_v - \rho_l} \times 100, \quad (5-1)$$

were, α is the void fraction present in the moderator, ρ_m is the void history calculated by S3, ρ_l is the density of the liquid and ρ_v is the density of the vapour.

5.2.4 Parameterization and generation of the cross section

Using the information calculated previously new S3 input decks, including the audit option are created. This option lets the user to verify/evaluate the cross section library used in a S3 calculation (Dean, et al., 2005).

Additionally, the audit option allows parameterizing, according to thermal-hydraulic state parameters, individual cross sections and assembly discontinuity factors (ADF) at nodal level. Here, the fuel temperature and moderator density are used as thermal-hydraulic state parameters. The expected range of variation of these state parameters should be considered in the parameterization. The range for the fuel temperature is [400, 800, 1200, 1600, 2000, 2400 °K] and for the moderator density is [177.2, 247.3, 317.4, 457.6, 597.8, 738 kg/m³]. The selected coolant density values correspond to an axial void fraction distribution along the BWR core of 80 %, 70%, 60 %, 40 %, 20 % and 0 % for a nominal system pressure of 70 bar.

For the selected time of the cycle, a new S3 input deck for every fuel subtype is automatically created, having in total 29 inputs. Here, the generation of the cross sections is considering history void and history control rod.

Finally, the cross section sets are extracted from SIMULATE-3 outputs and written in NEMTAB format.

In order to validate the GENSIM-XS methodology, the cross sections generated for the cycle 4 will be used in TRADYN to simulate the static core conditions. The obtained results will be compared to the ones of SIMULATE-3 in Chapter 7.

6 Validation of TRADYN using the Peach Bottom Turbine Trip test

For the validation of TRADYN the exercise 3 of the Boiling Water Reactor Turbine Trip (TT) benchmark was selected. It is a thermal-hydraulic initiated reactor transient event characterized by a pressurization in a BWR vessel, in which the coupling between core phenomena and system dynamics plays an important role. Also the availability of real plant measured data is very valuable. In this chapter, the definition of TT benchmark and the models used are given. Then, the results of TRADYN using PARCS and DYN3D as neutronics solvers for steady state and transient calculation are presented and discussed.

6.1 Definition of Peach Bottom Turbine Trip (TT) test and models

The TT benchmark is based on the Peach-Bottom-2 NPP test. This test was performed at the Peach Bottom-2 BWR/4 NPP prior to shut down for refuelling at the end of the cycle 2 in April 1977. At the moment of this test, the initial thermal power was 61.4 % rated 2030 MWth and the mass flow rate was 80.9% rated 10445 kg/s.

The TT transient begins at $t = 0$ s with a sudden closure of the turbine stop valve (TSV). As a consequence, the pressure wave propagates through the main steam line into the reactor core ($t = 0.4$ s) and downcomer with relatively little attenuation. The core pressure rise results in a higher boiling temperature and this leads to a significant void collapse in the core. This in turn yields to improve the neutron moderation within the core, causing a reactor power increase. The magnitude of the power and the corresponding neutron flux changes taking place in the core are strongly affected by the initial rate of pressure rise caused by the pressure oscillation (mainly due to secondary waves) and it has a strong spatial variation.

The TRACE core model includes a 2D vessel component with four radial rings and 14 axial levels. The 764 fuel assemblies are represented by 33 channels. The total fuel length is 365.75 cm, which is divided in 24 nodes; additionally two nodes were added to account for the lower and top reflector. This 33 channels model provides sufficient radial nodalisation in order to simulate a core pressurization transient like the turbine trip that is dominated by one-dimensional axial effects. Other components such as the recirculation loop including jet pumps, separator with dryers, feedwater, steam lines and bypass are also modelled. The Figure 6-1 depicts the TRACE model used as well as the flow directions.

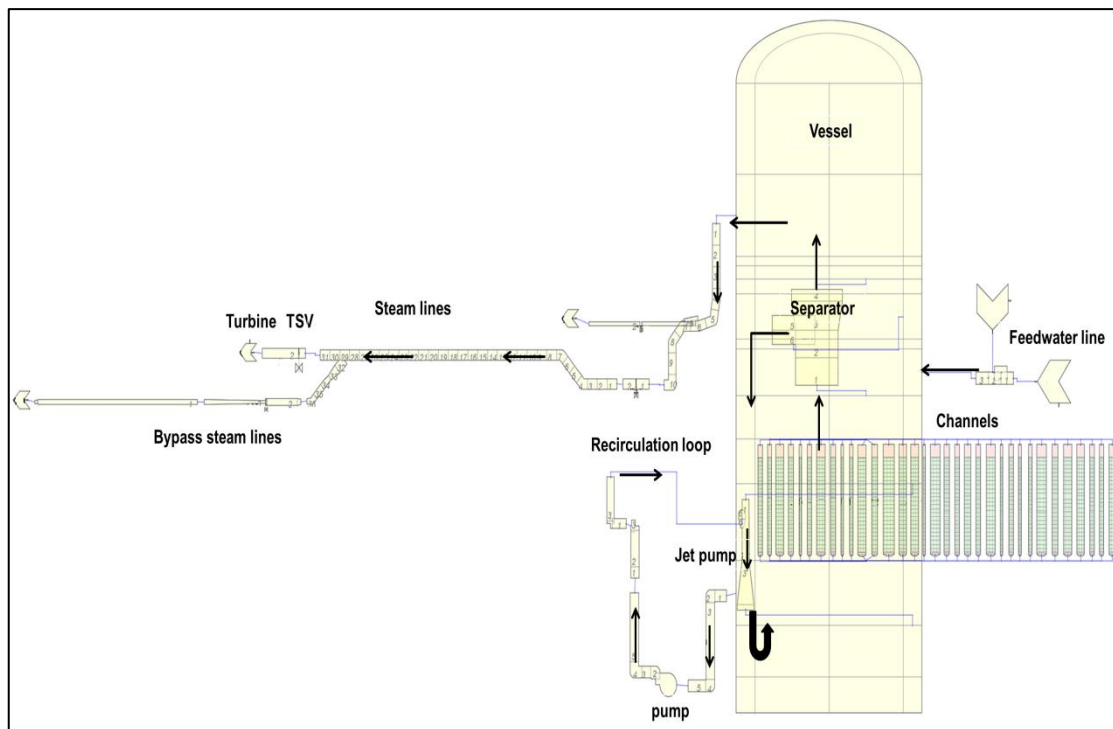


Figure 6-1 TRACE model used for the simulation of Peach Bottom Turbine Trip test.

In the PARCS and DYN3D models, each fuel assembly is represented explicitly as one radial neutronics node. Additionally, one channel is included for representing the radial reflector (see Figure 6-2). The mapping between TRACE and both PARCS and DYN3D is depicted in the Figure 6-3. The control rod position within the core at the beginning of the transient event is illustrated in Figure 6-4. In axial direction, both models are consistent with the TRACE channel nodalisation of 26 axial nodes including 2 reflectors (bottom and top). The calculations done with both codes PARCS and DYN3D use the 2 energy groups tabulated cross sections in NEMTAB format provided by the benchmark team. Then they have been converted into multi-group NEMTAB format which is readable by both neutronics codes. Therefore a converted program written in Python language was used.

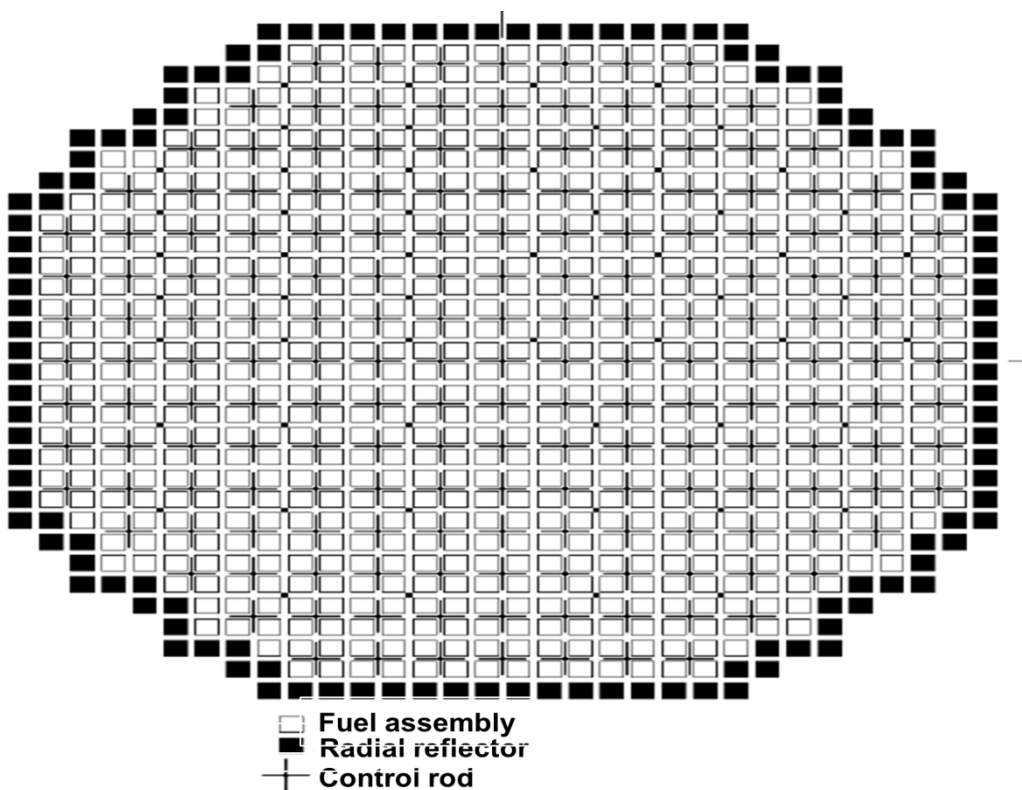


Figure 6-2 Cross sectional view of the Peach Bottom reactor core illustrating the fuel assemblies, control rods and radial reflectors (Solis, et al., 2001).

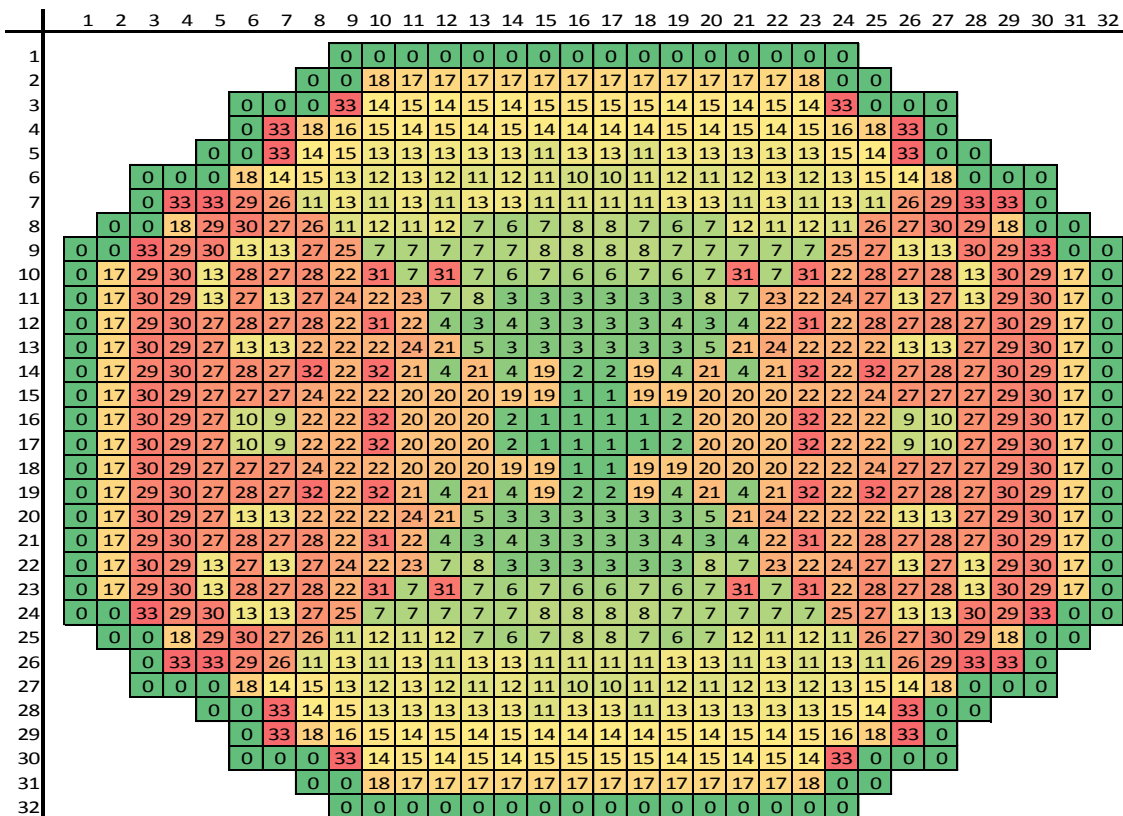


Figure 6-3 Reactor core thermal-hydraulic channel radial mapping scheme used to represent the Peach Bottom reactor core (Solis, et al., 2001).

(48 – full withdrawn, 0 – full insertion)

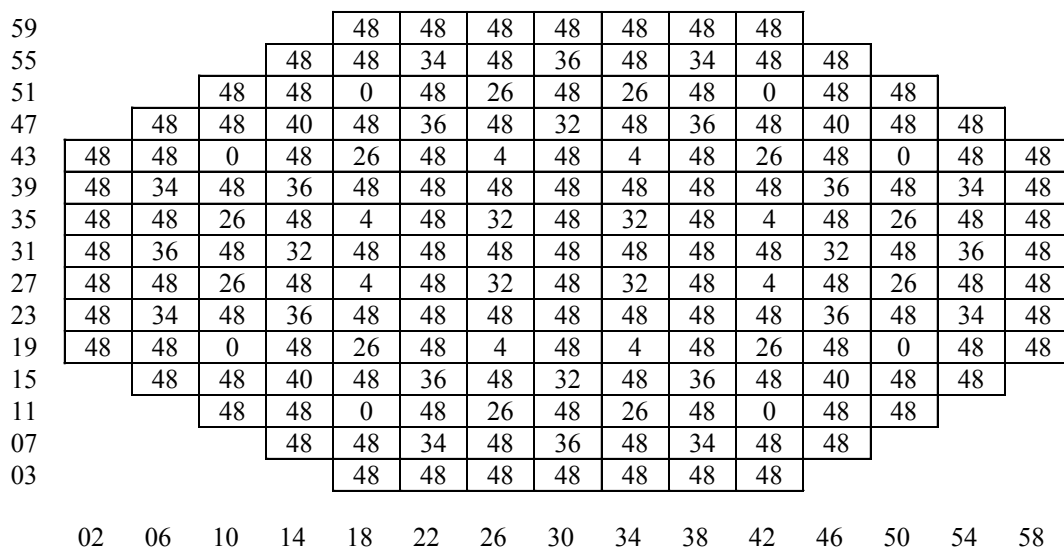


Figure 6-4 Control rod positions within the core at the beginning of the transient for the Peach Bottom Turbine (Solis, et al., 2001).

The initial thermal hydraulic boundary conditions were taken from the benchmark definition, shown in Table 6-1. It is worth to mention that a minimum time step of 1.0E-8 s and maximum time step size of 0.5 s were used in TRACE. The NK codes PARCS and DYN3D use the same time steps of the TH code during steady state and transient calculations.

Table 6-1: Peach Bottom Turbine Trip Initial Conditions as provided by (Solis, et al., 2001).

Parameter	Value
Core Thermal Power (MWth)	2030
Dome Pressure (MPa)	6.798
Feedwater Flow (kg/s)	980.26
Feedwater Temperature (°C)	191.17
Core Inlet Subcooling (J/kg)	48005.291
Jet Pump Driving Flow (kg/s)	2871.24
Inlet Temperature (°C)	274
Total Core Mass Flow (kg/s)	10445
Core Average Exit Quality (fraction)	0.097
Core Average Void (fraction)	0.304
Control Density (fraction)	0.159

6.2 Comparison of TRADYN steady state predictions against test data

The initial steady state conditions predicted with TRADYN using PARCS and DYN3D as neutronics codes are compared with the measurement data in Table 6-2. The comparison shows almost no difference in the dome pressure for both TRADYN calculations. The pressure drop across the core is overestimated by around 18 kPa in the TRADYN calculations. This is also reflected in the average void fraction. Similar differences were found by (Nikitin, et al., 2010), (Lee, et al., 2004). The reason for this difference can be attributed to the uncertainties inherent to the measurements and the model used in TRACE for the spacers and friction losses. However, this deviations in the pressure drop is not so significant, due to the fact that the operation pressure of the reactor is several orders of magnitude higher (7000 kPa) than the pressure losses.

Table 6-2: Measured turbine trip initial conditions comparison to TRADYN predictions.

Parameter	Measured	TRADYN (PARCS)	Rel. Dif (%)	TRADYN (DYN3D)	Rel. Dif ¹ (%)
Dome Pressure (MPa)	6.7985	6.7987	0.0029	6.799	0.007
Core Outlet Pressure (MPa)	-	6.825	-	6.826	-
Core Inlet Pressure (MPa)	-	6.927	-	6.927	-
Core Pressure Drop (MPa)	0.0835	0.102	22.053	0.101	20.86
Core Average Void (fraction)	0.304	0.336	10.526	0.321	5.59

Based on the results of the all participants of the benchmark (Akdeniz, et al., 2010), the average value of k_{eff} and its standard deviation (σ) including TRADYN results were recalculated. The new values are for $k_{eff} = 1.004249$ and for the standard deviation $\sigma = 0.00398$. The corresponding values of k_{eff} obtained by TRADYN and its respective deviations from the average value are displayed in Table 6-3. In the same table, it can be seen that the result of

¹ Rel. Dif(%) = $\frac{\text{predicted} - \text{reference}}{\text{reference}} \times 100$

TRADYN (DYN3D) has a larger deviation (-644 pcm) from the average than the predicted using PARCS (-180). However, the deviation in both calculations is within 2σ .

Table 6-3: Comparison of the effective multiplication factor k_{eff} , deviation, and difference of TRADYN predictions and average value of benchmark results.

	k_{eff}	Deviation ²	Diff (pcm)
Average Benchmark	1.004249	-	-
TRADYN (PARCS)	1.002353	-0.0019	-180
TRADYN (DYN3D)	0.99779	-0.00647	-644

The axially integrated power measurements are analysed. They have been normalized such that average axially integrated power is unity. Additionally, they were provided at the middle of each axial fuel level, thus the first value reported is 7.62 cm and the last one 358.14 cm. In the Figure 6-5, a comparison of the normalized axial power distribution as function of axial core height between the measurement data and TRADYN calculations is depicted. The predictions of TRADYN (PARCS) agree fairly well with the measurements. The maximum relative difference was found at the bottom (12%) and at the top (30%) of the core. This can be attributed to the reflector cross section and the uncertainties in the measurements. Respect TRADYN (DYN3D), the power shape presents a maximum relative difference of -52%, 14% and 34% in bottom, middle and top part of the core, respectively. These differences are a combination of cross section modelling and uncertainties in the measurements provided. The same conclusions were drawn by several other participants (Grundmann, et al., 2004), (Langenbuch, et al., 2004), (Mignot, et al., 2004), (Nikitin, et al., 2010), (Mori, et al., 2003).

However, this underprediction of the power by TRADYN (DYN3D) in the bottom part of the core leads to less void fraction in this zone (mainly up to 120 cm) as depicted in Figure 6-6. Therefore, a deviation² up to -0.046 is reached in the bottom part. But, TRADYN (PARCS) overpredicts the void slightly in this part of the core by a deviation² around 0.011. In both cases, the deviations² are more pronounced (around 0.022) at the heights, where the spacers are located.

² Deviation = $predicted - average$

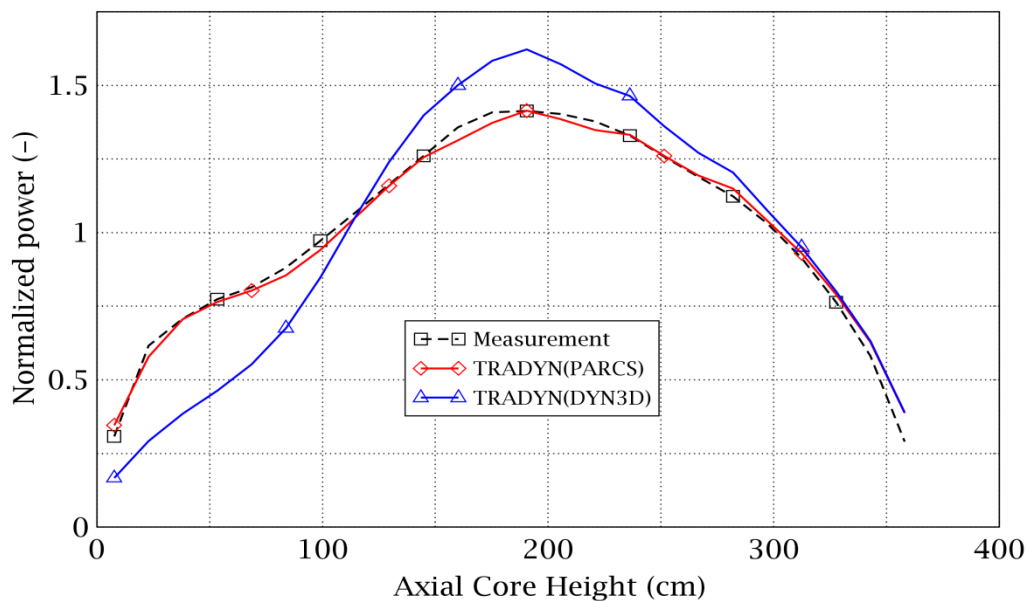


Figure 6-5 Core average relative axial power distribution comparison between the measurements and TRADYN predictions.

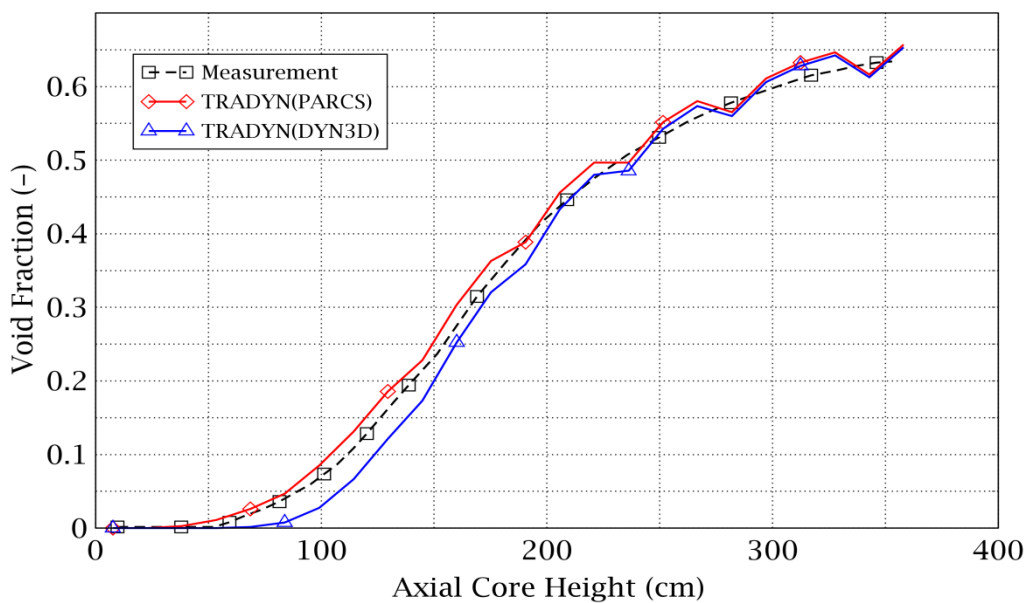


Figure 6-6 Core average axial void fraction comparison between the measurements and TRADYN predictions.

In TRADYN simulations, the generation of a MED file was activated (see section 4.5). Thus, a MED file containing the feedback parameters was automatically created. The figures showing the 3D representation of the power density, fuel Doppler temperature and moderator density are given in Appendix D.

Based on TRADYN results obtained for the steady state, it can be concluded that TRADYN is suitable to reproduce the measurements and its prediction are in agreement with other

participants. This confirms clearly not only the correct implementation of the physical models but also the consistency in the data transfers between the codes. The source of the differences exhibited in the prediction is mainly due to the several factors such as: homogenization of cross section, the uncertainty associated with the measurement and the number thermal-hydraulic channels.

6.3 Comparison of TRADYN transient predictions against test data

The transient is initiated by sudden closing of the turbine stop valve ($t=0$). The pressure wave coming from the turbine trip reaches the core following two main paths: single-phase (liquid) path through downcomer and recirculation loops with jet pumps and a two-phase path through the steam dryer and separators and the upper plenum. The induced core pressure wave collapses the void increasing the moderation and therefore the total power. The power excursion is stopped by the SCRAM bringing the reactor to shutdown conditions.

The steady state calculations presented in the previous section were used as start point for the transient calculations.

The Figure 6-7 depicts the evolution of the dome pressure evolution during the transient. There, the agreement of the predictions with the measured data is very good until the SCRAM is initiated (0.75s). Later on, the dome pressure calculated by TRADYN simulations is lower than the measured one. But the shape of the pressure evolution predicted by the codes follows qualitatively the evolution of the measured dome pressure. As consequence, a lower power increase is predicted by TRADYN simulations, since the void collapsing in the core is not so strong enough compared to the measurements, see Figure 6-8. Therefore, an underestimation in TRADYN predictions by around -30% has been obtained. This deviation cannot be only explained by the uncertainties in the measurements, cross section homogenizations or normalizations across fuel assemblies and the core, which can lead to another neutron flux distribution. Therefore an exhaustive revision of parameters including, but not limited to, power, mass flow rate, control rod position, time for closing TSV, SCRAM time initialization and control rod insertion velocity, has been carried out. Nevertheless, no significant differences with the benchmark specifications were found. For consistency, an execution of the original version of TRACE/PARCS system (without multigroup NEMTAB XS format) was carried out. In the Figure D-4 in the Appendix D, it can be seen that the results of the original version (referred as TRACE/PARCS_orig) for the power evolution are almost identical to the TRADYN (PARCS). Finally, it can be concluded that the new version of TRACE/PARCS (*version 5 patch 4*) is not able to predict correctly the height of the power peak during the transient. This problem is currently discussed with the main developers of TRACE/PARCS of

the University of Michigan to investigate the deviation of the current results respect to the ones reported by (Lee, et al., 2004).

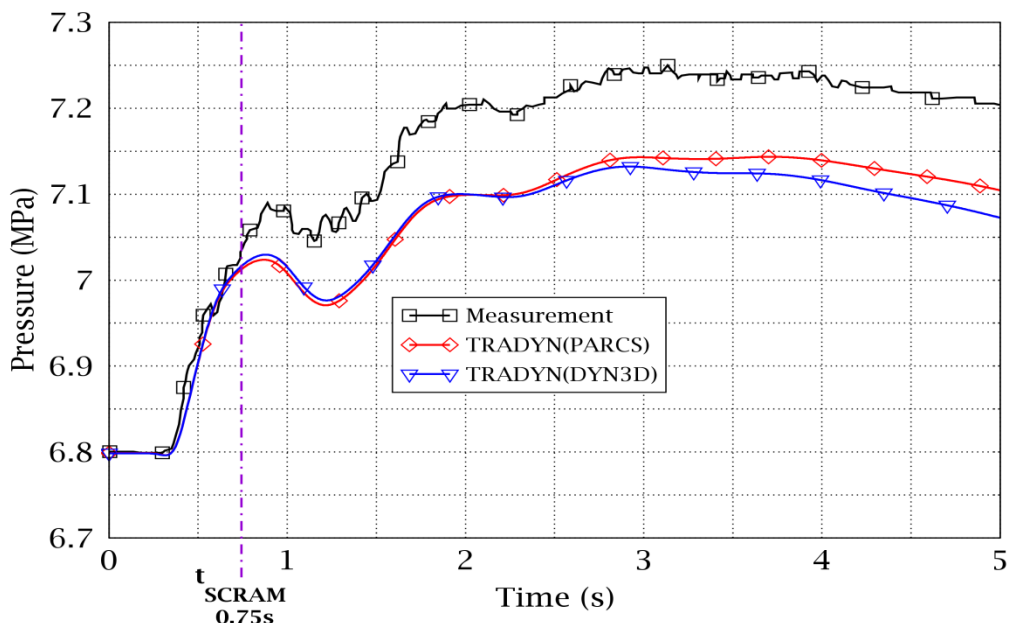


Figure 6-7 Steam dome pressure evolution comparison during the transient case between TRADYN and the measurements.

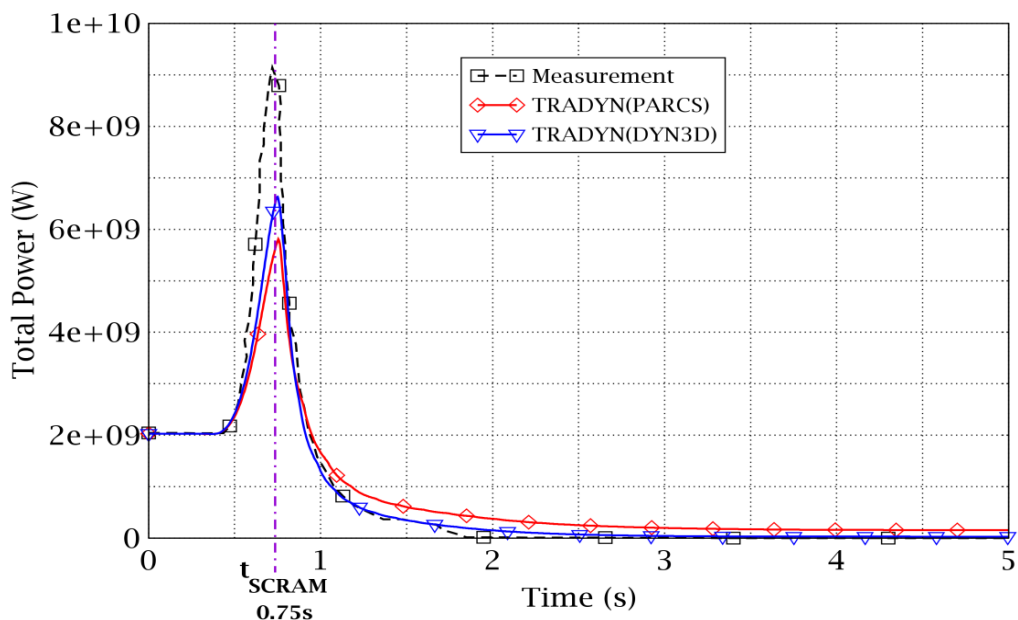


Figure 6-8 Total power comparison during transient between TRADYN calculations and the measurements.

During the execution of TRADYN using both neutronics solvers, the automatic creation of MED files was activated. Because the results obtained are quantitatively similar, just the post-processing of the PARCS MED file with the module ParaVis is presented. A 3D representation

of the core power evolution versus time for the transient calculation is depicted in the Figure D-5 in the Appendix D.

The Figure 6-9 depicts the core reactivity and its components calculated with TRADYN. The beta effective β_{eff} for PARCS and DYN3D is 549.34 (pcm) and 552.6 (pcm), respectively. A difference around 1\$ between the results obtained with PARCS and DYN3D is present after the first second of transient for the total reactivity (see Figure 6-9(a)). In the case of Doppler and moderator density reactivity (see Figure 6-9(b) and (c)), a good agreement until 2 seconds is observed. However, after this time more positive reactivity is inserted due to moderator density (void fraction), which implies that there is less void fraction in DYN3D calculations. Regarding the Doppler reactivity, the fact that less void fraction is present after 2 seconds improves the moderation and therefore the fission power. Finally, differences up to 12\$ in the control reactivity can be seen in the Figure 6-9(d). It can be inferred that DYN3D inserted the control rod faster than PARCS. This explains the differences in the other reactivity component and the total reactivity. However, a deeper analysis should be conducted in the future.

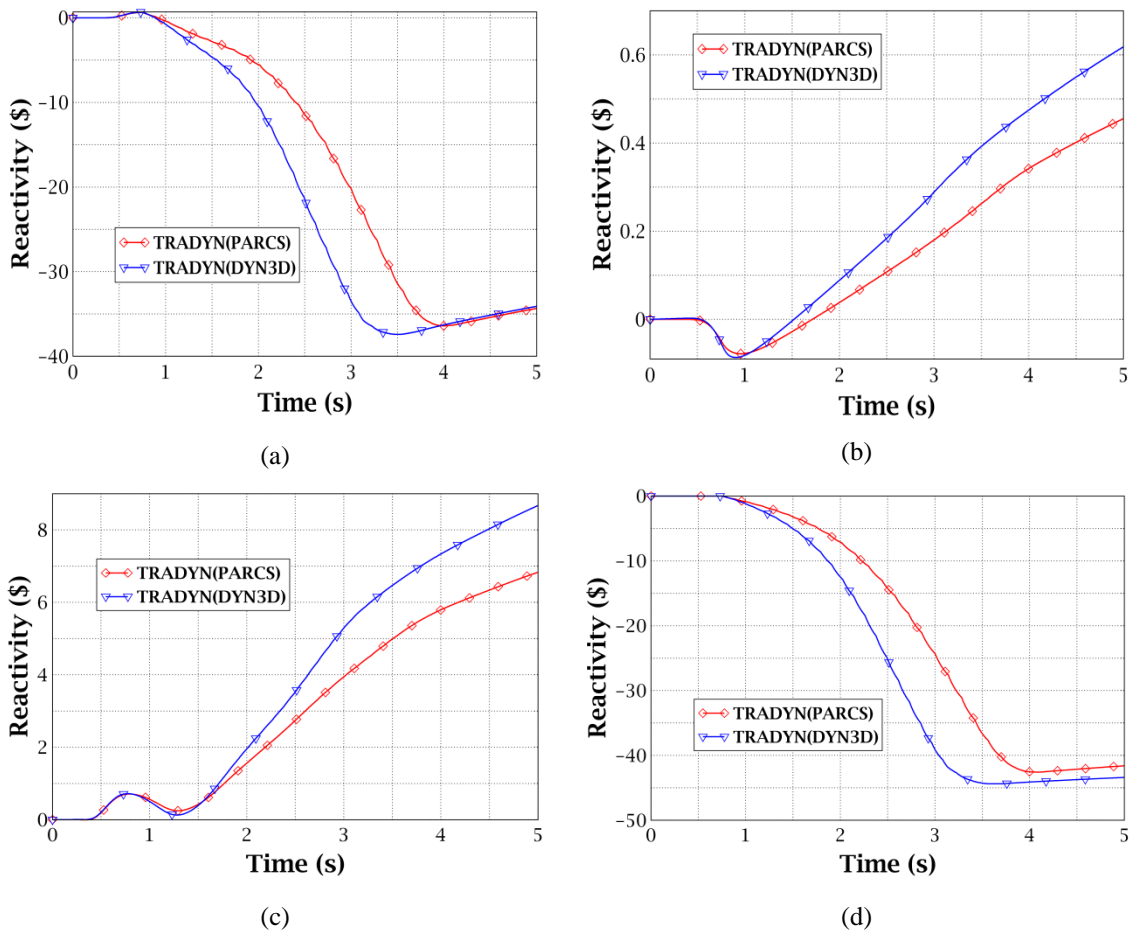


Figure 6-9 TRADYN results for the core total reactivity and its components. The total reactivity is given in (a), the Doppler reactivity in (b), the moderator density in (c) and the control rod reactivity in (d).

7 Analysis of the Laguna Verde core using SIMULATE-3 and TRADYN using cross sections generated with GENSIM-XS

Here, the GENSIM-XS methodology is validated by comparing the results of static simulations of the Laguna Verde core performed with TRADYN (using both PARCS and DYN3D) and SIMULATE-3. These investigations are also intended to validate not only the GENSIM-XS methodology but also the simulation capability of TRADYN itself. In this chapter, the reference SIMULATE-3 model and the thermal-hydraulic and neutronics models developed for TRADYN are firstly introduced. Then, the comparative study are shown and discussed.

7.1 The neutronics and thermal-hydraulic Laguna Verde core models

7.1.1 The SIMULATE-3 core reference model

The reference core model is composed by 444 fuel assemblies containing 9 different fuel designs, see Table 5-1. There are in total 536 assemblies, 444 fuel assemblies and 92 reflectors, additionally the 109 control rods are also included into the model (see Figure 7-1). Reflective boundary conditions are used in the neutronics simulations. Axially, the reactor core is divided into 27 layers (25 fuel layers plus bottom and top reflector) with a constant height of 15.24 cm. The total active core height is 381 cm. The axial nodalisation accounts for the material changes in the fuel design and for exposure and history variations. Therefore, SIMULATE-3 models every node explicitly producing in total 11,100 (active zones) plus 3 materials for the reflectors. The cross sections for these materials are previously generated with CASMO-4. The generated cross sections were put together into a master library using the CMSLINK code. Finally SIMULATE-3 uses this master library during the static calculations.

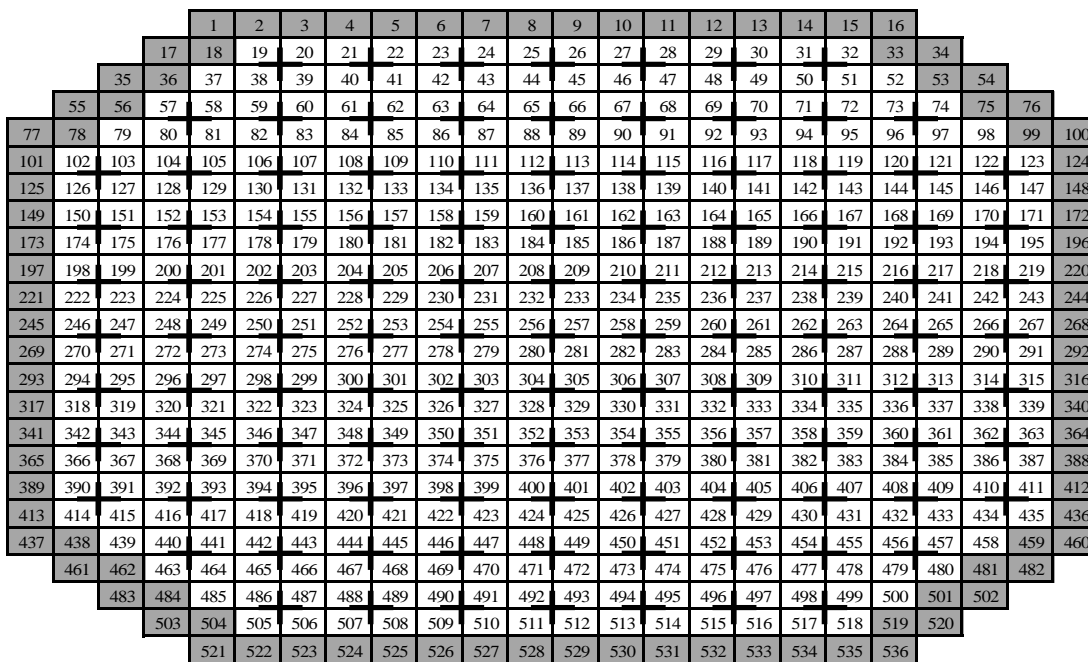


Figure 7-1 Fuel assembly and reflector arrangement used in SIMULATE-3 model (the same representation was used in PARCS and DYN3D) for LVNPP. Notice the 109 control rods present in the core.

The thermal-hydraulic model of SIMULATE-3 includes the lower and upper tie plates, a separator, a bypass region and parallel channels (are used for modelling the fuel assemblies). It is required to supply the core mass flow rate, the coolant inlet temperature and the system pressure as boundary conditions. The initial core static conditions are presented in Table 7-1 are used in SIMULATE-3 model. The control rod pattern used in the static simulations is given in Figure 7-2.

Table 7-1: Initial core static conditions for LVNPP used in S3 model

Parameter	Value
Core Thermal Power (MWth)	714.8 (37%)
Core Mass Flow Rate (kg/s)	2928.89 (37.8%)
Bypass Mass Flow Rate (kg/s)	250
Pressure Core Outlet (MPa)	6.51
Pressure Core Inlet (MPa)	6.55
Core Pressure Drop (MPa)	0.04
Core Inlet Temperature (°C)	268.66
Core Average Void (fraction)	0.364
k_{eff}	0.98296

(48 – full withdrawn, 0 – full insertion)

43		48	48	48	48	48	48	48	48		
39		48	48	0	48	18	48	0	48	48	
35	48	48	48	48	48	48	48	48	48	48	
31	48	0	48	0	48	0	48	0	48	0	
27	48	48	48	48	48	48	48	48	48	48	
23	48	0	48	0	48	6	48	0	48	0	
19	48	48	48	48	48	48	48	48	48	48	
15	48	0	48	0	48	0	48	0	48	0	
11	48	48	48	48	48	48	48	48	48	48	
07		48	48	0	48	18	48	0	48	48	
03		48	48	48	48	48	48	48	48		
	02	06	10	14	18	22	26	30	34	38	42

Figure 7-2 Control rod pattern for static state of the cycle 4 of LVNPP.

7.1.2 The PARCS and DYN3D core models

The neutronics core models for both core simulators, PARCS and DYN3D, are similar to SIMULATE-3 model. Then, the same radial and axial nodalisation and the same boundary conditions are used. However in TRADYN models, the fuel assemblies are grouped into 29 fuel types. The axial composition of the fuel assemblies is provided by the cross section generated by GENSIM-XS methodology. There are in total 1450 cross section sets plus three sets for bottom, top and radial reflector, respectively. The cross sections sets take into account the possible core states, because they depend on exposure, fuel temperature and moderator density. Furthermore, they consider history effects.

7.1.3 The TRACE thermal-hydraulic model

The thermal-hydraulic model of the LV core developed for the TRACE code consists of a VESSEL component with one radial ring and 4 axial levels. The 444 fuel assemblies are represented by 29 parallel channels corresponding to the 29 fuel assemblies subtypes obtained by GENSIM-XS methodology. Each thermal-hydraulic channel is divided axially in 27 nodes, 25 for the active core height and two for the lower and upper reflector. The core inlet mass flow rate, the coolant inlet temperature and the core outlet pressure are given as thermal-hydraulic boundary conditions. They are taken from SIMULATE-3 model, see Table 7-1.

In Figure 7-3, the TRACE model is represented. It illustrates the 1D VESSEL component, the 29 parallel channels, each one represented by a CHAN component. The inlet and outlet boundary conditions are taken into account by the FILL (inlet) and BREAK (outlet) component.

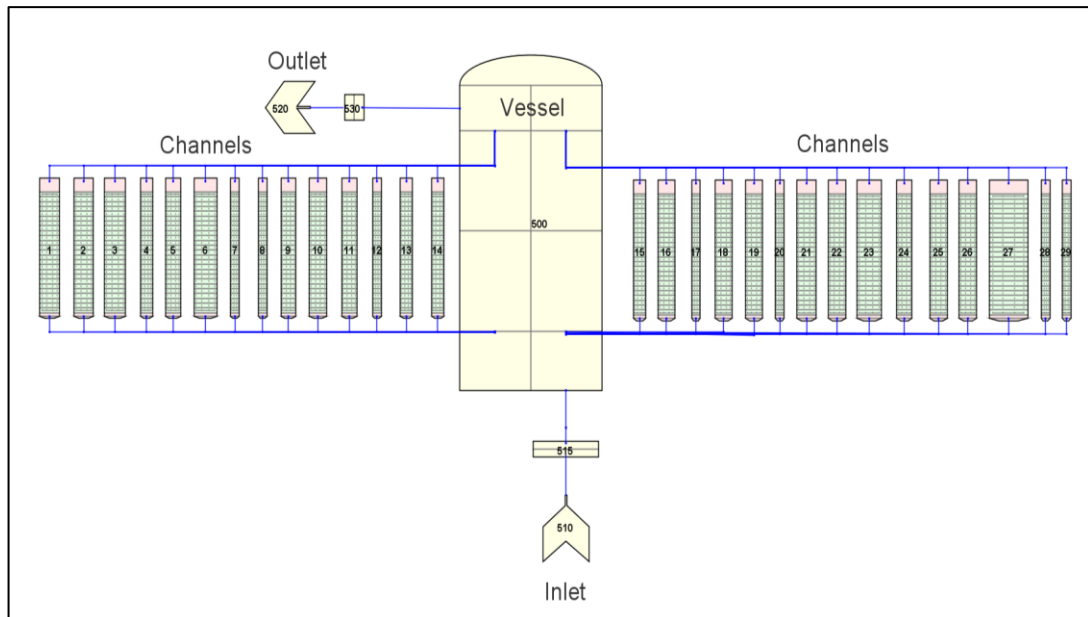


Figure 7-3 Thermal-hydraulic model for TRACE code used for the simulation of LV containing 29 channels for representing the core.

The 29 thermal-hydraulic channels shown in Figure 7-3 are coupled to the neutronics model in the radial plane shown in the Figure 7-4. The thermal-hydraulic channels identified as 0 are treated as reflectors regions.

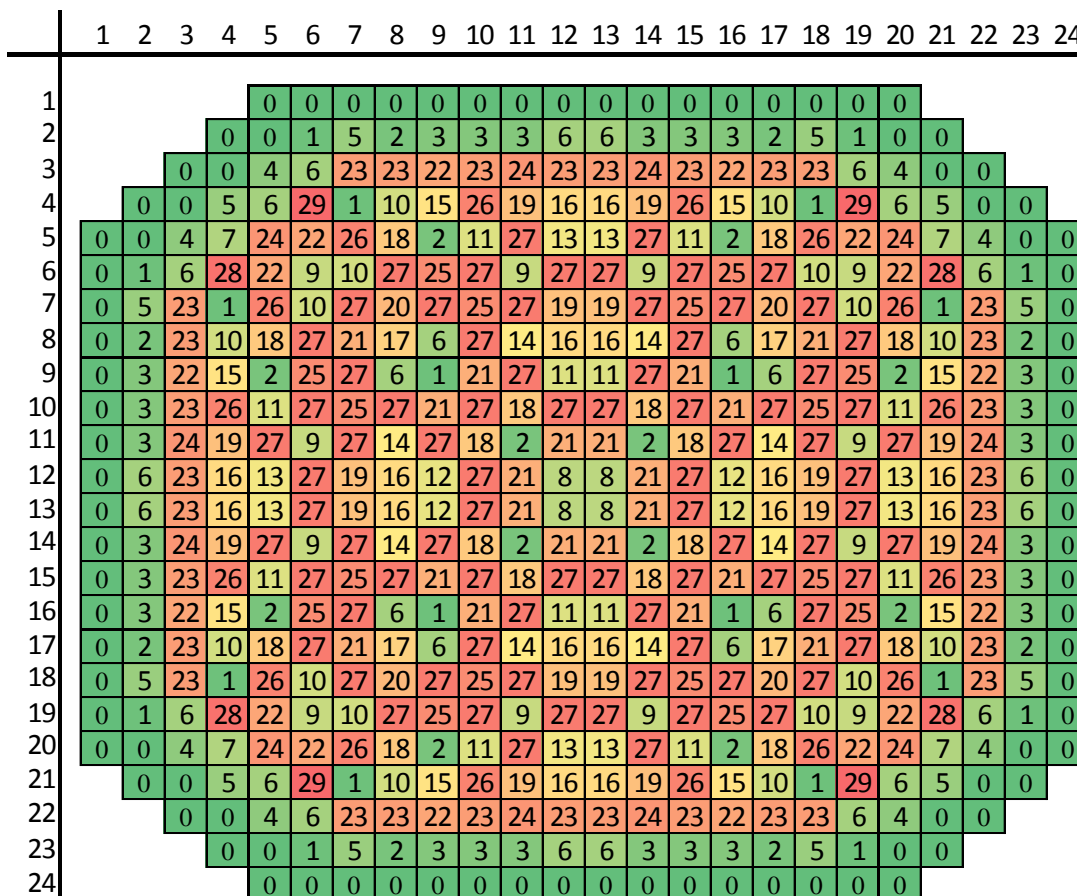


Figure 7-4 Reactor core thermal-hydraulic channel radial mapping scheme used to represent the LV core.

7.2 Comparison of TRADYN static core simulations with SIMULATE-3

In this subchapter, the selected results predicted by TRADYN (PARCS) and TRADYN (DYN3D) are discussed and compared to the ones obtained by the reference simulation (SIMULATE-3).

The static core simulations with TRADYN (PARCS) and TRADYN (DYN3D) were done for sets of nuclear data in NEMTAB format generated by the developed GENSIM-XS-methodology taking into account the history effects.

In the Table 7-2, the initial steady state conditions calculated with SIMULATE-3 and TRADYN (PARCS and DYN3D) are given. The comparison shows almost no difference in the important thermal-hydraulic core parameters. In the same table, it can be observed that the pressure drop is overestimated by around 8 kPa by TRADYN (PARCS) and one 1kPa by TRADYN (DYN3D). However, this difference in TRADYN (PARCS) is not so significant, due to the fact that the operation pressure of the reactor is several orders of magnitude higher (7000 kPa) than this

value. Additionally, the void fraction predicted by TRADYN (PARCS) is equal to the one calculated by SIMULATE-3. Whereas, the one predicted by TRADYN (DYN3D) is only underestimated by 1.2%.

Table 7-2: LVNPP initial conditions comparison to TRADYN predictions.

Parameter	S3	TRADYN (PARCS)	Rel. Dif (%)	TRADYN (DYN3D)	Rel. Dif (%)
Core Outlet Pressure (MPa)	6.51	6.51	0	6.51	0
Core Inlet Pressure (MPa)	6.55	6.558	0.122	6.551	0.152
Core Pressure Drop (MPa)	0.04	0.048	20	0.041	2.5
Core Average Void (fraction)	0.364	0.364	0	0.360	-1.2

The effective multiplication factor k_{eff} predicted by the codes is compared in Table 7-3. The results predicted by TRADYN (PARCS) exhibits a difference of -33 pcm, which is quite acceptable. On the other hand, the TRADYN (DYN3D) results underpredicts k_{eff} by 1210 pcm.

Table 7-3: Comparison of k_{eff} between SIMULATE-3 (reference) and TRADYN simulations.

	SIMULATE-3 (Reference)	TRADYN (PARCS)	Diff (pcm)	TRADYN (DYN3D)	Diff (pcm)
k_{eff}	0.98298	0.98265	-33.58	0.971064	-1210.22

This deviation in DYN3D results can be interpreted as either more neutron leakage or more neutron consumption in the reactor core, which can be originated by less fissile material or more absorption without producing a fission reaction. To find the root causes of this deviation, parameters including, but not limited to, power, mass flow rate, boundary conditions, fuel composition and position in the core, reflectors model, control rod pattern definition and position were exhaustively reviewed. Nevertheless, no significant differences were found regarding both TRADYN (PARCS) and S3 models. Additionally, a comparison of the initial thermal-hydraulic conditions at the first TH-NK iteration (see Figure 4-3) in TRADYN (PARCS) and TRADYN (DYN3D) has been performed. At this point TRACE supplies the same thermal-hydraulic conditions to DYN3D or PARCS to update the cross section (same library in both codes). Therefore, the differences can only be caused by the neutron flux

distribution calculated by DYN3D multigroup diffusion solver. This conclusion is discussed in the following sections.

In Figure 7-5, a comparison of the core average normalized (to unity) axial power distribution as function of the axial core height predicted by S3 and TRADYN simulations is depicted. It can be seen that the TRADYN (PARCS) predictions follow the shape of the curve but not the level, because the height of the power peak is underestimated by 14%. Additionally, deviations up to 17% can be found in the top part of the core. An explanation of these differences is mainly due to the simplification of the neutronics domains (XS) done during the cross section generation (see 5.2), similar observation has been found by (Demazière, et al., 2012). It can be stated that the exposure criterion (1.5 GWd/t) selected is not enough to catch all the heterogeneities of the fuels. It is expected a reduction in the differences by increasing the number of cross sections sets. However, the larger differences in the bottom (underprediction of 25%) and top (overprediction of 24%) part of the core obtained by TRADYN (DYN3D) cannot be fully explained by these arguments. Here, an almost flat power profile is predicted, which does not correspond to the reactor operating conditions.

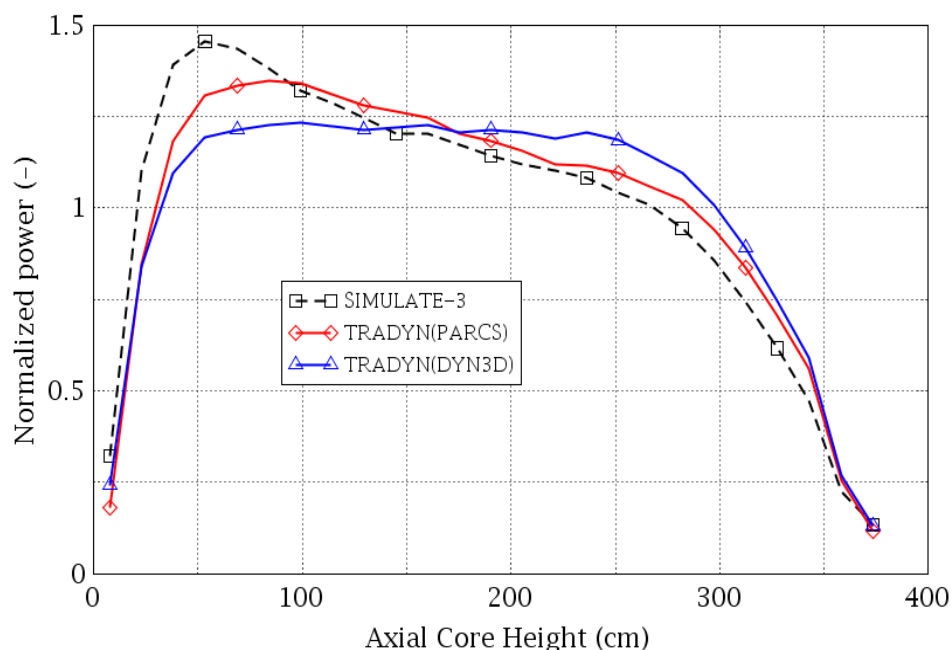


Figure 7-5 Core average normalized axial power distribution comparison between SIMULATE-3 and TRADYN (PARCS) predictions.

The axial power distribution leads to the core averaged axial void fraction distribution depicted in Figure 7-6. Here, it can be seen a deviation³ up to -0.02 in TRADYN (PARCS) predictions due to the pressure losses in the spacers locations. However, TRADYN (DYN3D) underpredicts the void in the bottom and middle part of the core by -0.04 . This is consequence of the flat power profile obtained.

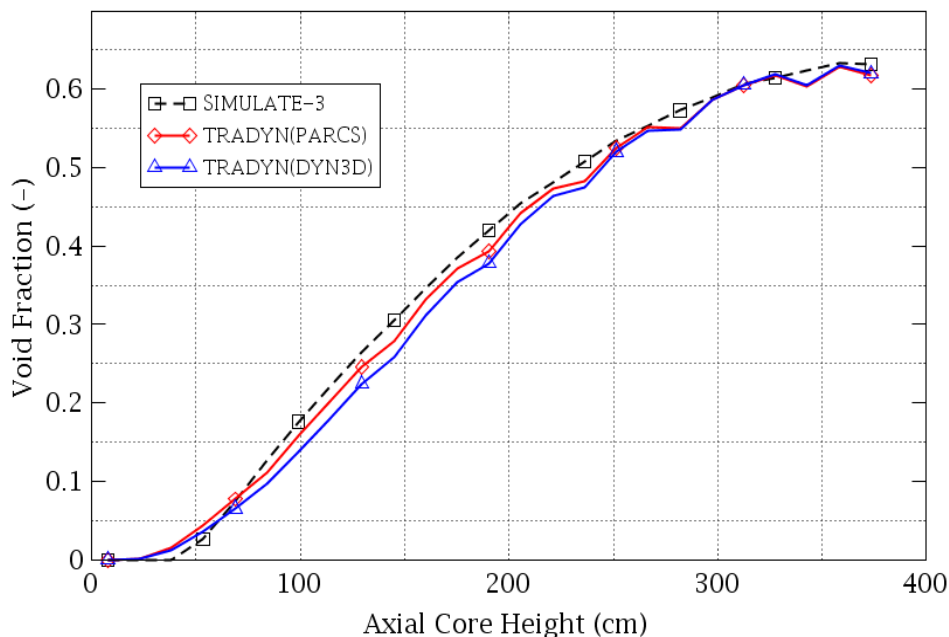


Figure 7-6 Core average axial void fraction comparison between S3 and TRADYN predictions.

It is important to remark that the results of TRADYN (PARCS) are satisfactory and for DYN3D similar results were expected and because the solvers of both codes are equivalent and both are using the same cross section sets in the same format (multigroup NEMTAB), the difference can be due to the predicted neutron flux in DYN3D, see equation (3-11). Thereby, to find the root causes of these deviations in the axial power profile in TRADYN (DYN3D), subroutines managing the transfer and reading of TRACE thermal-hydraulic data, the reading and updating of the cross sections for every node, the calculation of the nodal power and its transfer to TRACE, the modelling of control rods and their axial position, the reading of ADF and its use in the solver (this last activity could not be achieved due to the lack of documentation in the source code of DYN3D) were exhaustively reviewed. However, any inconsistency was detected.

Additionally, a comparison of the core average axial fast and thermal neutron flux predicted by S3 and TRADYN (DYN3D) simulations is performed. The Figure 7-7 and Figure 7-8 depict the

³ Deviation = $predicted - average$

comparisons for the fast and thermal flux, respectively. It can be seen that both neutron fluxes predicted by TRADYN have an order of magnitude of $1E-20$, which is 7 orders of magnitude higher than the ones predicted by SIMULATE-3. This fact is a confirmation that there are problems with the multigroup diffusion solver of DYN3D. A deeper analysis should be conducted in the future.

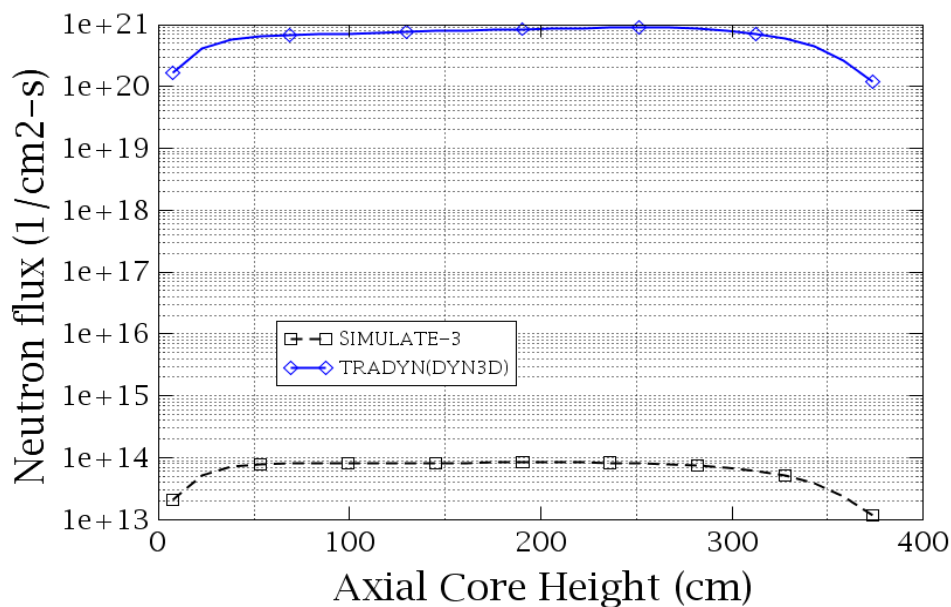


Figure 7-7 Comparison of the core average axial fast neutron flux predicted by S3 and TRADYN (DYN3D).

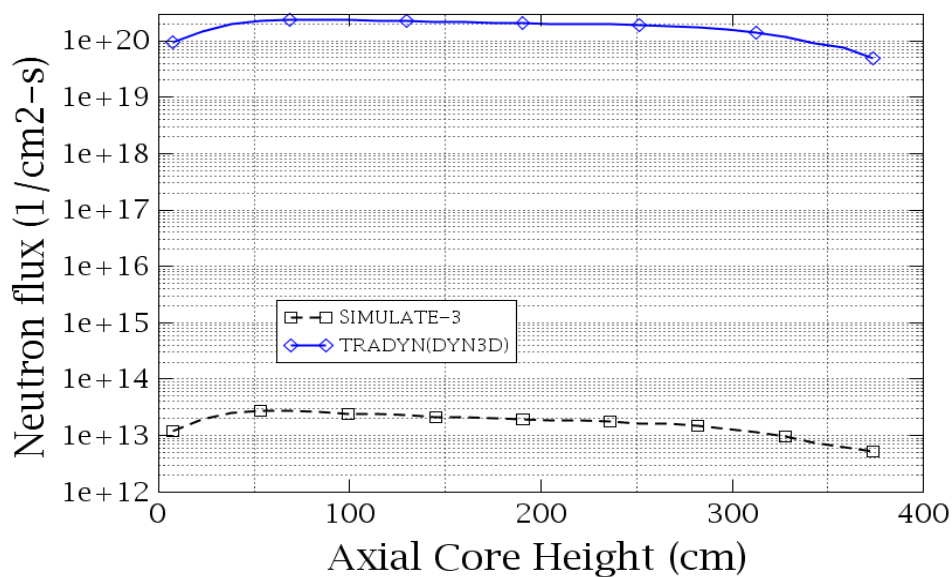


Figure 7-8 Comparison of the core average axial thermal neutron flux predicted by S3 and TRADYN (DYN3D).

Finally, an assessment of the local parameters has been performed. In the Figure 7-9, a comparison of the fuel assembly average relative power distribution between S3 and TRADYN (DYN3D) is depicted. However, a non-symmetrical distribution, with large differences where the control rods are inserted, is depicted. A checking of the ADF implementation in terms of their values, orientation depending on the control rod position has been carried out. They have been also compared with the ones used by PARCS, but any inconsistency was found.

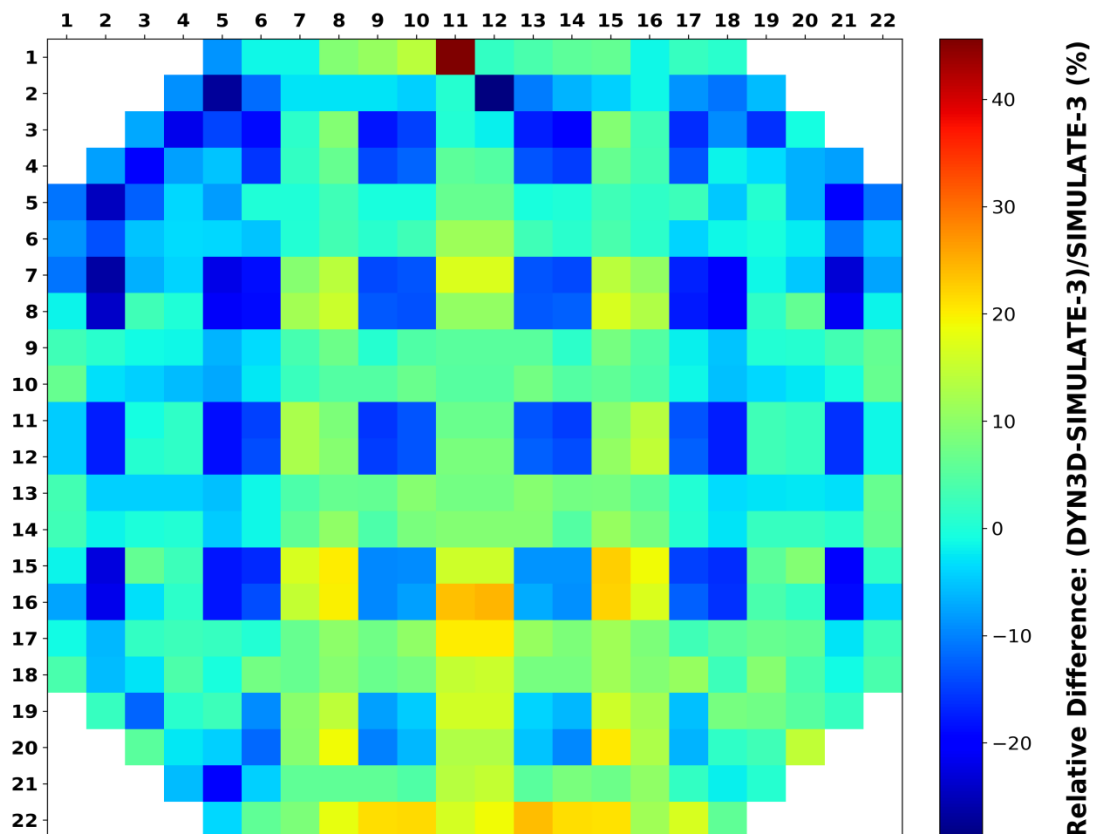


Figure 7-9 Relative difference of the core averaged radial power distribution between S3 and TRADYN (DYN3D).

In the Figure 7-9, the biggest relative difference (40%) is exhibited in the fuel assembly located in the position (11, 1). Consequently, the local parameters of the fuel assembly located in the position (11, 1) were evaluated in more detail. First, it has been verified that the XS sets used for describing correspond to materials in the fuel assembly.

Then, the fuel assembly averaged axial power at the position (11, 1) predicted by S3 and DYN3D using the different models included in DYN3D was compared to each other in Figure 7-10. It can be clearly seen that DYN3D is always overestimating the power in all the axial nodes. A comparison of the nodal fast and thermal neutron flux calculated by DYN3D and S3 is

depicted in Figure 7-11 and Figure 7-12, respectively. Here, it is also confirmed that there is a problem in the magnitude of the neutron flux calculated by the multigroup diffusion solver of DYN3D.

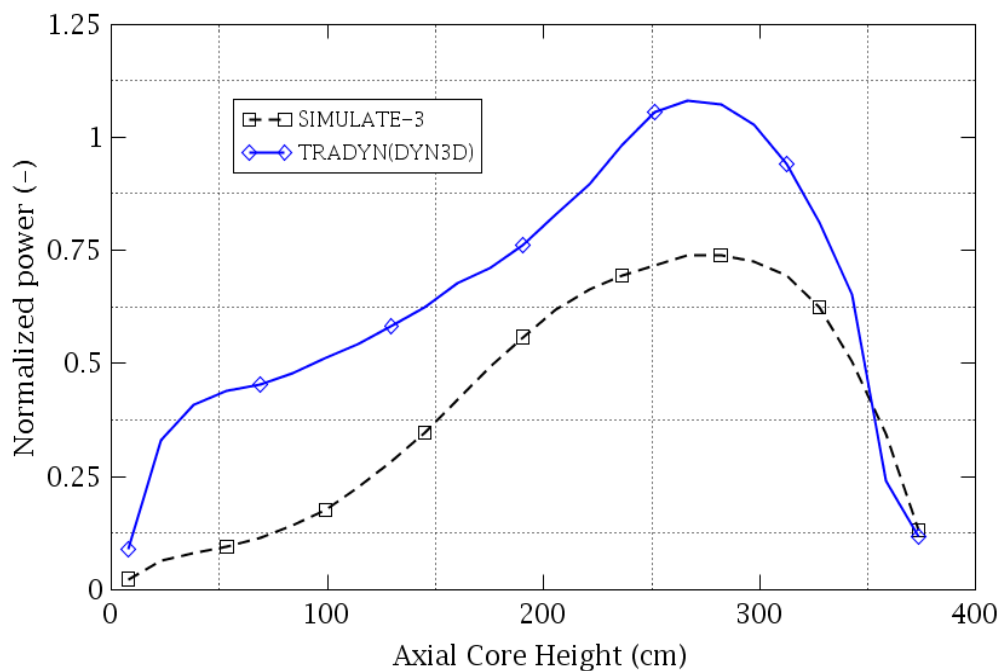


Figure 7-10 Fuel assembly normalized axial power distribution comparison between SIMULATE-3 and TRADYN (DYN3D) predictions, for the fuel assembly located in the position (11, 1).

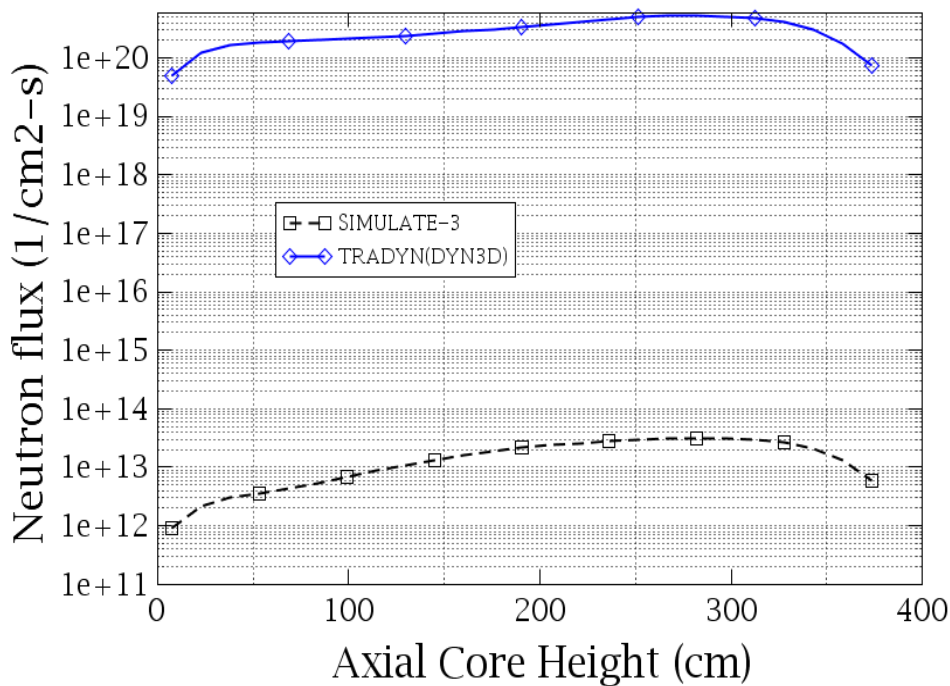


Figure 7-11 Comparison of the nodal fast neutron flux calculated with SIMULATE-3 and TRADYN (DYN3D) for the fuel assembly located in the position (11, 1).

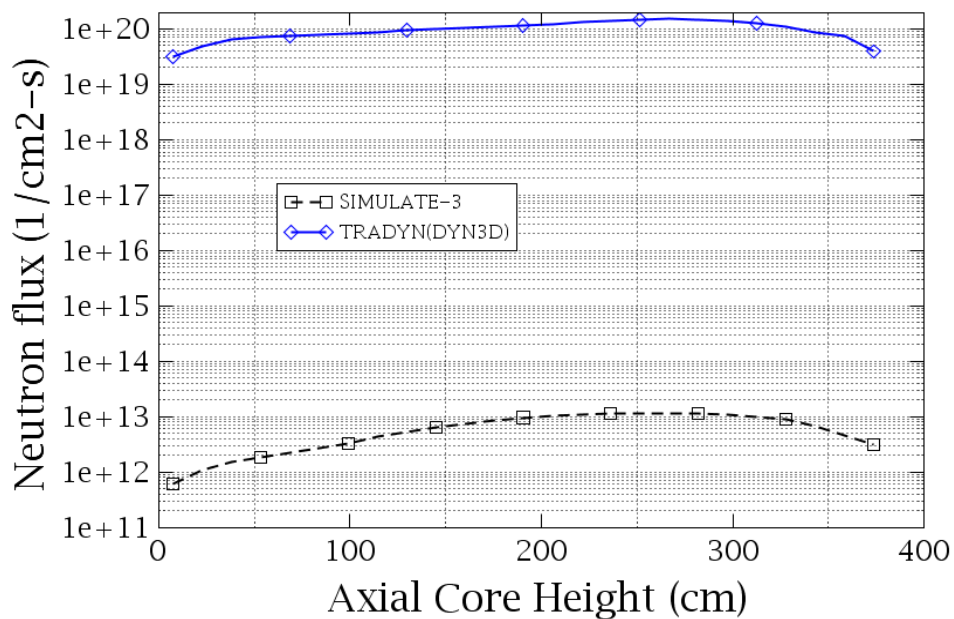


Figure 7-12 Comparison of the nodal thermal neutron flux calculated with S3 and TRADYN (DYN3D) for the fuel assembly located in the position (11, 1).

Finally, the new implemented post-processing capabilities of PARCS and DYN3D based on the ParaVis tool of the SALOME platform has been activated. 3D plots of the power density and fuel Doppler temperature in the core are exhibited in the Appendix E.

8 Summary

The main goals of this PhD work are on one hand the further development of multiphysics coupling methodologies based on thermal-hydraulic and neutronic domains for transient analysis of boiling water reactors in order to describe the main phenomena taking place in the reactor, and on the other hand the development of a new methodology for the generation of cross sections taken into account history effects for BWR.

First at all, a new coupled system code called TRADYN for the simulation of steady state and transient conditions on BWRs has been developed and described in chapter 4. In TRADYN, the best-estimate core simulator DYN3D was internally coupled with the widely used thermal-hydraulic code TRACE. Moreover, during this development, a computational route using FORTRAN preprocessor directives for coupling TRACE to any other core simulator was established. This has allowed the merging of DYN3D as an internal module of TRACE preserving all the capabilities of TRACE/PARCS. Now, in TRADYN the user has the option to select either PARCS or DYN3D as neutronic solver.

During the development of TRADYN, implementations in PARCS and DYN3D were done in order to improve the simulations of BWR. In the case of PARCS a new module for reading the cross sections in multigroup NEMTAB format was implemented. While in DYN3D, the inclusion of gamma heating, correction of the cross section by the density in the channel bypass and the ADF orientation were implemented.

A new in-house methodology called GENSIM-XS for the generation of nodal cross sections considering history void and history control rod effects for BWR cores has been developed. This methodology aims to simplify the number of the neutronics regions present in the reactor core in order to reduce the computational time preserving the accuracy on the calculation. The description and application of GENSIM-XS to the BWR Laguna Verde is given in the chapter 5.

From the validation of TRADYN against the Peach Bottom Turbine Trip Test presented in the chapter 6, the following conclusions can be drawn:

1. Steady state conditions: TRADYN is suitable to reproduce the measurements and its predictions are in good agreement with other participants. This confirms clearly not only the correct implementation of the physical models but also the consistency in the data transfers between the codes. The source of the differences exhibited in the predictions of the global parameters as well as k_{eff} is mainly due to the several factors

such as: homogenization of cross sections, the uncertainty associated with the measurement and the number thermal-hydraulic channels.

2. Transient conditions: The results of TRADYN match the measurements very well until the SCRAM is initiated. But after this time, both TRADYN (PARCS) and TRADYN (DYN3D) underestimate the value of dome pressure, the predictions qualitatively follow the shape of pressure evolution data. This lower pressure leads to lower power increase because less void collapsing is carried out in the core. Therefore, a deviation of 30% in the power peak height is obtained. Similar results are obtained using the original release of TRACE/PARCS version 5 patch 4. On-going investigations to overcome this problem are performed by main developers of TRACE/PARCS.

The static core of Laguna Verde has been simulated with TRADYN using the cross sections generated with GENSIM-XS, as presented in chapter 7. The results of TRADYN for the global parameters are in good agreement with SIMULATE-3 results. A small difference for k_{eff} (33 pcm) and core average normalized axial power (14%) between TRADYN (PARCS) and SIMULATE-3 results are obtained. The selection of smaller exposure criterion could reduce the errors introduced because of collapsing and averaging of fuels assemblies leading to improve the results in TRADYN. However, the TRADYN (DYN3D) results exhibit larger deviation in both k_{eff} (-1210 pcm) and core average normalized axial power (24%), respectively. Analyses performed to find the root of such deviations show problems in the prediction of the neutron flux distribution by DYN3D multigroup solver.

9 Outlook

Despite the described developments, extensions and implementations performed in the frame of this dissertation, areas of future work have been identified. Hereafter, a list of the most important issues to be tackled for TRADYN is given:

- Further verification and validation of TRADYN must be carried out in order to analyse other transient scenarios having a strong interaction between the thermal-hydraulic and neutronics domain. In this sense, at least 2 BWR cases have been identified: 1) the Oskarshamn-2 instability benchmark, recently a new cross section library on multi-group NEMTAB format was delivered, and 2) The instability event occurred in the cycle 4 of Laguna Verde Nuclear Power Plant.

The future investigations related to TRACE/PARCS system can be summarized hereafter:

- Further investigations have to be performed in the new models implemented in current versions of TRACE. Because they are not able to predict the previous results calculated for the Peach Bottom Turbine Trip test, specially the height of the peak power during transient.

Future work related to GENSIM-XS methodology is given below:

- To increase the cross section sets and reduce the errors (introduced due to collapsing and averaging of fuels assemblies) further investigations with more restrictive exposure criteria must be performed.
- The validation of the GENSIM-XS must be extended to other BWR cases in order to cover a major range of reactor sizes and conditions. This methodology can be also extended in order to be applied to PWRs. In fact, current efforts are been performed in this direction, but they are out of the scope of this dissertation.
- Additional history effects such as fuel temperature, moderator density, etc. can be included in order to quantify their impact on the simulations.
- The methodology can be complemented with uncertainty and sensitivity analysis tools, such as URANIE or SUSA (Glaeser, 2008).
- The use of different meshes for the thermal-hydraulic conditions considered for the generation of the cross section has been investigated in the recent years (Sanchez-Cervera, et al., 2014). Therefore, some efforts should be done in this direction in order to see the impact on the coupled simulations.

Finally, the future work related to DYN3D-MG core simulator is described hereafter:

- Because the development of the multi-group version of DYN3D was done (by the main developers) based on the two-group version, it is highly recommended to carry out an exhaustive review of all subroutines involved in this implementation with the goal to detect if some capabilities were not properly considered. During this PhD work some issues were detected: the xenon concentration input file was not processed, the output file was not able to manage the size of big BWR cores, the inclusion of ADFs is not well implemented, a new module for performing pin power reconstruction is necessary, etc.
- Other big area for improvements is related to the reduction of the computational time in DYN3D. This fact is directly linked to the lack of preconditioned solvers. Therefore, they should be implemented in DYN3D in order to make it competitive with other core simulators present in the nuclear field.
- The last topic points out the urgent necessity to refactor DYN3D, i.e. rewrite the code without changing its functionality. This is a challenging activity, because it implied to redesign DYN3D using a modular structure. But this structure has the advantage that one module is easier to conceive, understand, program and maintain. During the refactoring process, factors such as readability, automatic generation of documentation, use of preconditioned Krylov subspace solvers from third party libraries and use of parallel computing must be considered.
- Other option is to continue using the two-group version of DYN3D. This version was not only validated for BWRs (against PBTT) and other Benchmarks but also integrated in NURESIM platform. Furthermore, it can be coupled to TRACE following the coupling strategy developed during this PhD work.

List of figures

Figure 1-1 General scheme of a Nuclear Power Plant with a Boiling Water Reactor taken from (Chaparro-Vega, 2014). -----	8
Figure 1-2 Detailed display of a typical BWR pressure vessel and its internal structures taken from (ANS , 2012).-----	9
Figure 1-3 Example of a typical BWR fuel assembly taken from (ANS , 2012). -----	10
Figure 2-1 Internal Coupling between a neutron kinetic code and a system code from (Gomez-Torres, 2011).-----	16
Figure 2-2 External coupling between a reactor dynamics code and a system code from (Gomez-Torres, 2011). -----	17
Figure 2-3 Thermal-hydraulic channels of the radial mapping scheme used to represent the Peach Bottom reactor core (Solis, et al., 2001). -----	19
Figure 2-4 Scheme used for the axial mapping between Thermal-hydraulic and Neutronics domains used in the Peach Bottom Turbine Trip benchmark. -----	19
Figure 2-5 Explicit temporal coupling approach in TRACE/PARCS system; both codes use the same time step calculated by TRACE (master). -----	21
Figure 2-6 Global computational scheme for a deterministic reactor physics calculation. -----	22
Figure 3-1 Different vertical flow regimes available in TRACE for the Pre-CHF at the interface taken from (TRACE, 2013). -----	30
Figure 3-2 Schematic diagram of the data exchange between TRACE and PARCS via the General Interface (Barber, et al., 1998).-----	34
Figure 4-1 Flow of information between TRACE and DYN3D through the TDMR, GI and DDMR modules. -----	38
Figure 4-2 Schematic diagram of the data exchange between TRACE and DYN3D, now the user can select between PARCS and DYN3D as neutronics solver, just by changing a single variable (itdmr) in the TRACE input. -----	39
Figure 4-3 Flow diagram for the steady state calculation in TRADYN, when DYN3D is selected as neutronics solver. -----	40
Figure 4-4 Flow diagram for the transient calculation in TRADYN, when DYN3D is selected as neutronics solver. -----	41
Figure 4-5 Explicit coupling scheme between TRACE and DYN3D. It can be noticed the subdivision of the DYN3D time step within one time step of TRACE. -----	43
Figure 4-6 Channel bypass consideration in TRADYN for BWR fuel assemblies.-----	45

Figure 4-7 Fuel assembly orientation used by the lattice code CASMO-4 for ADF assignment, notice that the control rod is located in the top left corner. -----	45
Figure 4-8 Fuel assembly rotation index depending on the rotation degree considered in DYN3D, a) rotated assembly 90 degree (index = 1), b) rotated assembly 180 degree (index = 2) and c) rotated assembly 270 degree (index = 3). -----	46
Figure 5-1 Flowchart of the information transfer between SIMULATE-3 and the GENSIM-XS methodology. -----	50
Figure 5-2 Core configuration at the beginning of cycle 4 of Laguna Verde Nuclear Power Plant, which is composed of 9 different fuel types, the fuel type 0 represents the radial reflector. -----	52
Figure 5-3 Map of the radial fuel assembly exposure almost at the end of the cycle 4 of the LVNPP core. The range of exposure for the fuel type 1 (highlighted in yellow) is [18.42 - 22.13 GWd/t]. -----	53
Figure 5-4 Radial core mapping of fuel assembly subtypes according to the exposure criterion methodology (GENSIM-XS) for the cycle 4 of LVNPP. The fuel type 0 represents the radial reflector. -----	55
Figure 6-1 TRACE model used for the simulation of Peach Bottom Turbine Trip test. -----	60
Figure 6-2 Cross sectional view of the Peach Bottom reactor core illustrating the fuel assemblies, control rods and radial reflectors (Solis, et al., 2001).-----	61
Figure 6-3 Reactor core thermal-hydraulic channel radial mapping scheme used to represent the Peach Bottom reactor core (Solis, et al., 2001). -----	61
Figure 6-4 Control rod positions within the core at the beginning of the transient for the Peach Bottom Turbine (Solis, et al., 2001).-----	62
Figure 6-5 Core average relative axial power distribution comparison between the measurements and TRADYN predictions. -----	65
Figure 6-7 Core average axial void fraction comparison between the measurements and TRADYN predictions. -----	65
Figure 6-7 Steam dome pressure evolution comparison during the transient case between TRADYN and the measurements. -----	67
Figure 6-8 Total power comparison during transient between TRADYN calculations and the measurements. -----	67
Figure 6-9 TRADYN results for the core total reactivity and its components. The total reactivity is given in (a), the Doppler reactivity in (b), the moderator density in (c) and the control rod reactivity in (d). -----	68
Figure 7-1 Fuel assembly and reflector arrangement used in SIMULATE-3 model (the same representation was used in PARCS and DYN3D) for LVNPP. Notice the 109 control rods present in the core.-----	70

Figure 7-2 Control rod pattern for static state of the cycle 4 of LVNPP. -----	71
Figure 7-3 Thermal-hydraulic model for TRACE code used for the simulation of LV containing 29 channels for representing the core. -----	72
Figure 7-4 Reactor core thermal-hydraulic channel radial mapping scheme used to represent the LV core. -----	73
Figure 7-5 Core average normalized axial power distribution comparison between SIMULATE- 3 and TRADYN (PARCS) predictions. -----	75
Figure 7-6 Core average axial void fraction comparison between S3 and TRADYN predictions. -----	76
Figure 7-7 Comparison of the core average axial fast neutron flux predicted by S3 and TRADYN (DYN3D). -----	77
Figure 7-8 Comparison of the core average axial thermal neutron flux predicted by S3 and TRADYN (DYN3D). -----	77
Figure 7-9 Relative difference of the core averaged radial power distribution between S3 and TRADYN (DYN3D). -----	78
Figure 7-10 Fuel assembly normalized axial power distribution comparison between SIMULATE-3 and TRADYN (DYN3D) predictions, for the fuel assembly located in the position (11, 1). -----	79
Figure 7-11 Comparison of the nodal fast neutron flux calculated with SIMULATE-3 and TRADYN (DYN3D) for the fuel assembly located in the position (11, 1).-----	79
Figure 7-12 Comparison of the nodal thermal neutron flux calculated with S3 and TRADYN (DYN3D) for the fuel assembly located in the position (11, 1).-----	80

List of tables

Table 5-1: Different fuel designs present in cycle 4 of Laguna Verde Nuclear Power Plant.----	51
Table 5-2: Exposure ranges calculated by the GENSIM-XS methodology (based on delta exposure) for every fuel type present in the cycle 4. As a result, every fuel type is divided in subtypes resulting in 29 fuel subtypes. -----	54
Table 5-3: Determination of the nodal axial average exposure (GWd/t) of all fuel elements belonging to subtype 1, the Bottom and top reflectors were also added. -----	56
Table 6-1: Peach Bottom Turbine Trip Initial Conditions as provided by (Solis, et al., 2001). -	62
Table 6-2: Measured turbine trip initial conditions comparison to TRADYN predictions. -----	63
Table 6-3: Comparison of the effective multiplication factor k_{eff} , deviation, and difference of TRADYN predictions and average value of benchmark results. -----	64
Table 7-1: Initial core static conditions for LVNPP used in S3 model -----	70
Table 7-2: LVNPP initial conditions comparison to TRADYN predictions.-----	74
Table 7-3: Comparison of k_{eff} between SIMULATE-3 (reference) and TRADYN simulations. -----	74
Table A-1: New modules created due to the development of the DYN3D general interface. ---	91
Table A-2: New modules created due to the development of the DYN3D Specific Data Map routines (DDMR). -----	91

Appendix A

Table A-1: New modules created due to the development of the DYN3D general interface.

Module or Subroutine	Description
GiMd	GI main module containing the subroutines for the coupling between TRACE and DYN3D
Gi_varMd	Definition of the global variables needed by the GI
Gi_varmcopyMd	Definition of the shared buffer variables
Gi_varmapMd	Definition of the variables needed for mapping between TRACE and DYN3D
Gi_timeMd	Module containing the subroutines managing the time-dependent calculation in the GI
Gi_mapMd	Module containing the subroutines used during mapping process
Gi_initMd	Module containing the subroutines used during the initialization stage
Gi_errorMd	Module containing the subroutines used to verify the correct transfer of information
Gi_commMd	Module containing the subroutines used to communicate the the GI and DDMR and TDMR units
Gi_arfuncMd	Subroutine for calculating the arcsin and arctan
Gi_allocMd	Module containing the subroutines used to allocate the arrays
Gi_3dmapMd	Module containing the subroutines for the mapping between a 3D TH Core and a 3D Neutronics Core
Gi_1dmapMd	Module containing the subroutines for the mapping between a 1D TH Core and a 1D Neutronics Core

Table A-2: New modules created due to the development of the DYN3D Specific Data Map routines (DDMR).

Module or Subroutine	Description
DdmrM	DDMR main module containing the subroutines for transferring information between the GI and DYN3D
Ddmr_varM	Definition of the global variables needed by the DDMR
Ddmr_timeM	Module containing the subroutines managing the time-dependent calculation in the DDMR
Ddmr_mapM	Module containing the subroutines used during mapping process

Ddmr_initM	Module containing the subroutines used during the initialization stage
Ddmr_errorM	Module containing the subroutines used to verify the correct transfer of information
Ddmr_commM	Module containing the subroutines used to communicates with the GI
Ddmr_allocM	Module containing the subroutines used to allocate the arrays

Appendix B

New key features of TRADYN

The internal coupling between TRACE and DYN3D has been realized under the premise to preserve the original codes as much as possible. Then, if new versions of the codes are released, in principle only minor changes are required to update the coupled system. Because the structure of TRADYN is organized into FORTRAN 90 modules, the merging of DYN3D represented (from the programming point of view) the inclusion of one additional module.

In the Figure B-1, it can be seen that the main folder TRADYN system is integrated by 3 subfolders: 1) *Tag* that can contain previous versions of the code, 2) *Branches* that can contain parallel versions of the code and 3) *trunk*, the main folder containing all the necessary modules and subroutines for compiling the code. In this subfolder, the modules DYN3D, PARCS, among others are included. In order to compile TRADYN, the platform independent software construction tool SCons (<http://scons.org>) is used. A local version of SCons is also included in the source of TRADYN. Currently, both Windows and Linux operating systems with 32bit or 64bit architectures are supported.

On the other hand, because the integration of DYN3D is based on compiler preprocessor directives, it has the novel capability that the user can select one of the following optional computational routes in TRADYN:

- The original TRACE/PARCS system,
- TRACE/DYN3D and
- DYN3D

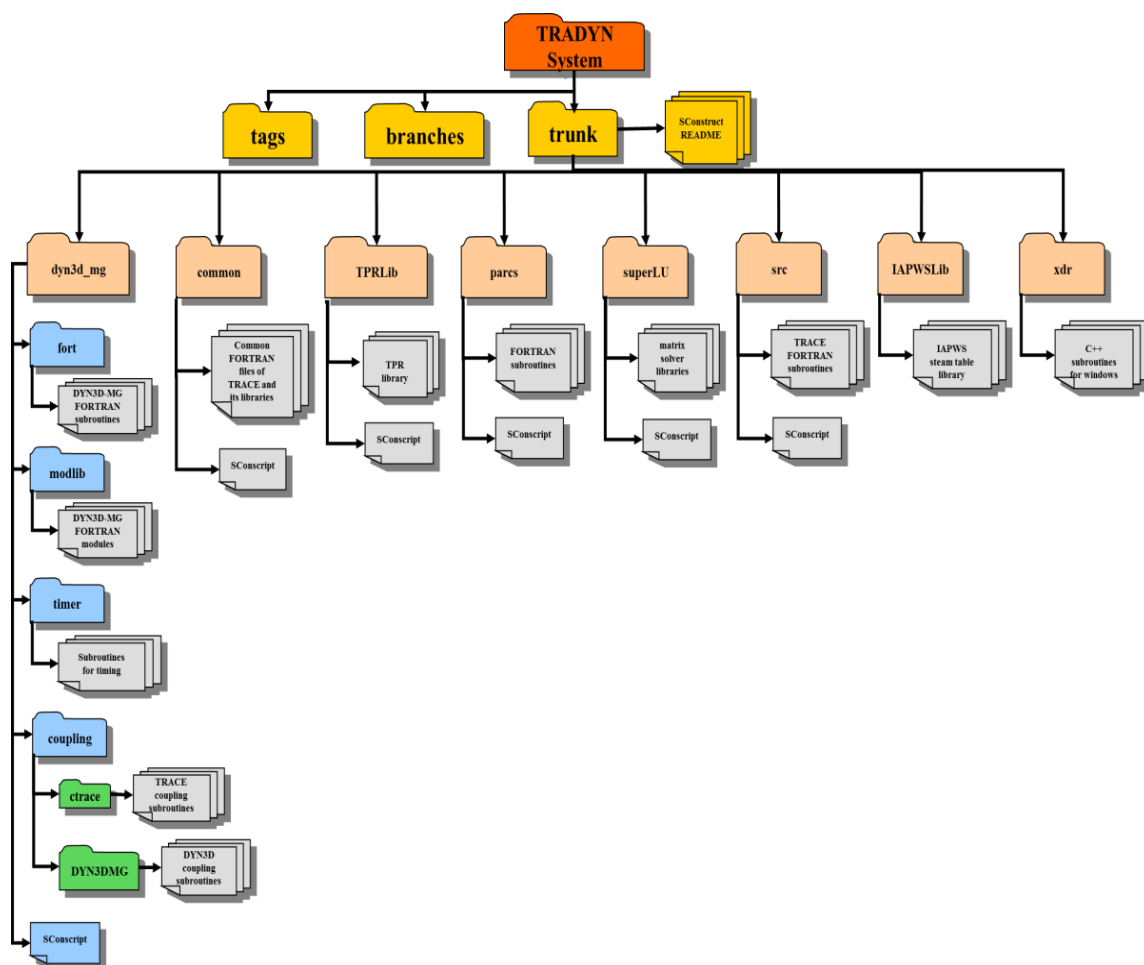


Figure B-1 Structure of TRADYN system as distributed project including DYN3D, PARCS among other modules.

Extensions of DYN3D input and output files

Because the multi-group version of DYN3D inside TRADYN has not been used for the modelling of BWR cores, extensions of the input/output files are implemented, e.g.:

- New card (“BWR”) for indicating the code the type of reactor.
- Allow the user to give core map bigger than 17x17 assemblies (~ PWR core size geometry).
- New card for activating the MED file capability (the same flag was implemented in PARCS).
- New card for activating ADF rotation. Additionally if the rotation is activated, a core map indicating the rotation index per fuel assembly must be given.

The aim of the extensions in the output file is twofold: on one hand to get better presentation of the results for BWRs and on the other hand to facilitate the code-to-code comparison with PARCS. The extensions done can be summarized as follow:

- Correct creation of the two-dimensional assembly normalized power distribution for BWRs geometry
- The creation of two-dimensional assembly maps for the thermal-hydraulic feedback parameters such as: Fuel temperature, moderator temperature and density. In fact, a 2-D map is also reported for every axial level in the assembly for all the parameters

Furthermore, the creation of a summary file during both steady state and transient calculation was implemented. Now, during a steady state simulation, variables such as: power, fuel temperature, moderator temperature and density at every thermal-hydraulic and neutronics iteration are reported. For transient calculations, in addition to variables reported during a steady state simulation, the reactivity coefficients due to Doppler temperature, moderator temperature and density, and control rod are also reported and plotted.

Last but not least, python scripts are created in order to extract selected data and obtain comparison graph automatically.

Appendix C

Example of a cross section set created by GENSIM-XS

```

*      Mod Dens      Boron ppm      Fuel Temp      Mod Temp
   6      0      6      0
  177.20  247.30  317.40  457.60  597.80  738.00
  400.00  800.00  1200.00  1600.00  2000.00  2400.00
*
*-----
* EXPOSURE 0.00000
*-----
*
* Diffusion Coefficient Table
*
* GROUP 1
  2.01503E+00  1.92986E+00  1.84500E+00  1.68229E+00  1.54596E+00  1.43996E+00
  2.02000E+00  1.93452E+00  1.84936E+00  1.68608E+00  1.54928E+00  1.44294E+00
  2.02512E+00  1.93932E+00  1.85383E+00  1.68995E+00  1.55267E+00  1.44599E+00
  2.02952E+00  1.94344E+00  1.85768E+00  1.69328E+00  1.55559E+00  1.44861E+00
  2.03340E+00  1.94707E+00  1.86106E+00  1.69621E+00  1.55816E+00  1.45092E+00
  2.03690E+00  1.95036E+00  1.86413E+00  1.69886E+00  1.56049E+00  1.45301E+00
*
* GROUP 2
  5.65368E-01  5.27728E-01  4.90357E-01  4.22608E-01  3.70577E-01  3.33185E-01
  5.66955E-01  5.29157E-01  4.91629E-01  4.23618E-01  3.71414E-01  3.33937E-01
  5.68665E-01  5.30700E-01  4.93007E-01  4.24716E-01  3.72321E-01  3.34744E-01
  5.70139E-01  5.32032E-01  4.94196E-01  4.25664E-01  3.73104E-01  3.35440E-01
  5.71438E-01  5.33204E-01  4.95244E-01  4.26499E-01  3.73794E-01  3.36053E-01
  5.72612E-01  5.34265E-01  4.96191E-01  4.27253E-01  3.74417E-01  3.36607E-01
*
* Absorption XSEC Table
*
* GROUP 1
  5.78559E-03  5.99125E-03  6.19529E-03  6.56107E-03  6.83670E-03  7.01872E-03
  5.92217E-03  6.13846E-03  6.35304E-03  6.73682E-03  7.02485E-03  7.21362E-03
  6.02701E-03  6.25148E-03  6.47419E-03  6.87187E-03  7.16952E-03  7.36378E-03
  6.11540E-03  6.34677E-03  6.57633E-03  6.98573E-03  7.29150E-03  7.49039E-03
  6.19328E-03  6.43072E-03  6.66631E-03  7.08604E-03  7.39896E-03  7.60194E-03
  6.26368E-03  6.50662E-03  6.74766E-03  7.17673E-03  7.49612E-03  7.70279E-03
*
* GROUP 2
  4.25715E-02  4.30836E-02  4.36000E-02  4.47042E-02  4.57665E-02  4.68180E-02
  4.24034E-02  4.29111E-02  4.34231E-02  4.45206E-02  4.55796E-02  4.66245E-02
  4.22397E-02  4.27420E-02  4.32485E-02  4.43374E-02  4.53916E-02  4.64292E-02
  4.20994E-02  4.25969E-02  4.30987E-02  4.41802E-02  4.52301E-02  4.62613E-02
  4.19758E-02  4.24691E-02  4.29667E-02  4.40417E-02  4.50879E-02  4.61135E-02
  4.18641E-02  4.23536E-02  4.28474E-02  4.39164E-02  4.49593E-02  4.59798E-02
*
* Nu-Fission XSEC Table
*
* GROUP 1
  2.90330E-03  2.97538E-03  3.04694E-03  3.17897E-03  3.28330E-03  3.35926E-03
  2.88767E-03  2.95967E-03  3.03116E-03  3.16311E-03  3.26746E-03  3.34348E-03
  2.87195E-03  2.94383E-03  3.01520E-03  3.14699E-03  3.25128E-03  3.32730E-03
  2.85845E-03  2.93023E-03  3.00149E-03  3.13313E-03  3.23738E-03  3.31338E-03
  2.84656E-03  2.91824E-03  2.98941E-03  3.12093E-03  3.22513E-03  3.30112E-03
  2.83580E-03  2.90740E-03  2.97849E-03  3.10989E-03  3.21406E-03  3.29004E-03
*
* GROUP 2
  5.47208E-02  5.49325E-02  5.51430E-02  5.55426E-02  5.58727E-02  5.61155E-02
  5.45122E-02  5.47188E-02  5.49242E-02  5.53173E-02  5.56459E-02  5.58824E-02
  5.43156E-02  5.45155E-02  5.47142E-02  5.50978E-02  5.54223E-02  5.56510E-02
  5.41474E-02  5.43414E-02  5.45344E-02  5.49096E-02  5.52304E-02  5.54523E-02
  5.39992E-02  5.41880E-02  5.43759E-02  5.47438E-02  5.50614E-02  5.52773E-02
  5.38653E-02  5.40494E-02  5.42326E-02  5.45939E-02  5.49087E-02  5.51191E-02
*
* Kappa-Fission XSEC Table
*
* GROUP 1
  3.57393E-14  3.66472E-14  3.75496E-14  3.92193E-14  4.05432E-14  4.15201E-14
  3.55339E-14  3.64409E-14  3.73427E-14  3.90113E-14  4.03358E-14  4.13134E-14
  3.53279E-14  3.62332E-14  3.71334E-14  3.88002E-14  4.01237E-14  4.11018E-14
  3.51509E-14  3.60553E-14  3.69540E-14  3.86186E-14  3.99418E-14  4.09196E-14
  3.49953E-14  3.58981E-14  3.67958E-14  3.84592E-14  3.97817E-14  4.07593E-14
  3.48545E-14  3.57564E-14  3.66530E-14  3.83148E-14  3.96371E-14  4.06142E-14
*
* GROUP 2
  6.73608E-13  6.76593E-13  6.79566E-13  6.85235E-13  6.89933E-13  6.93582E-13
  6.70794E-13  6.73725E-13  6.76644E-13  6.82239E-13  6.86932E-13  6.90505E-13
  6.68136E-13  6.70988E-13  6.73827E-13  6.79317E-13  6.83961E-13  6.87451E-13
  6.65861E-13  6.68649E-13  6.71422E-13  6.76810E-13  6.81416E-13  6.84825E-13
  6.63861E-13  6.66583E-13  6.69297E-13  6.74608E-13  6.79177E-13  6.82514E-13
  6.62053E-13  6.64721E-13  6.67381E-13  6.72613E-13  6.77156E-13  6.80423E-13
*
* A1 Xenon Macroscopic XSEC Table
*
* GROUP 1
  0.00000E+00  0.00000E+00  0.00000E+00  0.00000E+00  0.00000E+00  0.00000E+00
  0.00000E+00  0.00000E+00  0.00000E+00  0.00000E+00  0.00000E+00  0.00000E+00
  0.00000E+00  0.00000E+00  0.00000E+00  0.00000E+00  0.00000E+00  0.00000E+00
  0.00000E+00  0.00000E+00  0.00000E+00  0.00000E+00  0.00000E+00  0.00000E+00

```

```

0.00000E+00 0.00000E+00 0.00000E+00 0.00000E+00 0.00000E+00 0.00000E+00
0.00000E+00 0.00000E+00 0.00000E+00 0.00000E+00 0.00000E+00 0.00000E+00
* GROUP 2
1.03635E-03 1.03348E-03 1.03246E-03 1.03204E-03 1.03263E-03 1.03505E-03
1.03023E-03 1.02757E-03 1.02674E-03 1.02659E-03 1.02740E-03 1.02999E-03
1.02392E-03 1.02142E-03 1.02082E-03 1.02102E-03 1.02209E-03 1.02459E-03
1.01835E-03 1.01605E-03 1.01573E-03 1.01617E-03 1.01741E-03 1.02004E-03
1.01354E-03 1.01139E-03 1.01117E-03 1.01186E-03 1.01322E-03 1.01594E-03
1.00907E-03 1.00714E-03 1.00711E-03 1.00801E-03 1.00958E-03 1.01235E-03
*
* Ax Xenon Microscopic XSEC Table
*
* GROUP 1
0.00000E+00 0.00000E+00 0.00000E+00 0.00000E+00 0.00000E+00 0.00000E+00
* GROUP 2
1.32577E+06 1.34305E+06 1.36029E+06 1.39333E+06 1.42099E+06 1.44965E+06
1.31306E+06 1.33088E+06 1.34867E+06 1.38261E+06 1.41087E+06 1.43994E+06
1.29972E+06 1.31813E+06 1.33650E+06 1.37142E+06 1.40032E+06 1.42800E+06
1.28823E+06 1.30715E+06 1.32602E+06 1.36179E+06 1.39124E+06 1.42107E+06
1.27811E+06 1.29748E+06 1.31680E+06 1.35330E+06 1.38324E+06 1.41338E+06
1.26895E+06 1.28873E+06 1.30845E+06 1.34563E+06 1.37601E+06 1.40643E+06
*
* Scattering XSEC Table
*
* GROUP 1 -> 1
0.00000E+00 0.00000E+00 0.00000E+00 0.00000E+00 0.00000E+00 0.00000E+00
* GROUP 1 -> 2
9.10450E-03 1.03997E-02 1.17001E-02 1.46193E-02 1.75811E-02 2.04410E-02
9.03070E-03 1.03171E-02 1.16088E-02 1.45120E-02 1.74611E-02 2.03124E-02
8.97050E-03 1.02499E-02 1.15346E-02 1.44248E-02 1.73635E-02 2.02076E-02
8.91950E-03 1.01930E-02 1.14718E-02 1.43510E-02 1.72809E-02 2.01187E-02
8.87460E-03 1.01428E-02 1.14164E-02 1.42860E-02 1.72081E-02 2.00404E-02
8.83390E-03 1.00975E-02 1.13664E-02 1.42272E-02 1.71423E-02 1.99677E-02
* GROUP 2 -> 1
0.00000E+00 0.00000E+00 0.00000E+00 0.00000E+00 0.00000E+00 0.00000E+00
* GROUP 2 -> 2
0.00000E+00 0.00000E+00 0.00000E+00 0.00000E+00 0.00000E+00 0.00000E+00
*
* aw ADF3 Table
*
* GROUP 1
0.93356 0.93033 0.92709 0.92000 0.91300 0.90561
0.93356 0.93033 0.92709 0.92000 0.91300 0.90561
0.93356 0.93033 0.92709 0.92000 0.91300 0.90561
0.93356 0.93033 0.92709 0.92000 0.91300 0.90561
0.93356 0.93033 0.92709 0.92000 0.91300 0.90561
0.93356 0.93033 0.92709 0.92000 0.91300 0.90561
* GROUP 2
1.49850 1.48372 1.46900 1.44118 1.41835 1.40618
1.49850 1.48372 1.46900 1.44118 1.41835 1.40618
1.49850 1.48372 1.46900 1.44118 1.41835 1.40618
1.49850 1.48372 1.46900 1.44118 1.41835 1.40618
1.49850 1.48372 1.46900 1.44118 1.41835 1.40618
1.49850 1.48372 1.46900 1.44118 1.41835 1.40618
*
* as ADF4 Table
*
* GROUP 1
0.93325 0.92989 0.92652 0.91915 0.91186 0.90419
0.93325 0.92989 0.92652 0.91915 0.91186 0.90419
0.93325 0.92989 0.92652 0.91915 0.91186 0.90419
0.93325 0.92989 0.92652 0.91915 0.91186 0.90419
0.93325 0.92989 0.92652 0.91915 0.91186 0.90419
0.93325 0.92989 0.92652 0.91915 0.91186 0.90419
* GROUP 2
1.49719 1.48286 1.46859 1.44134 1.41866 1.40622
1.49719 1.48286 1.46859 1.44134 1.41866 1.40622
1.49719 1.48286 1.46859 1.44134 1.41866 1.40622
1.49719 1.48286 1.46859 1.44134 1.41866 1.40622
1.49719 1.48286 1.46859 1.44134 1.41866 1.40622
1.49719 1.48286 1.46859 1.44134 1.41866 1.40622
*
* ch Fission Spectrum
*
* GROUP 1 2
1.0 0.0
*
* Inverse Velocity
*
* GROUP 1 2
6.039e-08 2.6508e-06

```

```
*
* Delay Neutron Decay Constant (Lambda)
*
* GROUP      1      2      3      4      5      6
* 0.012775  0.031621  0.121590  0.321600  1.400200  3.845800
*
* Beta Delay Neutron Fraction
*
* GROUP      1      2      3      4      5      6
* 0.000194  0.001214  0.001085  0.002300  0.000827  0.000199
*
END
```


Appendix D

Results obtained using the new post-processing capability of TRADYN for the Peach Bottom Turbine Trip Benchmark

Steady state simulation with TRADYN (PARCS)

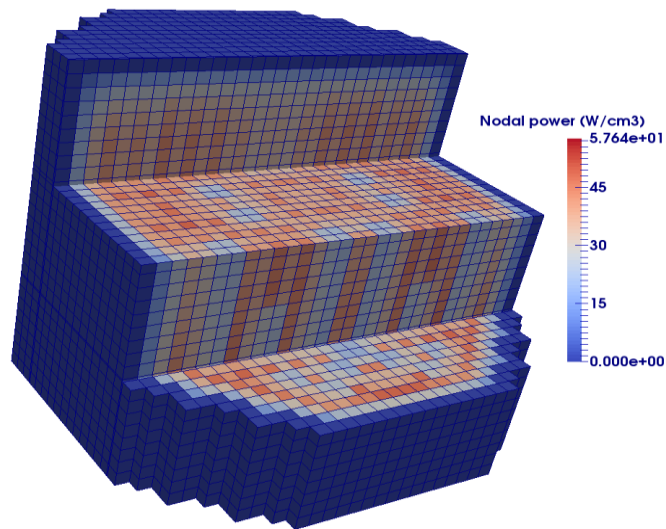


Figure D-1 3D power density distribution (W/cm³) of the Peach Bottom core. Data extracted from the MED file generated during a TRADYN (PARCS) simulation.

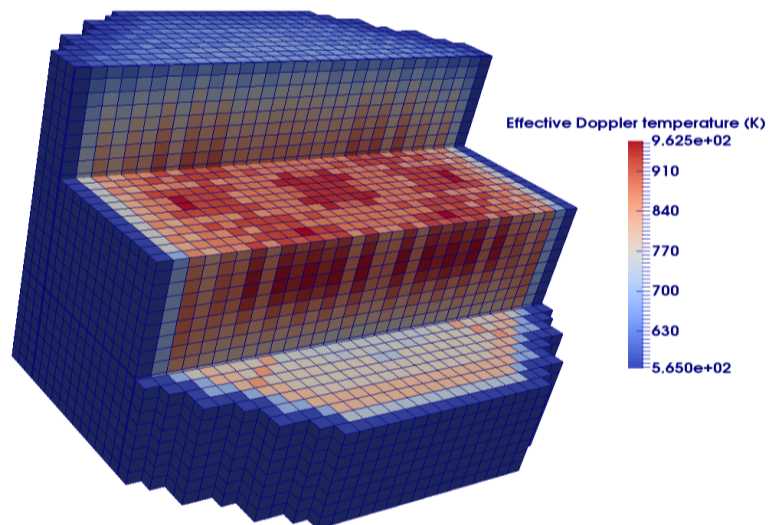


Figure D-2 3D Doppler fuel temperature (K) of the Peach Bottom core. Data extracted from the MED file generated during a TRADYN (PARCS) simulation.

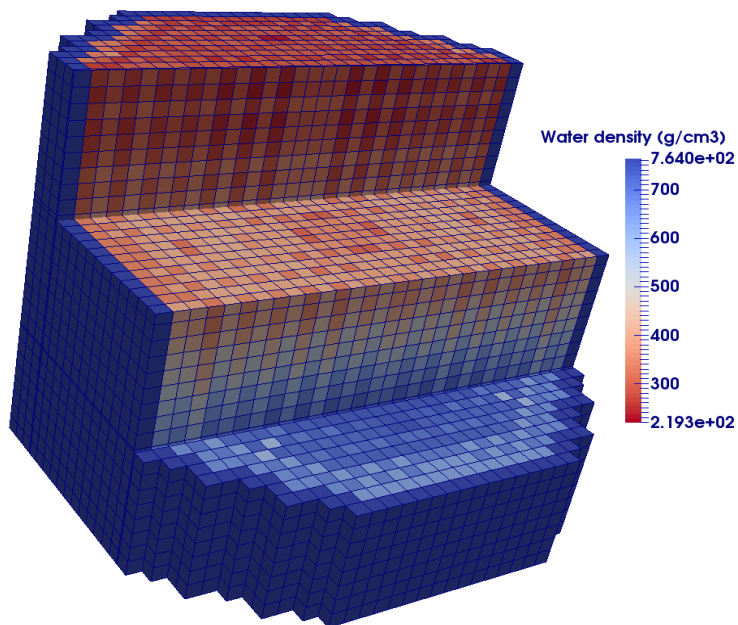


Figure D-3 3D moderator density distribution (g/cm³) of the Peach Bottom core. Data extracted from the MED file generated during a TRADYN (PARCS) simulation.

Transient simulation with TRADYN (PARCS)

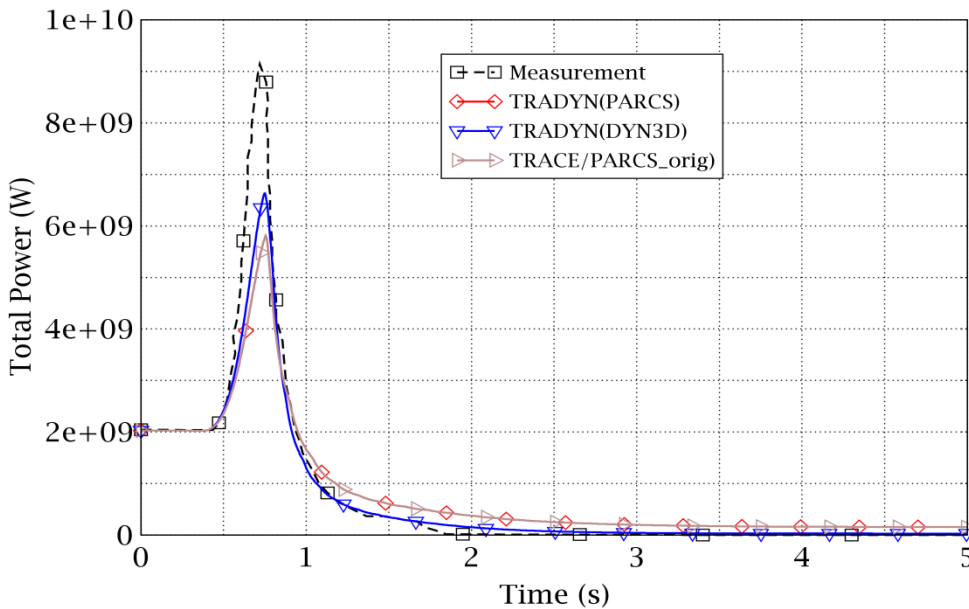


Figure D-4 Total power comparison during transient. Notice that the results of the original version TRACE/PARCS_orig are the same as in TRADYN (PARCS).

A 3D representation of the core power evolution versus time for the transient calculation is depicted in the Figure D-5. There, the increase of the nodal power until it is stopped by the SCRAM that started at 0.75 s after transient initiation is observed. Finally, the core reaches shutdown conditions.

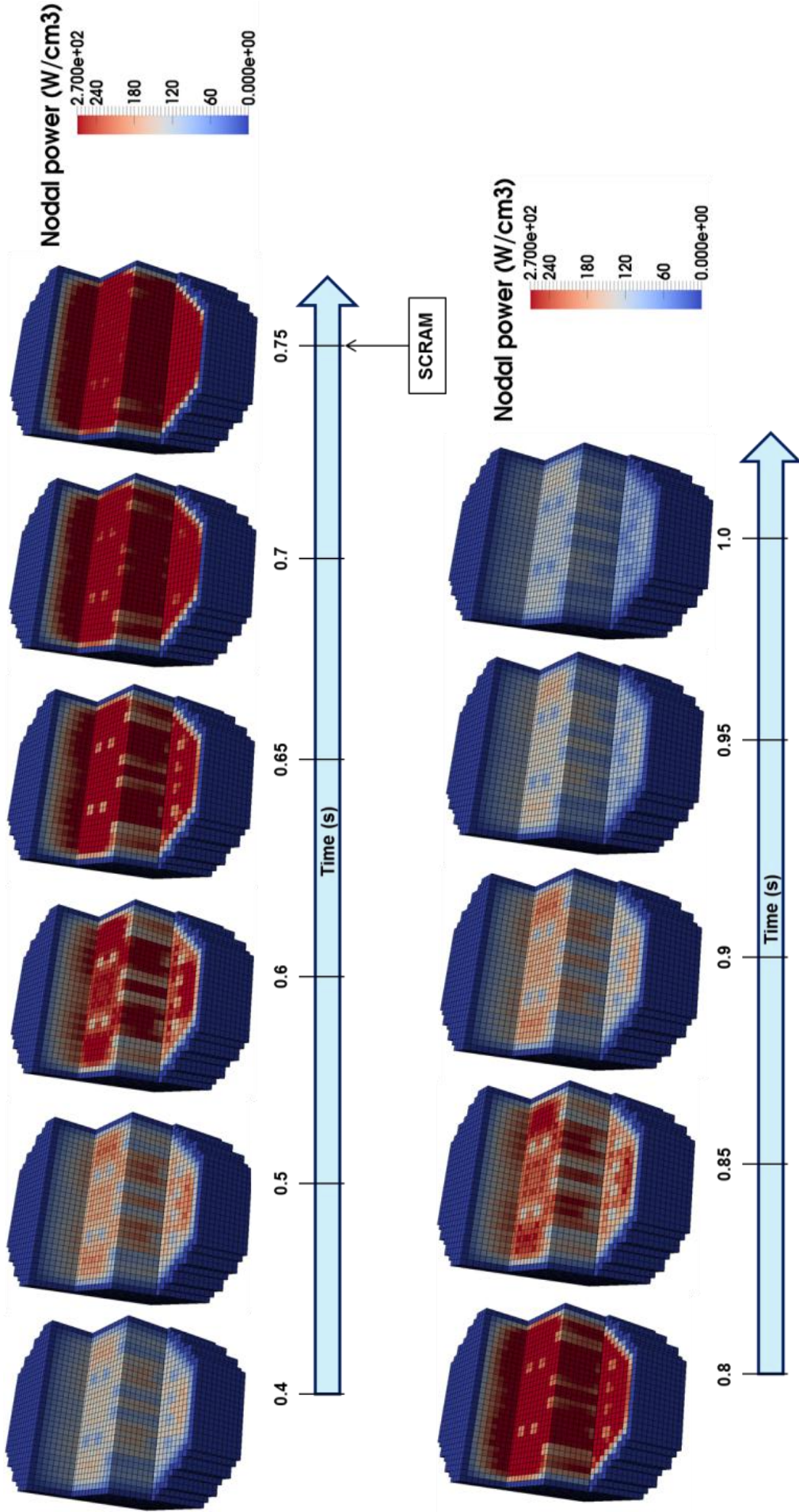


Figure D-5 3D nodal power evolution during the transient obtained by means of ParaVis module.

Appendix E

Results obtained using the new post-processing capability of TRADYN for the static core for Laguna Verde Nuclear Power Plant

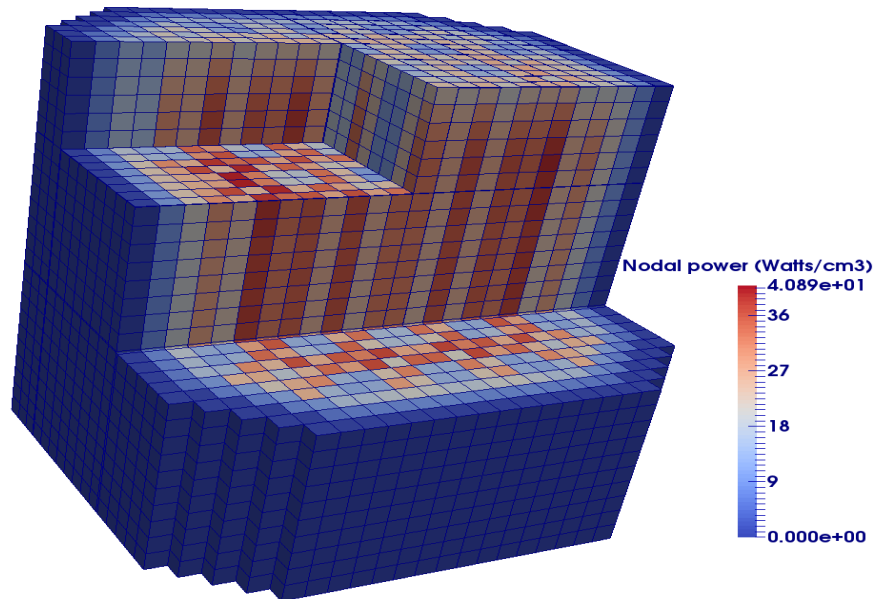


Figure E-1 3D power density distribution (W/cm^3) of the Laguna Verde core. Data extracted from the MED file generated during a TRADYN (PARCS) simulation.

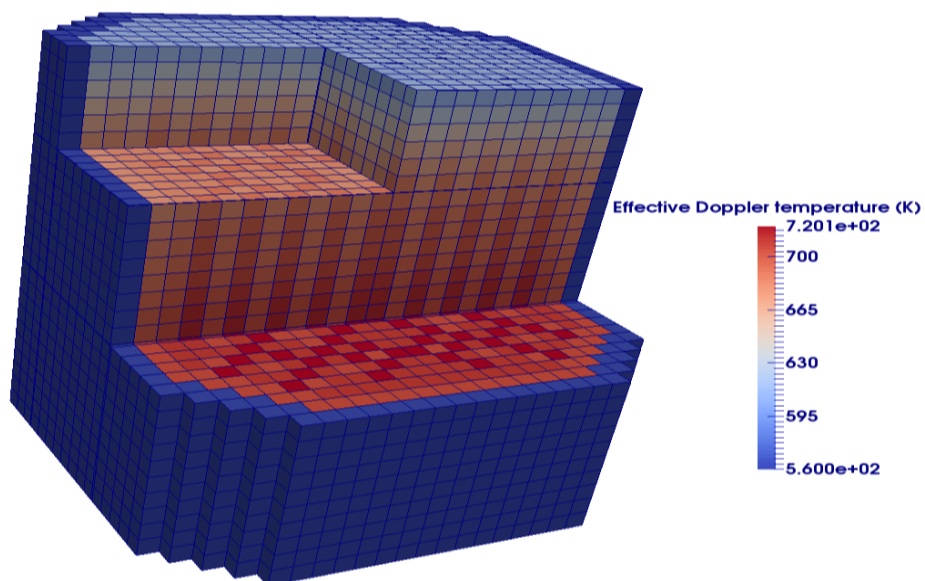


Figure E-2 3D Doppler fuel temperature (K) of the Laguna Verde core. Data extracted from the MED file generated during a TRADYN (PARCS) simulation.

References

1. **Akdeniz B. and Ivanov K., Olson, A.** Boiling Water Reactor Turbine Trip (TT) Benchmark Volume IV: Summary results of Exercise 3 [Report]. - [s.l.] : Nuclear Energy Agency, 2010. - NEA/NSC/DOC/(2010)11.
2. **ANS Special Committee on Fukushima** [Report]. - La Grange, IL : ANS, 2012.
3. **Bahadir Tamer** CMS-LINK User's Manual [Report]. - Newton, Massachusetts, USA : Studsvik of America, Inc., 1999.
4. **Barber D.A. and Downar T.J.** Software Requirements for the General Interface in the Coupled Code [Report] : PU/NE-98-8. - [s.l.] : Purdue University, 1998.
5. **Barber D.A., Downar, T.J., and Wang, W.** Final Completion Report for the Coupled RELAP5/PARCS [Report] : PU/NE-98-31. - [s.l.] : Purdue University, 1998.
6. **Basualdo J [et al.]** PARCS-SUBCHANFLOW-TRANSURANUS MULTIPHYSICS COUPLING FOR IMPROVED PWR'S SIMULATIONS [Conference] // ICAPP. - Fukui and Kyoto, Japan : American Nuclear Society, 2017. - CAMP Autumn Meeting.
7. **Beam Tara M. [et al.]** Nodal kinetics model upgrade in the Penn State coupled TRAC/NEM codes [Journal] // Annals of Nuclear Energy 26. - 1999. - pp. 1205-1219.
8. **Beckert Carsten and Grundmann Ulrich** Entwicklung einer Transportnäherung für das reaktordynamische Rechenprogramm DYN3D [Report] : FZD-497. - [s.l.] : Research Center Dresden-Rossendorf, 2008.
9. **Bell George I and Glasstone S** Nuclear Reactor Theory [Book]. - [s.l.] : Van Nostrand Reinhold Company, 1970.
10. **Borkowski J, Rettig W. H. and Wade N. L.** TRAC-BF1: And Advance Best-Estimate Computer Program for BWR Accident Analysis [Report]. - Washington, DC : NRC, 1992. - NUREG/CR-4356.
11. **Bousbia-Salah A [et al.]** Analysis of the Peach Bottom Turbine Trip 2 Experiment by Coupled RELAP5-PARCS Three-Dimensional Codes [Journal]. - [s.l.] : Nuclear Science and Engineering, 2004. - Vol. 148.
12. **Bousbia-Salah Anis and D'Auria Francesco** Use of coupled code technique for Best Estimate safety analysis of nuclear power plants [Journal]. - [s.l.] : Progress in Nuclear Energy, 2007. - Vol. 49. - pp. 1-13.
13. **Buongiorno J.** BWR Description // OpenCourseWare. - [s.l.] : MIT, 2010.

14. **Calleja M [et al.]** Coupling of COBAYA3/SUBCHANFLOW inside the NURESIM platform and validation using selected benchmarks [Journal]. - [s.l.] : Annals of Nuclear Energy, 2014. - Vol. 71.
15. **Castillo R and Alonso G, Ramirez, J** Validation of SIMULATE-3K for stability analysis of Laguna Verde nuclear plant [Journal] // Nuclear Engineering and Design. - [s.l.] : Nuclear Engineering and Design, 2013. - Vol. 265. - pp. 19-24.
16. **Chadwick M, Herman, M, Obložinský P and et.al.** ENDF/B-VII.1: Nuclear Data for Science and Technology: Cross Sections, Covariances, Fission Product Yields and Decay Data [Journal]. - [s.l.] : Nuclear Data Sheets, 2011. - 2887 : Vol. 112.
17. **Chanaron B [et al.]** Advanced multi-physics simulation for reactor safety in the framework of the NURESAFE project [Journal]. - [s.l.] : Annals of Nuclear Energy, 2015. - Vol. 84.
18. **Chaparro-Vega F** Safety Related Thermal Hydraulic Investigation with TRACE [Report]. - [s.l.] : Karlsruhe Institute of Technology, 2014.
19. **Chauliac C [et al.]** NURESIM - A European simulation platform for nuclear reactor safety: Multi-scale and multi-physics calculations, sensitivity and uncertainty analysis [Journal]. - [s.l.] : Annals of Nuclear Energy, 2011. - Vol. 241.
20. **CRISSEUV2** Neutronics/Thermal-hydraulics Coupling in LWR Technology: State-of-the art Report (REAC-SOAR), Vol. 2, CRISSEU-S I WP2 [Report] : No. 5436, ISBN 92-64-02084-5. - [s.l.] : NEA, 2004.
21. **Cronin James T., Smith, Kord S., Ver Planck, David M.** SIMULATE-3 Methodology, Advanced Three-Dimensional Two-Group Reactor Analysis Code [Report]. - Newton, Massachusetts, USA : Studsvik of America, Inc, 1995.
22. **Daeubler M [et al.]** Static and transient pin-by-pin simulations of a full PWR core with the extended coupled code system DYNSUB [Journal]. - [s.l.] : Annals of Nuclear Energy, 2015. - Vol. 84.
23. **Daeubler M** CreateXslib. - [s.l.] : Personal communication, 2015.
24. **Daeubler M, Jimenez J and Sanchez V** Development of a High-Fidelity Monte Carlo Thermal-Hydraulic Coupled Code System Serpent/Subchanflow - First Results [Conference] // Physor. - Kyoto, Japan : American Nuclear Society, 2014.
25. **Dean D, Rempe K and Umbarger J** SIMULATE-3 Advanced Three-Dimensional Two-Group Reactor Analysis Code [Report]. - [s.l.] : STUDSVIK SCANDPOWER, INC., 2005.
26. **Demazière C, Stálek M and Vinal P** Comparison of the U.S. NRC PARCS Core Neutronics Simulator Against In-Core Detector Measurements for LWR Applications [Report] : International Agreement Report. - Washington, DC, USA : Nuclear Regulatory Commission, 2012. - NUREG/IA-0414.

27. **Downar T, Xu Y and Seker V** PARCS v3.0 U.S. NRC Core Neutronics Simulator Theory Manual [Report]. - [s.l.] : University of Michigan, 2012.
28. **Downar T, Xu Y and Seker V** PARCS v3.0 U.S. NRC Core Neutronics Simulator User Manual [Report] : UM-NERS-09-0001. - [s.l.] : University of Michigan, 2013.
29. **Duderstadt J. J. and Hamilton L. J.** Nuclear Reactor Analysis [Book]. - [s.l.] : John Wiley & Sons, Inc, 1976.
30. **Emonot P [et al.]** CATHARE-3: A new system code for thermal-hydraulics in the context of the NEPTUNE project [Journal]. - [s.l.] : Nuclear Engineering and Design, 2011. - Vol. 241.
31. **Fridman E and Leppänen J** On the use of the Serpent Monte Carlo code for few-group cross section generation [Journal]. - [s.l.] : Annals of Nuclear Energy, 2011. - Vol. 38.
32. **Glaeser H** GRS Method for Uncertainty and Sensitivity Evaluation of Code Results and Applications [Journal]. - [s.l.] : Science and Technology of Nuclear Installations, 2008.
33. **Godfrey A [et al.]** Watts Bar Unit 2 Startup Results with VERA [Report] : CASL Technical Report: CASL-U-2017-1306-00. - 2017.
34. **Gomez Torres A [et al.]** AZTLAN: Mexican Platform for Analysis and Design of Nuclear Reactors [Conference] // ICAPP. - Nice, France : American Nuclear Society, 2015.
35. **Gomez-Torres A [et al.]** DYNSUB: A high fidelity coupled code system for the evaluation of local safety parameters – Part I: Development, implementation and verification [Journal]. - [s.l.] : Annals of Nuclear Energy, 2012a. - Vol. 48.
36. **Gomez-Torres A [et al.]** DYNSUB: A high fidelity coupled code system for the evaluation of local safety parameters - Part II: Comparison of different temporal schemes [Journal]. - [s.l.] : Annals of Nuclear Energy, 2012b. - Vol. 48.
37. **Gomez-Torres Armando** Further Developments of Multiphysics and Multiscale Methodologies for Coupled Nuclear Reactor Simulations. - Munich : Technischen Universität München, 2011. - Doctoral Thesis.
38. **Gonzalez-Vargas Jose Angel** Plotting Capabilities for Reactor Dynamics Codes [Report] : Wissenschaftliche Berichte. - [s.l.] : Karlsruhe Institute of Technology, 2017.
39. **Gonzalez-Vargas Jose Angel, Sanchez-Espinosa V and Jimenez J** Internal Coupling of the Code DYN3D with the USNRC Code TRACE - First Results [Conference] // Physor 2016. - Sun Valley, USA : [s.n.], 2016.
40. **Gonzalez-Vargas Jose Angel, Sanchez-Espinosa, V., Stieglitz R and Macian-Juan R** Development and Validation of the New Coupled Code System TRADYN [Journal]. - [s.l.] : Submitted to Annals of Nuclear Energy, 2017.
41. **Grahn A, Kliem S and Rohde U** Coupling of the 3D neutron kinetic core model DYN3D with the CFD software ANSYS-CFX [Journal]. - [s.l.] : Annals of Nuclear Energy, 2015. - Vol. 84.

-
42. **Grandi Gerardo M** SIMULATE-3K Models & Methodology [Report]. - Newton, Massachusetts, USA : Studsvik Scandpower, 2005.
 43. **Grundmann U** DYN3D – MG – V2.0: Code for Calculation of Steady States and Transients of Reactors by using the Multigroup Neutron Diffusion approximation for hexagonal or quadratic fuel Assemblies or the Multigroup SP3 approximation for quadratic fuel assemblies. [Bericht]. - [s.l.] : Forschungszentrum Dresden-Rossendorf, 2009.
 44. **Grundmann U, Kliem S and Rohde U** Analysis of the Boiling Water Reactor Turbine Trip Benchmark with the Codes DYN3D and ATHLET/DYN3D [Journal]. - [s.l.] : Nuclear Science and Engineering, 2004. - Vol. 148.
 45. **Grundmann U. [et al.]** DYN3D Version 3.2 Code for Calculation of Transients in LWR with Hexagonal or Quadratic Fuel Elements – Description of Models and Methods [Report] : FZR-434. - [s.l.] : Research Centre Rossendorf, 2005.
 46. **Hagrman Dan** CMS-View Users Guide [Report]. - Newton, Massachusetts, USA : Studsvik of America, Inc., 1999.
 47. **Hagrman Daniel T.** INTERPIN-3 Model Improvements and Verification [Report]. - Newton, Massachusetts, USA : Studsvik of America, Inc, 2004.
 48. **Hartmann C.** Advanced Methodology to Simulate Boiling Water Reactor Transient using coupled Thermal-hydraulic/Neutron-kinetic Codes // PhD thesis. - Karlsruhe : Karlsruhe Institute of Technology, 2016.
 49. **Holt L [et al.]** Development of a general coupling interface for the fuel performance code TRANSURANUS - Tested with the reactor dynamics code DYN3D [Journal]. - [s.l.] : Annals of Nuclear Energy , 2015. - Vol. 84.
 50. **Hudson N [et al.]** PARCS Updates and Status. - Prague : [s.n.], 2015. - Presentation during the Spring 2015 CAMP meeting.
 51. **Ikonen T [et al.]** Multiphysics simulation of fast transients with the FINIX fuel behaviour module [Journal]. - [s.l.] : EPJ Nuclear Science & Technologies, 2016. - 37 : Vol. 2.
 52. **Imke U and Sanchez V** Validation of the Subchannel Code SUBCHANFLOW Using the NUPEC PWR Tests (PSBT) [Journal]. - [s.l.] : Science and Technology of Nuclear Installations, 2012. - Article ID 465059 : Vol. 2012.
 53. **Ivanov A [et al.]** High fidelity simulation of conventional and innovative LWR with the coupled Monte-Carlo thermal-hydraulic system MCNP-SUBCHANFLOW [Journal]. - [s.l.] : Nuclear Engineering and Design, 2013. - Vol. 262.
 54. **Ivanov A. [et al.]** High fidelity simulation of conventional and innovative LWR with the coupled Monte-Carlo thermal-hydraulic system MCNP-SUBCHANFLOW [Article] // Nuclear Engineering and Design 262. - 2013. - pp. 264-275.

-
55. **Ivanov A. [et al.]** Large-Scale Monte Carlo calculations with thermal-hydraulic feedback [Conference]. - Kyoto, Japan : Proceedings of PHYSOR 2014 conference, 2014.
 56. **Ivanov B [et al.]** VVER-1000 Coolant Transient Benchmark, Phase 1 (V1000CT-1), Vol. I: Main Coolant Pump Start-up – Final Specifications [Report] : NEA/NSC/DOC(2002). - [s.l.] : Nuclear Energy Agency, 2002.
 57. **Ivanov K, Beam T and Barratta A** PWR Main Steam Line Break (MSLB) Benchmark, Volume I: Final Specification [Report] : NEA/NSC/DOC(99). - [s.l.] : Nuclear Energy Agency, 99.
 58. **Ivanov Kostadin and Avramova Maria** Challenges in coupled thermal-hydraulics and neutronics simulations for LWR safety analysis [Journal]. - [s.l.] : Annals of Nuclear Energy, 2007. - Vol. 34. - pp. 501-5013.
 59. **Jackson C, Cacuci D and Finnemann H** Dimensionally Adaptive Neutron Kinetics for Multidimensional Reactor Safety Transients-I: New Features fo RELAP5/PANBOX [Journal]. - [s.l.] : Nuclear Science and Engineering, 1999. - Vol. 131.
 60. **Jessee M [et al.]** POLARIS: A New Two-Dimensional Lattice Physics Analysis Capability for the SCALE Code System [Conference] // Physor. - Kyoto : American Nuclear Society, 2014.
 61. **Jessee M and DeHart M** NEWT: A New Transport Algorithm for the Two-Dimensional Discrete Ordinates Analysis in non-orthogonal Geometries [Report]. - [s.l.] : Oak Ridge National Laboratory, 2015.
 62. **Jimenez J, Cuervo D and Aragonés J** A domain decomposition methodology for pin by pin coupled neutronic and thermal–hydraulic analyses in COBAYA3 [Journal]. - [s.l.] : Nuclear Engineering and Design, 2010. - Vol. 240.
 63. **Joo H [et al.]** Methods and Performance of a Three-Dimensional Whole-Core Transport Code DeCART [Conference] // Physor. - Chicago, Illinois : American Nuclear Society, 2004.
 64. **Jung Y.S., Joo H.G. and Yoon J.I.** Core Follow Calculation with the nTRACER Numerical Reactor and Verification using Power Reactor Measurement Data [Conference]. - Sun Valley, Idaho, USA : Proceedings of M&C 2013 conference, 2013.
 65. **Knott Dave Bengt H., Forssén, Malte Edenius** CASMO-4 A FUEL ASSEMBLY BURNUP PROGRAM Methodology [Report]. - Newton, Massachusetts, USA : Studsvik of America, Inc, 1995.
 66. **Kochunas B [et al.]** Coupled Single Assembly Solution with COBRA-TF/MPACT (Problem 6) [Report] : CASL Technical Report: CASL-U-2013-0280-000. - 2013.
 67. **Kozlowski T [et al.]** BWR Stability Event Benchmark based on Oskarshamn-2 1999 Feedwater Transient [Report]. - [s.l.] : OECD/NEA, 2014.

-
68. **Kozlowski T., Downar, T.,** OECD/NEA AND U.S. NRC PWR MOX/UO₂ CORE TRANSIENT BENCHMARK- Final Specification [Report]. - [s.l.] : OECD Nuclear Energy Agency/ Nuclear Science Committee, 2003.
 69. **Kozmenkov Y [et al.]** Calculation of the VVER-1000 coolant transient benchmark using the coupled code systems DYN3D/RELAP5 and DYN3D/ATHLET [Journal]. - [s.l.] : Nuclear Engineering and Design, 2007. - 15-17 SPEC. ISS. : Vol. 237.
 70. **Kozmenkov Y, Kliem S and Rohde U** Validation and verification of the coupled neutron kinetic/thermal hydraulic system code DYN3D/ATHLET [Journal]. - [s.l.] : Annals of Nuclear Energy, 2015. - Vol. 84.
 71. **Langenbuch S, Schmidt K and Velkov K** Analysis of the OECD/NRC BWR Turbine Trip Benchmark by the Coupled-Code System ATHLET-QUABOX/CUBBOX [Journal]. - [s.l.] : Nuclear Science and Engineering, 2004. - Vol. 148.
 72. **Langenbuch S.** QUABOX/CUBBOX-HYCA, Ein Dreidimensionales Kernmodell mit parallelen Kühlkanälen für Leichtwasser-reaktoren [Report] : GRS-A-926. - [s.l.] : Gesellschaft für Anlagen- und Reaktorsicherheit (GRS) gGmbH, 1984.
 73. **Lee D [et al.]** Analysis of the OECD/NRC BWR Turbine Trip Transient Benchmark with the Coupled Thermal-Hydraulics and Neutronics Code TRAC-M/PARCS [Journal]. - [s.l.] : Nuclear Science and Engineering, 2004. - Vol. 148.
 74. **Leppänen J.** Serpent a Continuous-energy Monte Carlo Reactor Physics Burnup Calculation Code [Report]. - [s.l.] : VTT Technical Research Centre of Finland, 2013.
 75. **Lerchl G. and H. Austregesilo** ATHLET Mod 1.2 Cycle A – User’s Manual [Report] : GRS-P-1, Vol. 1., - [s.l.] : Gesellschaft für Anlagen- und Reaktorsicherheit (GRS) mbH, 1998.
 76. **MacFarlane R [et al.]** The NJOY Nuclear Data Processing System, Version 2012 [Report] : LA-UR-12-27079. - [s.l.] : Los Alamos National Laboratory, 2012.
 77. **Magedanz J [et al.]** High-fidelity multi-physics system TORT-TD/CTF/FRAPTRAN for light water reactor analysis [Journal]. - [s.l.] : Annals of Nuclear Energy, 2015. - Vol. 84.
 78. **Marleau G** DRAGON THEORY MANUAL PART 1: COLLISION PROBABILITY CALCULATIONS [Report] : Technical report . - Montreal : Ecole Polytechnique de Montréal, 2001. - IGE-236 Rev 1.
 79. **Mignot G [et al.]** Computation of a BWR Turbine Trip with CATHARE-CRONOS2-FLICA4 Coupled Codes [Journal]. - [s.l.] : Nuclear Science and Engineering, 2004. - Vol. 148.
 80. **Miller R.M. and Downar T.J.** Software Design and Implementation Documents for the TRAC-M-Specific Data Map Routine in the Coupled TRAC-M/PARCS Code [Report] : PU/NE-00-20. - [s.l.] : Purdue University, 2000.
 81. **Mori M [et al.]** RETRAN-3D MOD003 Peach Bottom Turbine Trip 2 Multidimensional Kinetics Analysis Models and Results [Journal]. - [s.l.] : Nuclear Technology, 2003. - Vol. 142.

-
82. **Mylonakis A [et al.]** Optimization of an Integrated Neutronic/Thermal-Hydraulic Reactor Core Analysis Model [Conference] // 23rd International Conference Nuclear Energy for New Europe. - Portoro, Slovenia : [s.n.], 2014.
 83. **Nikitin K [et al.]** PEACH BOTTOM 2 TURBINE TRIP 2 SIMULATION by TRACE/S3K COUPLED CODE [Conference] // Physor. - Pittsburgh : American Nuclear Society, 2010.
 84. **Puente-Espel F, Avramova M and Ivanov K** NEW DEVELOPMENTS OF THE MCNP/CTF/NEM/NJOY CODE SYSTEM – MONTE CARLO BASED COUPLED CODE FOR HIGH ACCURACY MODELING [Conference] // Physor. - Pittsburgh, Pennsylvania : American Nuclear Society, 2010.
 85. **RELAP RELAP5-3D©** Code Manual, INEEL-EXT-98-00834 – Rev.2.4 [Report]. - [s.l.] : Idaho National Laboratory, 2005.
 86. **RELAP5 RELAP5/MOD3.3** CODE MANUAL, VOLUME I: CODE STRUCTURE, SYSTEM MODELS, AND SOLUTION METHODS [Report]. - Washington, DC : USNRC, 2001.
 87. **Rohde U [et al.]** The reactor dynamics code DYN3D e models, validation and applications [Journal]. - [s.l.] : Progress in Nuclear Energy journal, 2016. - Vol. 89.
 88. **Romano P and Forget Benoit** The OpenMC Monte Carlo particle transport code [Journal]. - [s.l.] : Annals of Nuclear Energy, 2013. - Vol. 51.
 89. **Roselló O.** Desarrollo de una metodología de generación de secciones eficaces // PhD. Thesis. - [s.l.] : Universidad Politécnica de Valencia, 2004.
 90. **Ryu M. [et al.]** Solution of the BEAVRS benchmark using the nTRACER direct whole core transport code [Conference]. - Kyoto, Japan : Proceedings of PHYSOR 2014 conference, 2014.
 91. **Sanchez R [et al.]** APOLLO2 Year 2010 [Journal]. - [s.l.] : Nuclear Engineering and Technology, 2010. - 5 : Vol. 42.
 92. **Sanchez V and Al-Hamry A** DEVELOPMENT OF A COUPLING SCHEME BETWEEN MCNP AND COBRA-TF FOR THE PREDICTION OF THE PIN POWER OF A PWR FUEL ASSEMBLY [Conference] // International Conference on Mathematics, Computational Methods & Reactor Physics. - Saratoga Springs, New York : American Nuclear Society, 2009.
 93. **Sanchez V. [et al.]** SUBCHANFLOW: A Thermal-Hydraulic Sub-Channel Program to Analyse Fuel Rod Bundles and Reactor Cores [Conference]. - Cancun, Mexico : Proceedings of the 17th Pacific Basin Nuclear Conference, 2010.
 94. **Sanchez-Cervera S [et al.]** Optimization of multidimensional cross-section tables for few-group core calculations [Journal]. - [s.l.] : Annals of Nuclear Energy, 2014. - Vol. 69.
 95. **Santamarina A [et al.]** The JEFF-3.1.1 Nuclear Data Library [Report] : JEFF Report 22. - [s.l.] : NEA, 2009.
 96. **Schmidt R [et al.]** An approach for coupled-code multiphysics core simulations from a common input [Journal]. - [s.l.] : Annals of Nuclear Energy, 2015. - Vol. 84.

-
97. **Schöffel P, Ceuca S and Hristov H** Schnelllaufendes 3D-Thermohydraulikmodell für ATHLET (AC2). - Karlsruhe : [s.n.], 2016. - Lecture given during the KTG Fachtagung.
 98. **Schunert S and Azmy Yousry** Using the Cartesian Discrete Ordinates Code DORT for Assembly-Level Calculations [Journal]. - [s.l.] : Nuclear Science and Engineering, 2013. - 3 : Vol. 173. - pp. 233-258.
 99. **Smith K** Assembly Homogenization Techniques for Light Water Reactor Analysis [Journal]. - [s.l.] : Progress in Nuclear Energy, 1986. - 3 : Vol. 17.
 100. **Solis J, Avramova M and Ivanov K.** Temporal Adaptive Algorithm for the TRAC-BF1/NEM/COBRA-TF Coupled Calculations in BWR Safety Analysis [Journal]. - [s.l.] : Annals of Nuclear Energy , 2002. - Vol. 29.
 101. **Solis Jorge [et al.]** Boiling Water Reactor Turbine Trip (TT) Benchmark [Report]. - [s.l.] : US Nuclear Regulatory Commission and OECD Nuclear Energy Agency, 2001.
 102. **Studsvik Staff** CMS System Overview: User Interface // Lecture given during a training course in Laguna Verde Nuclear Power Plant. - Veracruz, Mexico : [s.n.], 2006.
 103. **TRACE** TRACE V5.0 Theory Manual - Field Equations, Solution Methods, and Physical Models [Report]. - [s.l.] : U.S. Nuclear Regulatory Commission, 2013.
 104. **Turinsky P** Modeling & Simulation Goals and Accomplishments [Conference] // Joint International Conference on Supercomputing in Nuclear Applications + Monte Carlo. - Paris, France : [s.n.], 2013. - Lecture given during SNA + MC. - CASL-U-2013-0217-000.
 105. **Ward A [et al.]** PARCS Updates and Status // Presentation given during the Fall CAMP meeting. - Washington : [s.n.], 2013.
 106. **Watson J and Ivanov K** Improved cross-section modeling methodology for coupled three-dimensional transient simulations [Journal]. - [s.l.] : Annals of Nuclear Energy, 2002. - Vol. 29.
 107. **Watson J.** Implicit time-integration method for simultaneous solution of a coupled non-linear system [Report] : PhD Thesis. - [s.l.] : The Pennsylvania State University, 2010.
 108. **Wemple C [et al.]** Recent Advances in the HELIOS-2 Lattice Physics Code [Conference] // Physor. - Interlaken, Switzerland : American Nuclear Society, 2008.
 109. **X-5 Monte Carlo Team** MCNP — A General Monte Carlo N-Particle Transport Code, Version 5, Volume I: Overview and Theory [Report] : Technical Report LA-UR-03-1987. - [s.l.] : Los Alamos National Laboratory, 2003.
 110. **Xu Yunli [et al.]** Application of TRACE/PARCS to BWR stability analysis [Journal] // Annals of Nuclear Energy. - [s.l.] : Annals of Nuclear Energy, 2009. - pp. 317-323.
 111. **Yoshioka K [et al.]** Multi-Group Constants Generation System for 3D-Core Simulation Using a Continuous Energy Monte Carlo Technique [Journal]. - [s.l.] : Progress in Nuclear Science and Technology, 2011. - Vol. 2.